The Institute of Paper Chemistry

Appleton, Wisconsin

Doctor's Dissertation

An Investigation of the Peroxyacetic Acid Delignification of White Birch

Allan J. Glinski

June, 1976

AN INVESTIGATION OF THE PEROXYACETIC ACID DELIGNIFICATION OF WHITE BIRCH

A thesis submitted by

Allan J. Glinski

B.S. 1970, University of Wisconsin — Stevens Point

M.S. 1972, Lawrence University

in partial fulfillment of the requirements
of The Institute of Paper Chemistry
for the degree of Doctor of Philosophy
from Lawrence University,
Appleton, Wisconsin

June, 1976

TABLE OF CONTENTS

SUMMARY

White birch (Betula papyrifera) wood chips were continuously reacted with peroxyacetic acid (PAA) under mild conditions with continuous removal of solubilized materials and rapid quenching of excess oxidant. The solubilized materials were collected at six consecutive reaction stages down to about 82% wood yield and fractionated on Porasil B. Fractionation showed that as delignification proceeded, a greater proportion of larger molecules was removed from the wood, and no evidence was found for ionic or polar interactions with the column packing.

Over one-half of the fractionated materials were obtained as light tan freeze-dried powders which were examined for their physical and chemical properties. Variation in absorptivity at 280 nm as a function of fraction number and percent delignification showed that there were chemical differences between the fractions. Relatively low absorptivity values (av. 6.6 liters/g cm) reflected lower aromaticities arising from ring degradation. Significant losses in methoxyl groups tied in with lowered absorptivities are indicative of loss of aromaticity. Carboxyl contents of 0.49-0.79 per C_9 lignin unit were significantly higher than the 0.20 carboxyls per C_9 believed by others to represent a minimum amount of degradation needed to achieve water solubility. Variation in the infrared absorption band near 1510 cm^{-1} tended to follow the absorptivity trends relating aromatic content to fraction number and percent delignification.

The freeze-dried fractions contained from 5-25% carbohydrates with significant and orderly trends in the amount and composition of the carbohydrate components. Paper electrophoresis was not capable of separating the lignin and carbohydrates in the freeze-dried fractions. Enzymolysis of freeze-dried materials using a polysaccharidase reduced the hydrodynamic size of the lignin remaining after hydrolysis. These results gave inductive evidence for a lignin-carbohydrate bond.

Variation in specific rotation at 546 nm as a function of fraction number and percent delignification followed trends in polysaccharide amount and composition, particularly xylan, glucan, and galactan content. This variation is believed to occur because fractionation is according to hydrodynamic size, and size is systematically related to composition.

When specific rotations at different wavelengths of light (ORD) were determined for certain fractions, Cotton effects* were observed in the aromatic electronic transition regions. ORD and circular dichroism (CD) curves had positive Cotton effects for early fractions near the start of the delignification where glucan and galactan were major components of the total polysaccharide content. Negative Cotton effects were observed for late fractions near the end of the delignification where xylan was by far the major component of the total polysaccharide content. This was likely to have occurred because xylans are known to have negative rotations while glucans (cellobiose to cellopentose) and galactans have positive rotations.

The differences between the ORD curves of the fractions again showed that there were significant and orderly chemical differences between the fractions ex-Porasil B. Even though each fraction is composed of a heterogeneous mixture of molecular structures, the Cotton effects for each of these samples probably reflect greater homogeniety of molecular structures than would be expected for a polydisperse system.

Cotton effects in the ORD and CD curves for several of these samples provided positive evidence for a lignin-carbohydrate bond. When the lignin and carbohydrates are bonded, delignification involves not only removal of lignin but

*Cotton effects in this system are the result of an intramolecular coupling of the optical activity of the carbohydrates with the aromatic electronic transitions.

also removal of bonded carbohydrates, which are many times larger than lignin of equivalent molecular weight. Therefore even small amounts of bonded carbohydrates can be a controlling factor in the transport of lignin through the microporous structure of wood during PAA delignification.

INTRODUCTION

GENERAL

To produce a high-yield pulp, one must selectively remove lignin from the wood. In the early 1950's, Poljak (1-3) observed that peroxyacetic acid, which is a strong oxidant, degraded lignin to soluble products much more readily than it degraded carbohydrates. It was then suggested (4-6) that PAA be used to prepare holocelluloses, and later workers used PAA as a pulping (7-9) and bleaching (10-14) agent.

Although much is known about PAA reactions with wood and lignin model compounds, the complete delignification mechanism of wood by PAA is not fully understood. Present knowledge of this mechanism is limited mostly to work done on batch reaction systems (15,16) and a study by Albrecht on the continuous delignification of a softwood (17). Under the mild reaction conditions used by Albrecht, the delignification was very selective. When secondary reactions were minimized, the solubilized softwood lignin more closely resembled the lignin as it existed in the wood. From the results of his study, Albrecht hypothesized that molecular size was a limiting factor in the transport of solubilized materials from the microporous structure of wood during delignification.

This investigation involved the study of solubilized materials obtained from the reaction between PAA and a hardwood in a continuous flow reactor to minimize secondary reactions. A study of the lignin and carbohydrate parts of the solubilized materials was expected to add to the understanding of the PAA delignification mechanism.

RAW MATERIALS

CHOICE AND PREPARATION OF WOOD CHIPS

White birch (Betula papyrifera), a common hardwood species of relatively low extractive content with light-colored sapwood and heartwood, was used as the wood substrate in this study. The sapwood region from a 30-year-old white birch which was both straight grained and had pores of uniform size and distribution (18,19) was removed and cut into chips as described in the Experimental section. Chips from the white birch sapwood were easily shaped and had final dimensions of 12 x 8 x 0.5 mm in the longitudinal, tangential, and radial directions.

The radial thickness of 0.5 mm corresponded to 20-25 fiber diameters, thus assuring rapid and uniform penetration of reactant. Extractives were removed from the wood chips by acetone extraction. After being air dried, these chips were likely to be stable at room temperature indefinitely. Chips prepared in this way were easily packed in the reaction apparatus (described later), and comparison of results to the softwood case (17), where the chip dimensions were the same, was more readily made.

CHOICE OF OXIDANT

Peroxyacetic acid was chosen because it is known to be a selective delignifying agent (1-9). The mechanism of lignin removal by PAA is not yet fully understood. Evidence has been summarized (20,21) which suggests that the delignification mechanism involved aromatic ring opening. Analyses of the PAA-solubilized materials from a softwood indicated that wood pore size and carbohydrate in these materials had an important role in delignification (17).

Some practical advantages of using freshly generated PAA to delignify were the following:

(1) High purity PAA, devoid of stabilizers, was generated in aqueous solution as described in the Experimental section; the procedure developed by FMC Corporation (22) and described in Appendix I was used.

(2) Inorganic salts were not present in generator PAA.

(3) Standard Pyrex glassware was used in all apparatus contacted by PAA.

(4) Purification of PAA-solubilized materials for example, by dialysis, was not needed prior to exclusion chromatography.

PEROXYACETIC ACID

SOME ASPECTS OF DELIGNIFICATION

In aqueous solution, PAA forms a stable 5-membered ring (23,24) whose outer peroxide oxygen is assumed to have a partial positive charge. Thus, it is likely that PAA reactions with lignin molecules proceed through polarized intermediates with attack of the peroxy oxygen on electron-rich sites (16,21,25,26).

Peroxide reactions are commonly associated with free radical mechanism. However, there is no evidence for free radicals through the addition of free radical scavengers (20) or by electron spin resonance spectroscopy (27).

Delignification by PAA involves the heterogeneous reaction of PAA with wood samples following the penetration of an aqueous solution of PAA into the wood chip matrix. To avoid a nonuniform reaction throughout the chip, the rate of penetration of PAA must be greater than the rate of reaction by PAA. Thus, the final wood chip dimensions must be small enough to ensure that the penetration of PAA has occurred before PAA reactions begin.

Of the main components of wood, lignin has many electron-rich sites for the peroxy oxygen to react with in comparison to the carbohydrates, for example. But, there are other components of wood that have electron-rich sites such as extractives which have been found to be reactive with PAA (28,29). To avoid their influence on delignification by PAA, one usually removes these extractives prior to reaction.

Several electron-rich sites suitable for attack by the peroxy oxygen are present within hardwood lignins as typified in Fig. 1. Such lignins are known to have about a 1:1 guaiacyl to syringyl ratio for white birch. Although PAA reactions with syringyl type compounds have not been studied in detail, extensive

studies have been made on the guaiacyl type (20,21,30-43). On the basis of these and other studies it is known that lignin degradation is accomplished through demethoxylation, side-chain, and ring cleavage reactions.

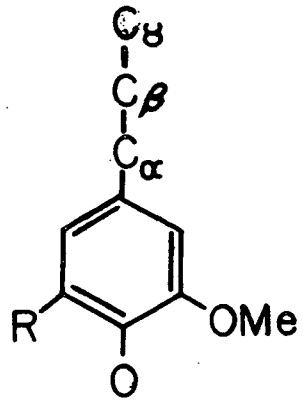

where R = H (guaiacyl) and OMe (syringyl) for hardwoods.

Figure 1. Typical Hardwood Lignin Skeleton

Demethoxylation by PAA occurs with the breakage of aryl-alkyl ether bonds. This is depicted in Pathway A of Fig. 2.

Phenyl propane groups with oxidizable C-3 side-chains are initially attacked by PAA (40,41,44). Side-chain oxidations occur in lignin units containing hydroxyl, carboxyl, or olefinic groups in the α-position of the C-3 side-chain (20,21,30-37) as shown in Pathways B and C of Fig. 2.

Several studies (20,21,30) show that the ease of ring cleavage increases as the number of electron-donating substituents increase. Those results suggest that a hardwood would undergo delignification more rapidly than a softwood. Ring cleavage results in muconic acid systems and related lactones (15,16,21). Muconic acid groups are predominant because the intermediate o-quinones are likely to cleave to give muconic acids. p-Quinones are visualized as oxidizing to lactones. The

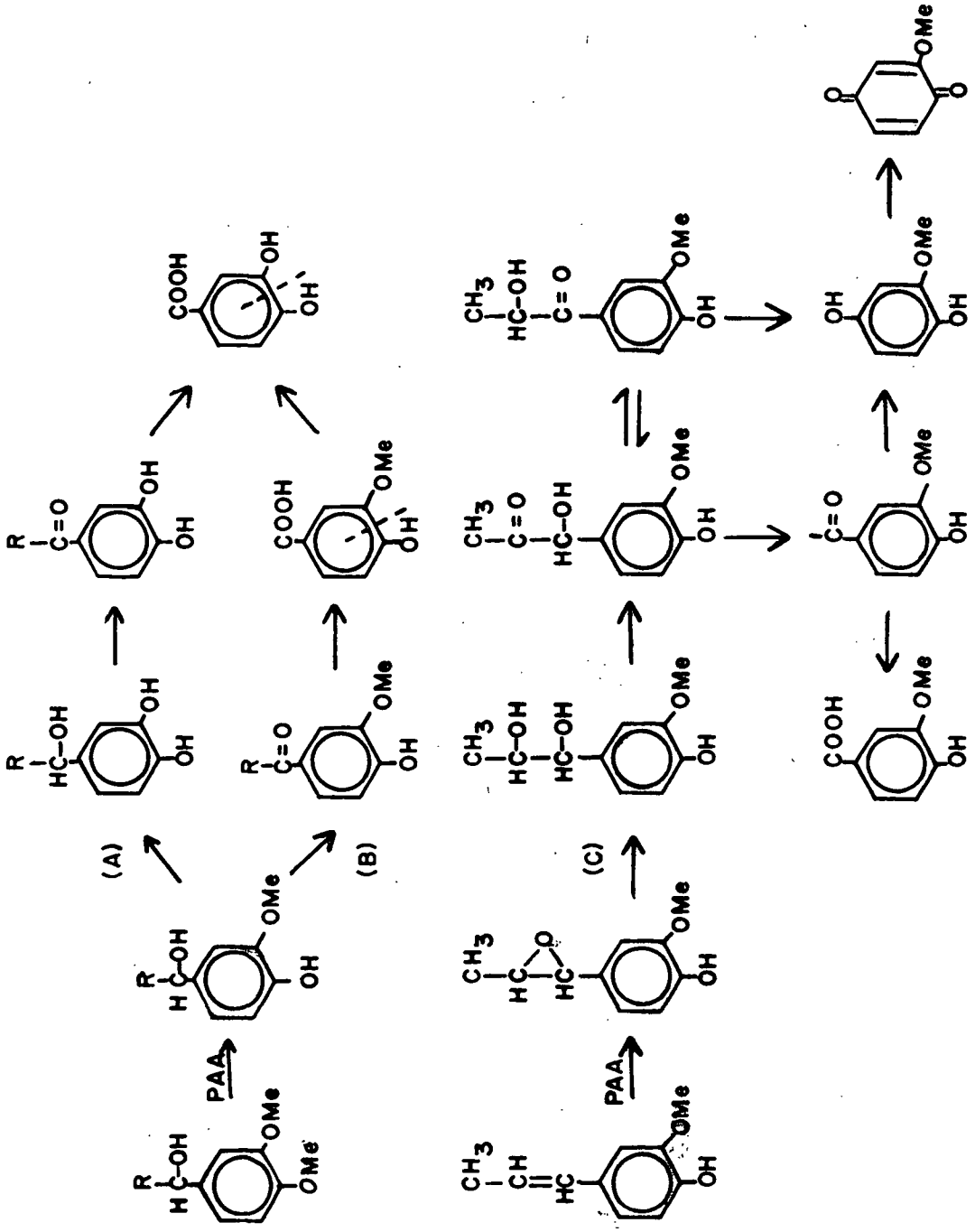

Figure 2. Proposed Reaction Pathways for Peroxyacetic Acid Oxidations of Aromatic Rings (A) and C-3 Side-Chains (B and C) (34,35)

reaction pathways that lead to muconic acids and lactones are shown in Fig. 3 for the PAA oxidations of 4-methyl phenols and their methyl esters as described by Farrand (20). Those results are consistent with the finding of muconic acid systems and related lactones as products of the reaction of PAA with hardwoods and softwoods for prolonged periods and at relatively high temperatures by Sarkanen and Suzuki (15) and Sarkanen and Lai (16).

When birch dioxane lignin was reacted with PAA (45), solubilization occurred at a carboxyl content of about 0.2 equiv./equiv. mol.wt. This led to the postulation by Sakai and Kishimoto (45) that the generation of carboxyl groups may be the rate-limiting step for the solubilization of lignin. The rate of demethoxylation and solubilization were also closely related (41,46). This indicated that the rate-limiting step in lignin solubilization may involve the loss of loosely bound methoxyl groups.

For the continuous reaction of a loblolly pine with PAA under mild conditions (17), carboxyl contents for the isolated lignin samples were higher than those at which loblolly pine dioxane lignin became soluble (45). These results indicated that after initial solubilization, these materials continued to react until they were able to escape from the cell wall matrix. From the physical and chemical properties of the solubilized materials from a softwood, it is apparent that in addition to initial solubilization by PAA, hydrodynamic volumes of these materials (which are related to their ability to escape from the cell wall matrix) are an important factor in the delignification of a softwood.

PREPARATION AND STORAGE OF OXIDANT

There are various methods used to generate peroxyacetic acid (47-50). The method of preparation used in this study is described in Appendix I and involves the hydrogen peroxide oxidation of acetic acid as in Equation (1).

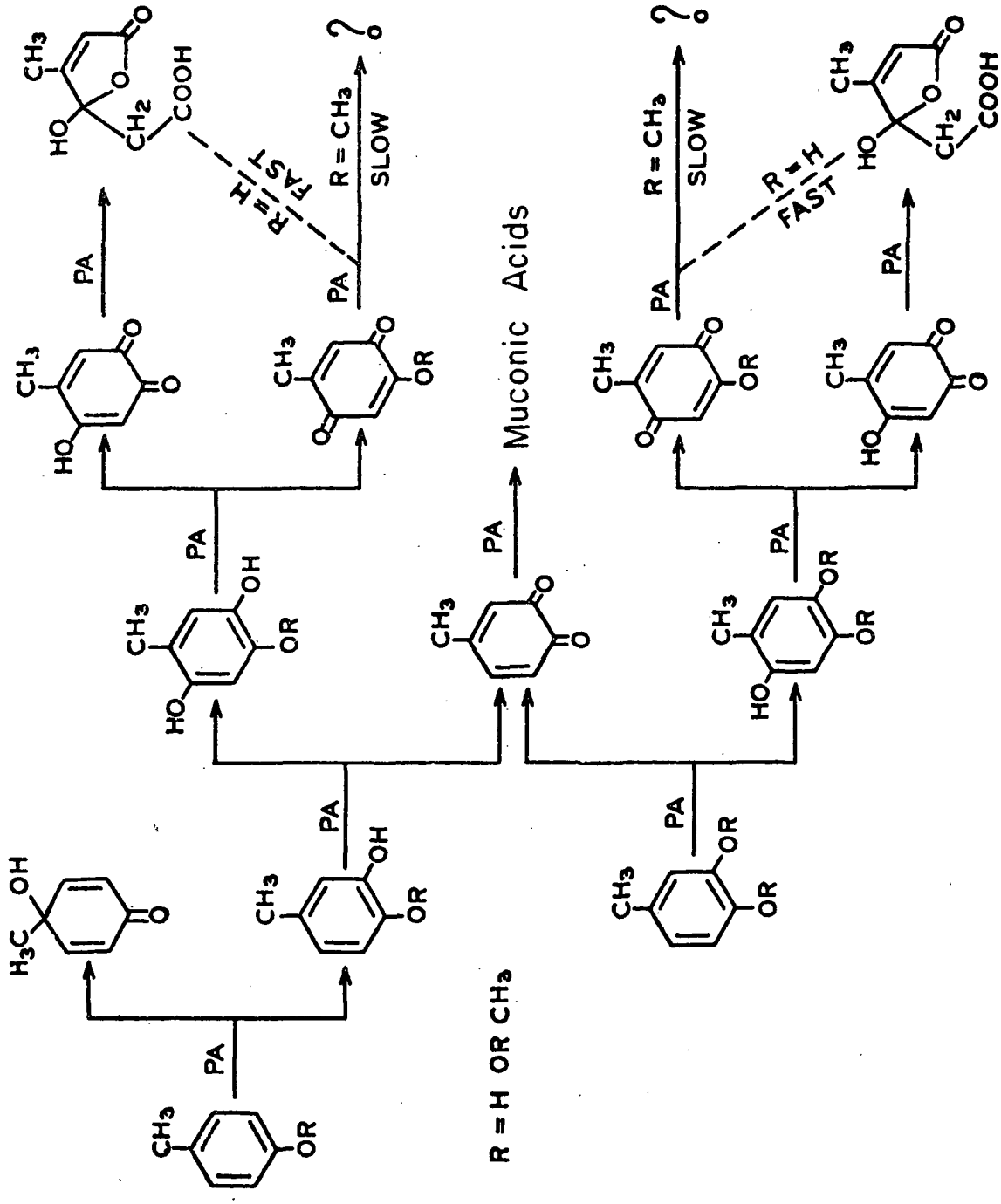

Figure 3. Overall Reaction Scheme for Peracetic Acid Oxidation of 4-Methyl Phenols and Their Methyl Ethers (20)

$$H_2O_2 + CH_3CO_2H \rightleftharpoons CH_3CO_3H + H_2O \qquad (1)$$

High purity PAA, produced in aqueous solution by this method as developed by the FMC Corporation (22), is devoid of stabilizers and inorganic ions. The same method was used previously by Albrecht and Farrand (17,20).

On standing for long periods of time, generator PAA (without stabilizers) is subject to hydrolysis to H_2O_2, thus, generator PAA should be used as soon as possible after preparation. At room temperature, a typical generator PAA can lose 2% concentration per day. Storage below 20°C in colored, vented glass bottles minimizes heat and light decomposition reactions of PAA and avoids excessive pressures in the storage vessel.

REACTION WITH WHITE BIRCH

CONTINUOUS FLOW APPARATUS

The continuous flow reaction apparatus used in this study is shown in Fig. 4. Simplicity of the apparatus and its operation were two advantages of this system, which was constructed from Pyrex glass, teflon, polyethylene, and stainless steel. Wood chips for delignification were packed into the reaction vessel, and adequate flow rates were maintained by gravity flow, thus eliminating the need for pumping and monitoring devices.

As the reaction proceeded, the solubilized materials were readily removed from the reaction site and cooled with the excess oxidant being immediately quenched by acetaldehyde according to Equation (2).

$$CH_3CO_3H + CH_3CHO \rightleftharpoons CH_3CH(OH)\text{-}O\text{-}O\text{-}CO\text{-}CH_3 \rightarrow 2CH_3CO_2H \qquad (2)$$

Rapid removal of solubilized materials and quenching of excess oxidant minimized secondary degradation reactions which can occur in batch reaction systems.

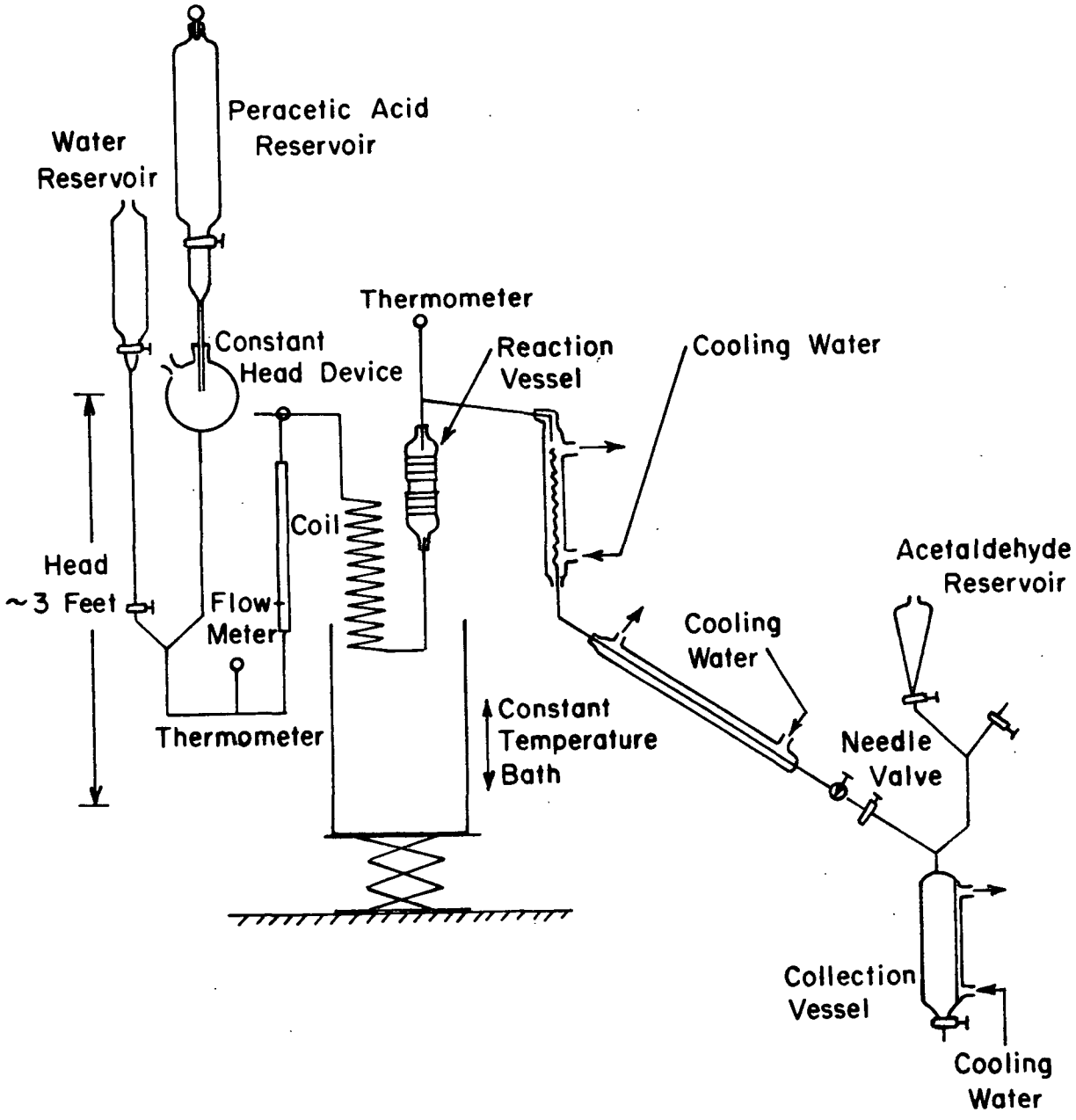

Figure 4. Continuous Flow Reaction Apparatus

Quenching was also necessary to avoid the possibility of explosion due to organic peroxides as the solubilized materials were concentrated. Use of acetaldehyde to quench excess oxidant kept inorganic ions out of the system. When excess oxidant was reduced by Na_2SO_3 (51) or by colloidal platinum (15), subsequent extractions, filtrations, and regenerations were needed. Sulfuric acid contamination can also become a problem in the sulfite system.

The continuous flow apparatus lent itself to the collection of solubilized materials at various stages in the reaction. This allowed comparisons of the physical and/or chemical properties of the solubilized materials to be made as the delignification proceeds.

PRELIMINARY EXPERIMENTS AND SELECTIVITY

Several preliminary reactions at various temperatures and reaction times were used to delignify white birch chips to two different yields. The results are presented in Table I. The flow rate and PAA concentration were held constant as before.

Table I shows that, if anything, lower temperatures appear to result in the lowest carbohydrate loss and highest lignin removal at a given yield. Average values showed more clearly that there was a greater loss of carbohydrate when more lignin had been removed, which is supported by other results (4).

In accord with these preliminary experiments, 50°C was the chosen delignification temperature mainly because at this temperature, most of the lignin was removed in a reasonable time without need for excessive amounts of PAA, and also because a minimal amount of carbohydrate was removed under these conditions (8 hr, 12 liters of PAA).

TABLE I

DATA FOR PRELIMINARY DELIGNIFICATION EXPERIMENTS[a]

Temp., °C	Time, hr	Yield, %	Klason[b] Lignin	Acid-[b] Soluble Lignin	Total[c] Lignin	Lignin[d] Removed	Yield + Lignin Removed	Apparent Loss	Carbohydrates[e] Total	Carbohydrates[e] Loss
Control		100.0	17.4	4.8	22.2	None	100.0	None	63.5	None
44	2.5	87.6	9.1	3.6	12.7	9.5	97.1	2.9	59.4	4.1
44	5.0	86.1	6.3	4.3	10.6	11.6	97.7	2.3 (Av.)	61.0	2.5 (Av.)
51	2.0	87.2	9.2	4.2	13.4	8.8	96.0	4.0 3.3	60.7	2.8 3.5
52	1.5	87.1	9.6	3.7	13.3	8.9	96.0	4.0	58.9	4.6
51	4.0	82.1	3.4	4.1	7.5	14.7	96.8	3.2	58.9	4.6
52	4.0	79.7	2.4	3.0	5.4	16.8	96.5	3.5 (Av.)	59.3	4.2 (Av.)
60	2.0	80.7	3.7	3.7	7.4	14.8	95.5	4.5 3.7	57.5	6.0 5.2
60	2.0	79.6	2.4	2.9	5.3	16.9	96.5	3.5	57.5	6.0

[a] All analyses are expressed on the basis of g/100 g oven dry unreacted, solvent extracted wood.

[b] All values are the average of two determinations.

[c] Calculated by the addition of the two preceding columns.

[d] Calculated by the difference in total lignin from lignin content at 100% yield.

[e] Sum of the individual sugars.

Selectivity of white birch PAA delignification under these conditions was observed. For the low yield reactions, about 70% of the lignin was removed while only about 11% of the carbohydrate material was removed.

UNIFORMITY

It is known that because of the heterogeneous nature of the system used, the rate of penetration of the wood chip must be much faster than the rate of reaction with PAA. To determine whether this was the case, some means of detection of the rate of penetration as compared with the rate of reaction was needed. This was accomplished by staining the chip with an appropriate stain and then examining any differences in the typical color reaction of that stain across the wood chip (through the center) early in the reaction.

It is known that lignified substances have characteristic color reactions with certain organic reagents. On contact with wood, phloroglucinol has been found (52) to give a violet-red color. The question of which substance(s) in wood react in this way and how the color results has been the subject of many studies as reviewed by Hagglund (53).

As a result of studies by Adler, et al. (54) and Adler and Ellmer (55), it was finally shown that the phloroglucinol reaction was quite specific and the reactive substances were of the cinnamaldehyde type. On substitution of the carbon-carbon double bond in the C-3 side-chain, the substituted cinnamaldehyde group was no longer phloroglucinol-reactive. Thus, the proposed reaction pathway had been attributed to the condensation reaction of cinnamaldehyde type groups with phloroglucinol as shown in Equation (3).

The question of whether or not the cinnamaldehyde type groups were part of the lignin macromolecule was answered in later studies (54-56). The typical phloroglucinol reaction was found for the so-called "native" lignin isolated

by Brauns (56). Cinnamaldehyde type groups were present in a lignosulfonic acid sample which gave the phloroglucinol reaction (54,55).

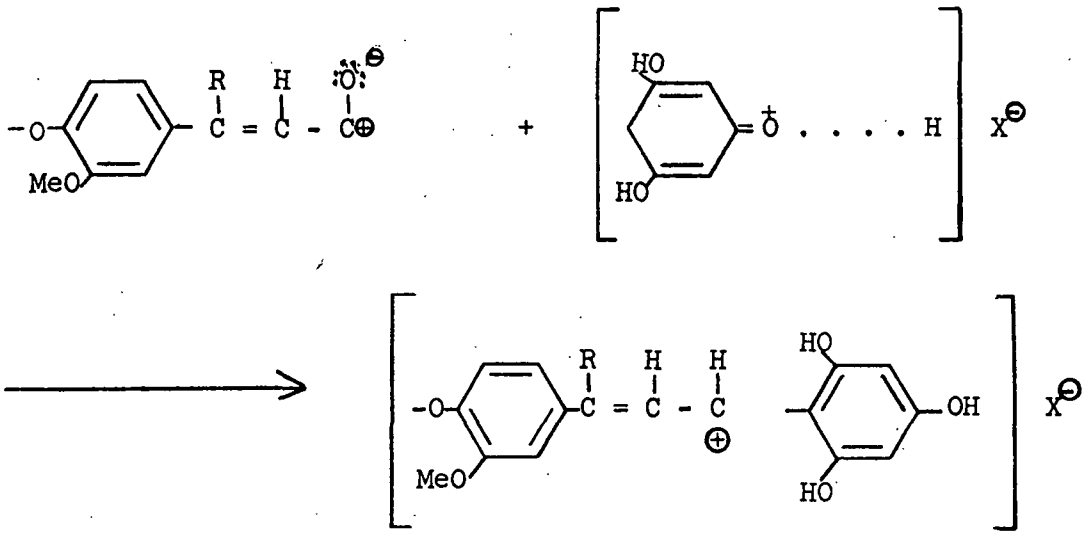

(3)

When a white birch chip was stained with phloroglucinol in this study, a violet-red color resulted. When a reacted white birch chip (98% yield) was stained with phloroglucinol, a tannish-brown color resulted. In addition, this change in color was uniform throughout the reacted chip thus demonstrating uniformity of reaction by PAA throughout the chip. These results also indicated that early in the reaction, PAA reacted with the cinnamaldehyde groups of lignin and were analogous to observations made on softwoods by Albrecht (17) and Fleck (57).

COLLECTION OF SOLUBILIZED MATERIALS

The solubilized materials from the continuous reaction with PAA were collected in two ways. First, a composite liquor which consisted of all the solubilized materials from the reaction was collected. This composite liquor was used for some of the preliminary fractionation studies and electrophoresis.

Second, the solubilized materials from the continuous reaction with PAA were collected in six reaction stages as the delignification proceeded. The first

reaction stage represented the first solubilized materials removed from the wood chips, the second represented the second materials removed, etc. Examination of the physical and/or chemical properties of these solubilized materials is discussed in the following section.

FRACTIONATION

FRACTIONATION OF LIGNIN

Most separations of lignin molecules have been accomplished by gel permeation chromatography (GPC) using Sephadex, a cross-linked dextran gel which swells in water. Previous work (58-68) on lignosulfonate fractionation by GPC on Sephadex showed few chemical differences in the molecular populations obtained upon fractionation. Larger molecular weight lignosulfonates on longer cooking times or higher temperatures for shorter times were found by GPC in one study (68).

Exclusion chromatography as used in this study involved the following steps:

(1) The sample was added onto the top of the column.

(2) The sample was eluted through the column by means of flowing solvent.

(3) The sample was fractionated in the pores of the packing.

Molecules too large to enter any pores came out first. The very small molecules entered most of the pore volume and thus spent more time diffusing through the porous medium.

The mechanism of size sorting has been argued from three different mechanistic points of view: 1) steric exclusion (69), 2) restricted diffusion (70), and 3) thermodynamic (71) hypotheses. All of these hypotheses agree that the separation was according to hydrodynamic volume for chemically uniform materials, as discussed in reviews given in the literature (72-74). Changes in composition of the materials being separated can also have an influence on their fractionation. In addition, retardation of certain substances (75,76) is frequently observed during gel chromatography and is known as reversible adsorption. These effects are strongly dependent upon the composition of the eluant.

Outside forces such as Coulombic interactions between ions and charged regions in the gel, Van der Waals interactions between the solute and the support, or adsorption, can cause the delay of the elution of the solute. These forces were minimized by deactivating the support (17) prior to fractionation to insure that the primary separation mechanism was by hydrodynamic volume.

The packing used to perform the fractionation needed to be both capable of performing the fractionation and inert to the materials being fractionated. Porasil packings, which are spherical porous silica beads that are not gels, have been shown (77) to be capable of fractionating aqueous solutions of various polymer calibration standards according to hydrodynamic volume. Previous work (17) on PAA solubilized materials from a loblolly pine has demonstrated that Porasil B is a suitable packing for fractionating PAA solubilized materials.

The advantages of using Porasil as a support for the fractionation are numerous. Porasil is rigid, chemically inert, heat resistant, nonbiodegradable, and easily washed. Once packed in a column, Porasil does not change its volume or porosity and sufficient flow rates can be maintained by hydrostatic head alone, thus eliminating expensive and complicated pumping and monitoring devices.

The PAA solubilized materials from white birch were fractionated by exclusion chromatography using Porasil B as described later.

FRACTIONATION OF SOLUBILIZED MATERIALS

PRELIMINARY TESTS

Concentration Determination by Beer's Law

Absorbance at 280 nm divided by the absorptivity of the sample was used to semiquantitatively determine the concentrations of PAA solubilized materials.

This was done through the application of Beer's Law which states the following:

$$A = abc$$

where A = absorbance at a given wavelength

a = absorptivity of a species at that wavelength, liter/(g cm)

b = path length of absorbing solution, cm

c = concentration of absorbing species, g/liter

To demonstrate that Beer's Law was applicable to this system, a plot of A versus c was obtained for a sample of Fraction 45 from reaction stages (1-6) and shown to be a straight line.

Acceptability of Porasil B as Packing

A small Porasil B column was constructed for preliminary tests on the fractionating capabilities and inertness of Porasil B packing toward the PAA solubilized materials. The first materials came off the column immediately after the void volume was reached. However, not all materials came off the column at this elution volume, but rather came off at later elution volumes. Thus, a fractionation of the PAA solubilized materials was accomplished by Porasil B packing.

There was no difference in the weight of materials eluted from the small column and an equal amount dried in a vacuum oven. This result showed that there was no permanent adsorption of the PAA solubilized materials on Porasil B. However, all materials were not off the column prior to the total liquid volume, thus indicating some drag occurring in the column. This will be discussed in more detail later.

Ultraviolet absorbance measurements for solubilized materials which had been in contact with Porasil B for up to two weeks and solubilized materials which had

never been in contact with Porasil B showed no differences. Infrared spectra of Porasil B which had been in contact with the PAA solubilized materials and Porasil B which had never been in contact showed no differences. Thus, no evidence was obtained that the PAA solubilized materials were permanently adsorbed on Porasil B.

Concentration of Different Reaction Stages

Following the above tests, the equipment described in an earlier work (17) was used for the fractionation in this study. Differences in solute concentrations have led to changes in the proportion of excluded molecules when lignosulfonates were fractionated on Sephadex columns (66). Variation in concentrations of the solutions to be fractionated have been shown in this study to affect the fractionation results. Thus, fractionations were made for equal gravimetric concentrations of the six reaction stages with monitoring by ultraviolet absorbance at 280 nm.

FRACTIONATION CURVES

Ultraviolet absorbance at 280 nm versus fraction number curves were obtained for each of the six reaction stages during fractionation on the Porasil B column with corrections for PAA quenched by acetaldehyde. A computer program shown in Appendix II was used to normalize all curves to the same area under the curve. The results of the fractionations of three reaction stages can be seen in a plot of the normalized absorbance versus fraction number shown in Fig. 5. The complete fractionation plot for all six reaction stages can be seen in Appendix III. Because of the uncertainty in the absorptivity determinations due to the nature of the products, absorbance values rather than some other relationships such as absorptivity or concentration was used in these plots. Accounting for absorptivities of these samples does not alter significantly the character of the curves.

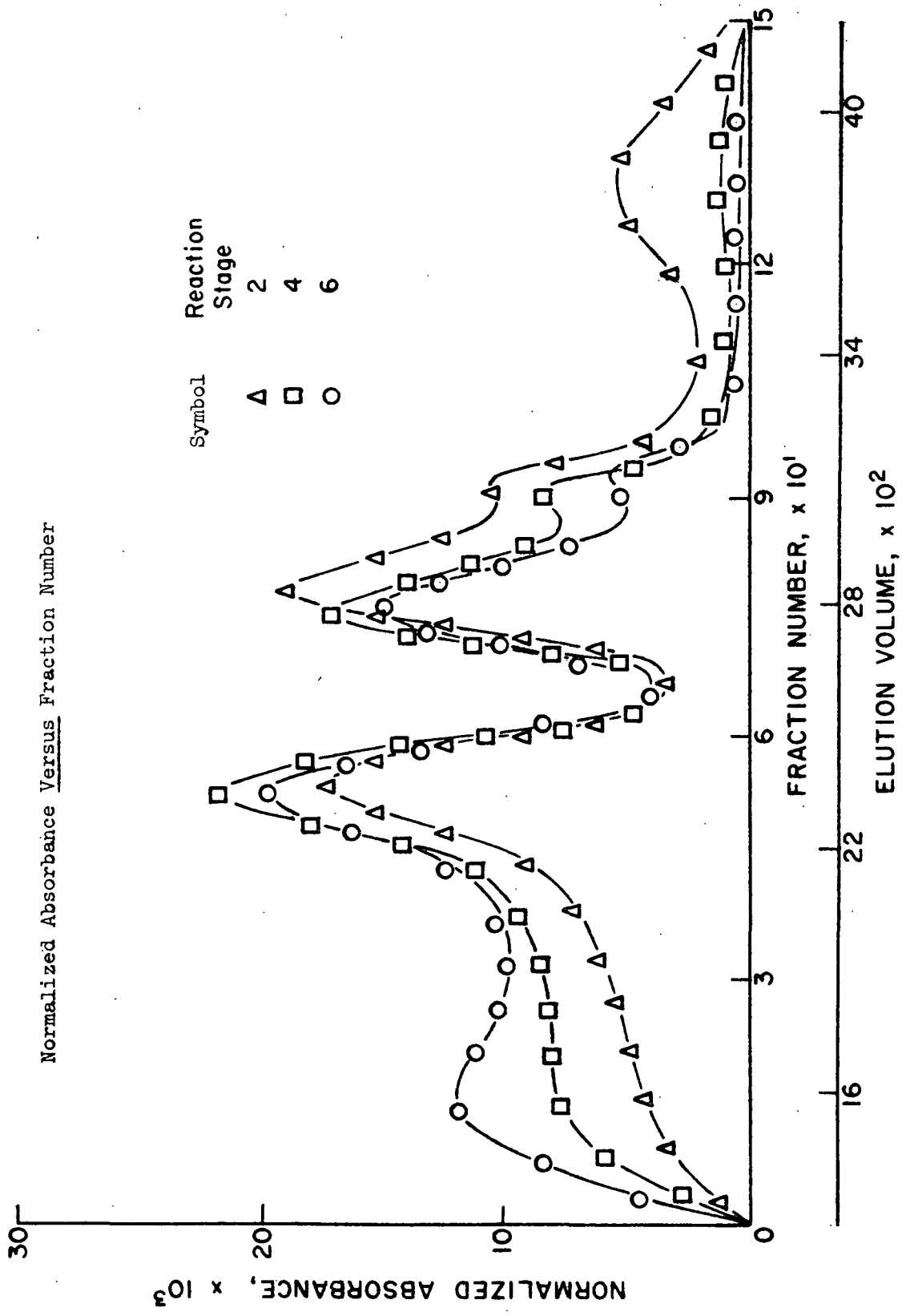

Figure 5. Normalized Absorbance Versus Fraction Number for Three Reaction Stages

Absorptivity at 280 nm of Fractionated Materials

The sums of the absorbance values at 280 nm for all fractions from the six reaction stages are shown in Table II. Absorbance values were at a maximum for Reaction Stage 3. Since equal concentrations of solubilized materials were fractionated for each reaction stage, the sum of the absorbance at 280 nm is proportional to the absorptivity, which is a measure of the proportion of aromatic nuclei present in the sample being examined. Thus, the largest value for the sum of absorbance at 280 nm (aromatic nuclei absorbance) for Reaction Step 3 implied that the proportion of aromatic nuclei to the remainder of the molecules was likely to be at its maximum at this reaction step.

TABLE II

PEROXYACETIC ACID REACTION TIME WITH CORRESPONDING LIQUOR REACTION STAGES AND DISSOLVED SOLIDS, AS DELIGNIFICATION PROCEEDS

Reaction Time, hr	Liquor		Delignification, %
	Reaction Stage	Dissolved Solids, % o.d.w.	
0-1.3	1	2.6	6.3[b]
1.3-2.7	2	4.8	23.9[a]
2.7-4.0	3	5.1	45.9[a]
4.0-5.3	4	5.0	63.1[b]
5.3-6.7	5	4.3	77.5[b]
6.7-8.0	6	3.5	84.5[a]

[a]By analysis for Klason and acid soluble lignin.

[b]By graphical estimation.

Absorptivity values at 280 nm for Fractions 1-65 for each of the six reaction steps are listed in Appendix IV and in Fig. 6. Early fractions (1-11) had low absorptivity values around 4 liters/(g cm), middle fractions (12-45) had absorptivities around 6.5 liters/(g cm), and later fractions (46-61) had absorptivities around 8 liters/(g cm). After Fraction 65, the absorptivities dropped below 2 liters/(g cm), but the concentration of the syrips could not be

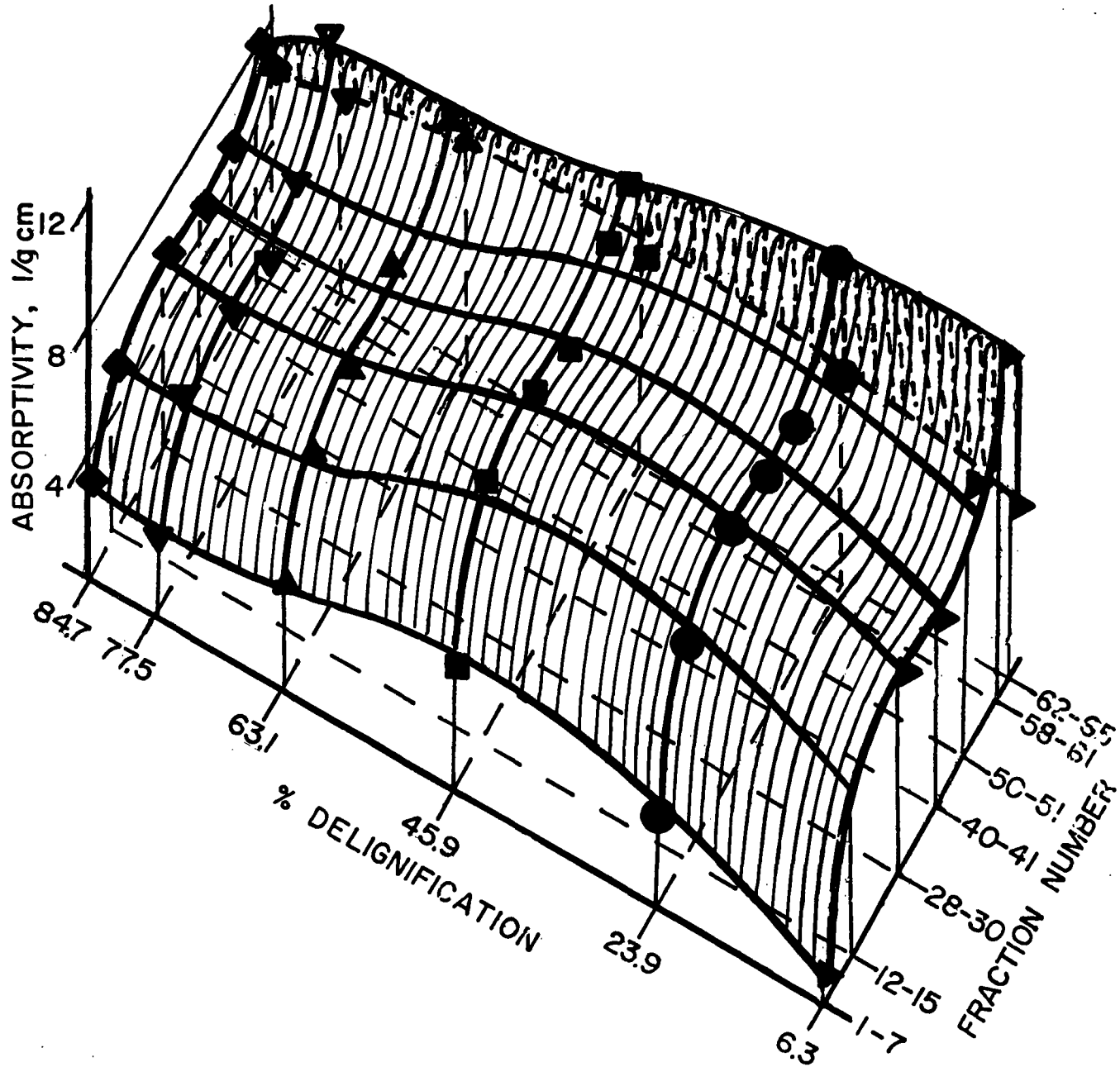

Figure 6. Absorptivities as Delignification and Fractionation Proceed

accurately determined. Differences in absorptivity values from fraction to fraction indicate that there were chemical differences between the various fractions. Assuming that ultraviolet (UV) absorptivity at 280 nm was related to the proportion of aromatic nuclei present in the sample, these results indicated that there was a greater aromatic content to the remainder of the solubilized materials as the molecular populations became smaller in size up to Fraction 65 where the reverse was true.

The range of absorptivities, namely 0.8-11.3 liters/(g cm), brackets the range found for PAA degraded softwood lignin (17). Compared with absorptivities of 12.1 and 13.1 liters/(g cm) reported for birch milled wood and dioxane lignins (78,79), respectively, a significant decrease in most of the absorptivities is apparent. This indicated that the lignin being removed in this study was somewhat degraded from its original state even under the mild conditions used in this study.

Normalized Absorbance Versus Fraction Number

Five peaks (I-V in Fig. 5) can be seen in the early reaction stages while only the first four are present in the later stages. The first fractions (20 ml/fraction) ex-Porasil B were detected immediately after the void volume of the column had been reached. Absence of a large sharp peak at this elution volume indicated that only a relatively small proportion of the solubilized materials had a hydrodynamic volume large enough to be excluded entirely from the packing.

When successive liquor fractions from a chlorite delignification were obtained using a different experimental approach by Ahlgren, et al. (80), the freeze-dried materials after dialysis were found to have constant weight average molecular weights. From those results, it was concluded that the average size of the lignin macromolecules was constant up to 60% delignification.

An increase in the weight average molecular weight was found by Rezanowich, et al. (81) and Yean and Goring (82-83) for nondialyzable lignins from successive pulping liquor fractions from kraft and sulfite delignifications. This trend was associated with a significant removal of hemicelluloses early in the delignification.

For the continuous PAA delignification of a softwood, it was found that as delignification proceeded, fractionation on Porasil B showed that there were fewer of the smaller molecules and more of the larger ones being removed from the wood sample, without change in the overall size range (84). The softwood PAA lignins had significantly smaller molecular weights than those dissolved at a comparable level of delignification in the sulfite or kraft processes. Because accompanying hemicelluloses can have a decisive influence on the hydrodynamic volume of the lignin-carbohydrate molecules being removed from the wood, it was thought by Albrecht that the hemicelluloses had a significant influence on the fractionation results, especially if the hemicelluloses and lignin were linked.

As the reaction proceeded in this work, the proportion of molecules contributing to the first peak (Fractions 1-30) increased, while the proportion of molecules in the late peaks (Fractions 90-160) decreased. In other words a greater proportion of larger molecules and a lesser proportion of smaller molecules were being removed as delignification proceeded similar to the softwood case.

Upon freeze-drying, the first 65 fractions were obtained as fluffy light-tan powders. Later fractions were obtained as gummy syrips. For practical purposes, the first 65 fractions for each of the six reaction stages which were obtained as powders and came off the column prior to the total liquid volume of eluate, were used for the tests described below. To further simplify the system, each

set of 65 fractions was made into 20 groups of fractions of equal mass (composite liquor basis) to give a total of 120 groups.

Effect of Methyl Esterification

The possibility of adsorption by Porasil B of the solubilized materials during fractionation either by ion exchange or dipole-dipole interactions was examined by methylating the functional group(s) most likely to undergo these interactions and then noting changes, if any, in the fractionation on Porasil B. A sample of combined Fractions 1-65 from Reaction Stages 3-6 was methylated. The most polar functional groups in the freeze-dried samples, such as carboxyl groups, were expected to be the largest contributers to the types of interactions described above, if these interactions were present. Carboxyl groups are also the most easily methylated. Potentiometric titrations brought the percentage carboxyl from 14.49% for unmethylated to 0.58% for the methylated.

Results of the fractionation of the methylated and unmethylated fractions can be seen in Fig. 7. There was little change in the fractionation profile upon methylation of Fractions 1-65. Methylation of acid groups was not expected to substantially influence absorptivity at 580 nm because the methyl esterification has not taken place on the aromatic ring. Thus, the fractionation was primarily by hydrodynamic volume and not by ion exchange or dipole interactions of the solute with the packing.

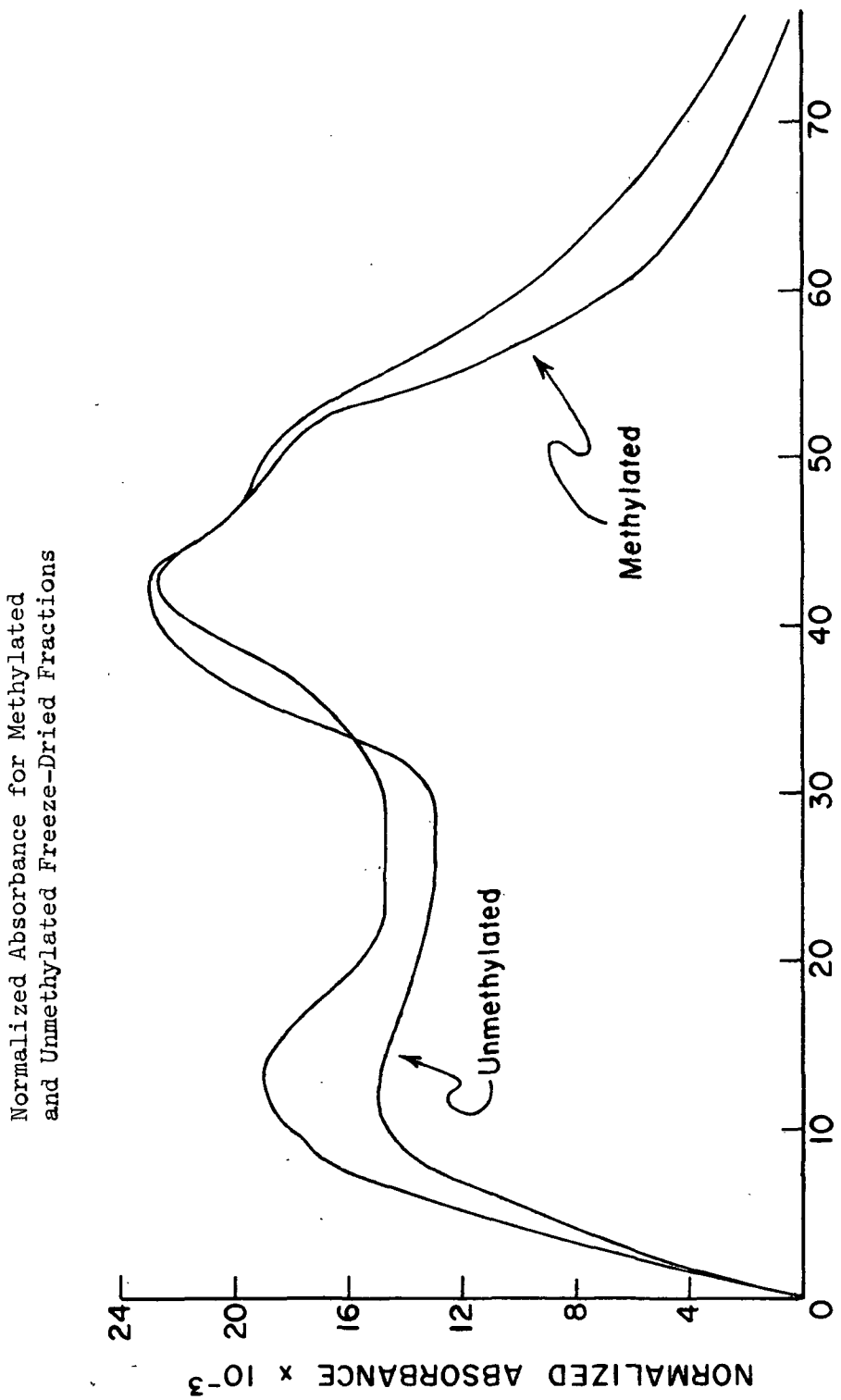

Figure 7. Normalized Absorbance Versus Fraction Number for Methylated and Unmethylated PAA Solubilized Materials

EXAMINATION OF FRACTIONS EX-PORASIL B

CARBOHYDRATE COMPONENT

In the concluding remarks* concerning the polymer properties of lignin, Goring (85) had this brief admonition to lignin chemists:

> "Advances in the elucidation of the lignin problem are now going to depend on deeper understanding of the intimate chemical and morphological relationship of lignin to the other important constituents of the xylem. And we can predict with certainty that such further understanding will lead to a wider and more efficient use of wood as a basic source of fiber and chemial."

One such important relationship involves the possible lignin-carbohydrate bond which will be discussed in more detail in a later section (see Effect on Lignin Hydrodynamic Volume). During delignification, various amounts of polysaccharides are always removed. Losses of polysaccharides have been observed in the chlorite delignification of both softwoods and hardwoods (86,87). It has been reported that there was a trend toward more polysaccharide removal at later stages of delignification (85). Similar trends have been inferred from the results for PAA delignifications of softwoods (4-6).

The role of polysaccharides in the delignification mechanism is not yet fully understood. The ease of a chlorite delignification of white birch has been examined by Kerr (87) for a sample from which the hemicelluloses had been previously removed by a mild caustic extraction. Delignification was significantly facilitated by the initial removal of the hemicelluloses. From those results it has been concluded that the ease of delignification was increased after hemicellulose removal because there were bigger cell pores after hemicellulose

*Concluding remarks by Goring from Chapter 17 of Sarkanen and Ludwigs' "Lignins" book dealing with the polymer properties of lignin (85).

removal, and larger lignin molecules could escape the matrix of the cell, thus minimizing the amount of lignin degradation needed to remove the lignin from the matrix of the cell.

In a more extensive study of the polysaccharides removed on PAA delignification of loblolly pine under mild conditions, it has been observed at the Institute that as delignification proceeded, there were more polysaccharides removed (84). It was also observed that the smallest molecules eluted from a Porasil B column were associated with the greatest amount of polysaccharides as shown in Fig. 8. In addition to studying the total polysaccharide content, the trends in the various pentoses and hexoses present in the fractions ex-Porasil B were determined. These previous results on a softwood showed that as delignification proceeded, the relative amount of xylose and mannose increased. Moreover, the greatest percentage of xylose was found in the largest molecules, while the reverse was true of mannose as shown in Fig. 9.

Under severe reaction conditions, it has been found (88) that hemicelluloses were degraded by PAA with chain rupture. Thus, finding saccharides in the products of PAA delignifications and greater amounts of saccharides at later stages in the reaction was not entirely surprising. However, the study on loblolly pine PAA lignins (84) gave the first evidence for orderly trends in the relative amounts of the individual sugars being removed during delignification. Although the noncellulosic region of wood may not be crystalline in the same sense as cellulose fibrils, the orderly trends described above for the softwood PAA lignins (84) suggest that there is organization of some type within the wood which may have significant implications on the understanding of the PAA delignification mechanism.

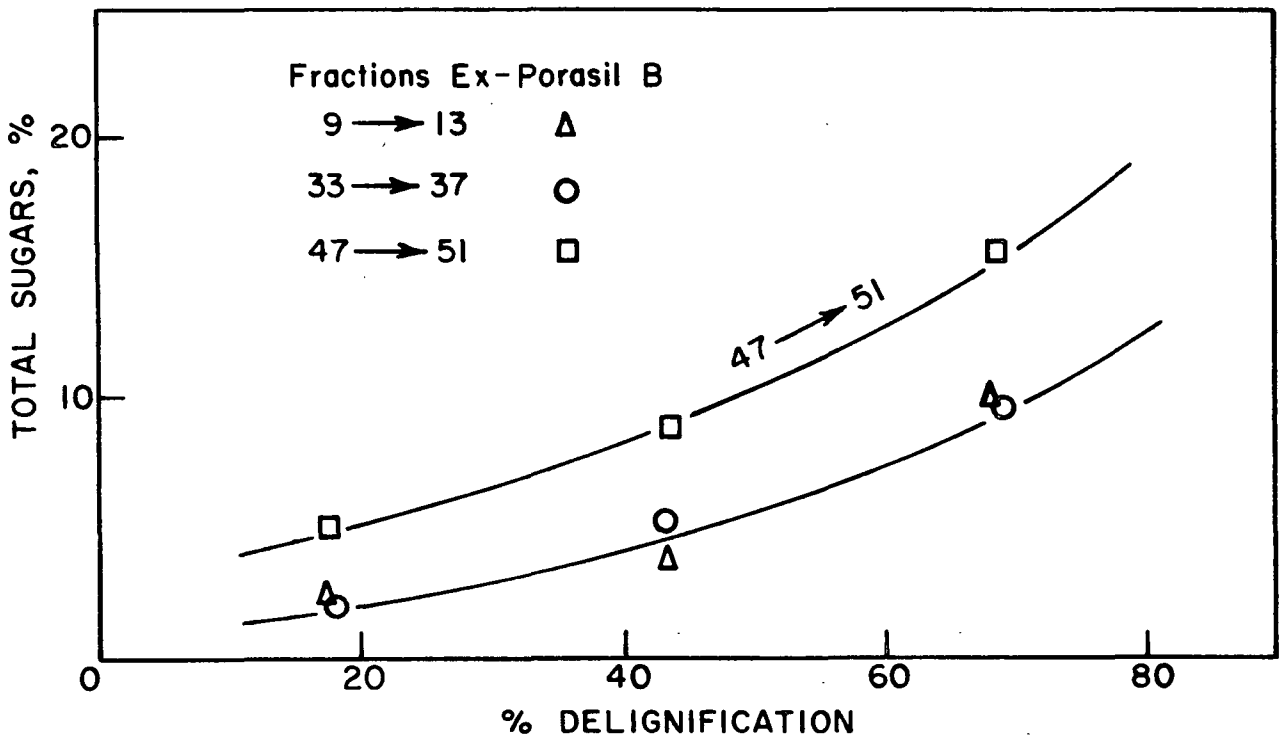

Figure 8. Total Sugars in Freeze-Dried Solids from Fractions 9→13, 33→37, and 47→51 ex-Porasil B as Delignification Proceeds (84)

In this study on white birch, polysaccharide analyses were made on the column-fractionated materials from PAA delignifications to determine whether any analogous trends in polysaccharide removal could be observed both as delignification and column fractionation proceeded. Relationships between lignin removal and polysaccharide content of the fractions ex-Porasil B were examined to determine whether any implications about the role of polysaccharides in delignification could be observed.

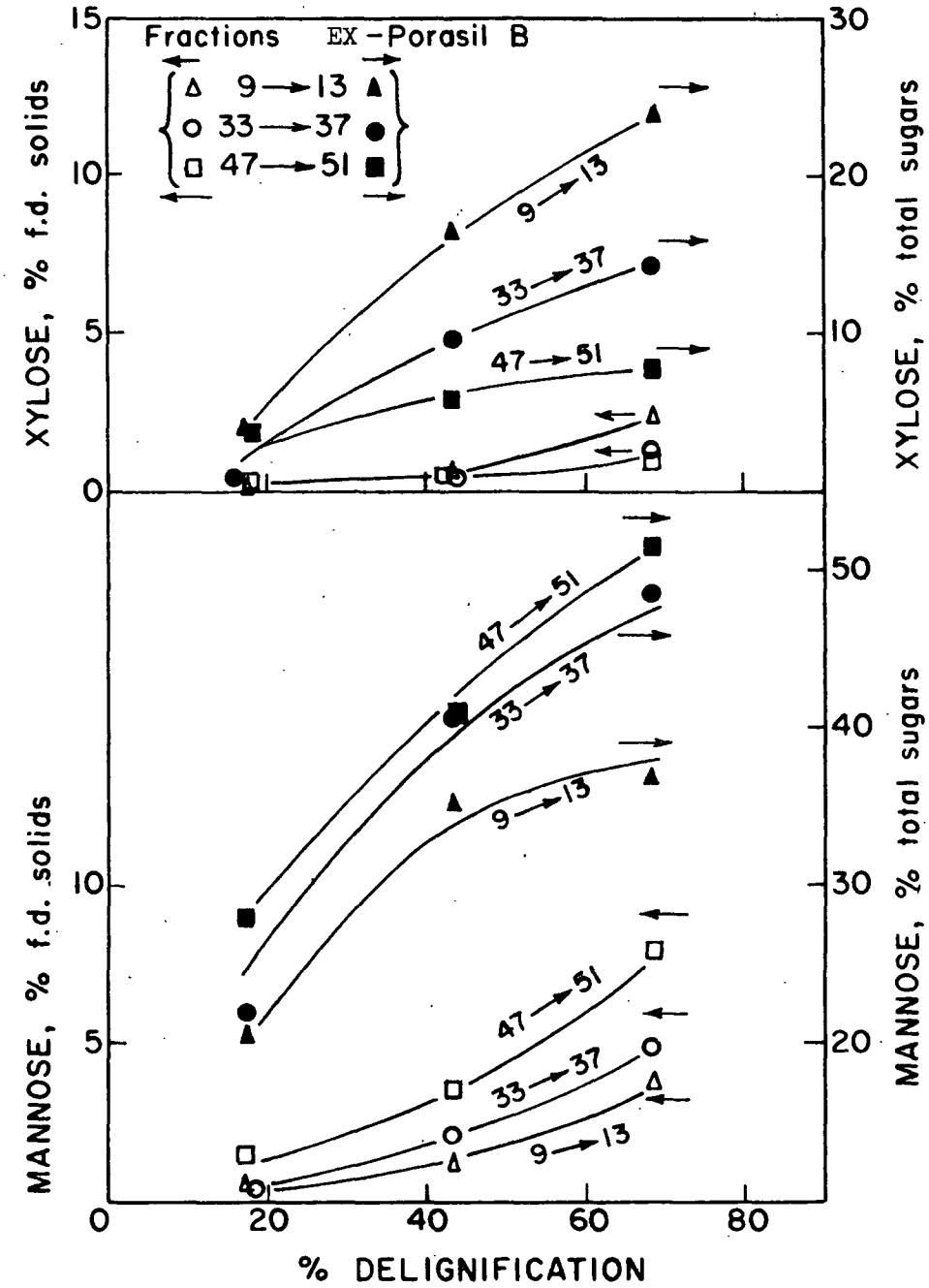

Figure 9. Comparison of Xylose and Mannose Contents of Fractions ex-Porasil B as a Percentage of Freeze-Dried Solids and Total Sugars as Delignification Proceeds (84)

SACCHARIDE DISTRIBUTIONS

Trends in polysaccharide content both as delignification and column fractionation (going from Fraction 1-65) proceeded were determined on the basis of the polysaccharide analyses as presented in Appendix V. An arithmetic average of about 8% of the freeze-dried fractions (range: 2-25%) was polysaccharide.

Trends in total sugars expressed as a percentage of freeze-dried solids were plotted as a function of degree of delignification and column fraction number as shown in Fig. 10. This shows not only that as the delignification proceeded, the relative amount of total polysaccharide being removed from the wood increased, but also, the early fractions ex-Porasil B, which represent the fractions with the largest hydrodynamic volume, always had a greater total sugar content than any other fractions for any degree of delignification. In addition, the total sugars after the early fractions (12-15) drop to a lower value and remain relatively constant for the middle fractions, and then begin to rise for the late fractions (58-61).

Trends in xylose expressed as a percentage of freeze-dried solids were plotted as a function of degree of delignification and column fraction number as shown in Fig. 11. This shows that the trends in xylose content as delignification and column fractionation proceeded were similar to those of the total sugars.

Considering Fig. 11 on the basis of xylose content versus fraction number, the extent of similarity of the xylose case in Fig. 11 with that of the total sugars in Fig. 10 tended to be a reflection of the content of xylose in the total sugars, as illustrated by the data in Table III. There is a marked similarity between the shape of the curve at later stages of delignification in Fig. 10 and 11 when xylose is by far the major sugar component. On the

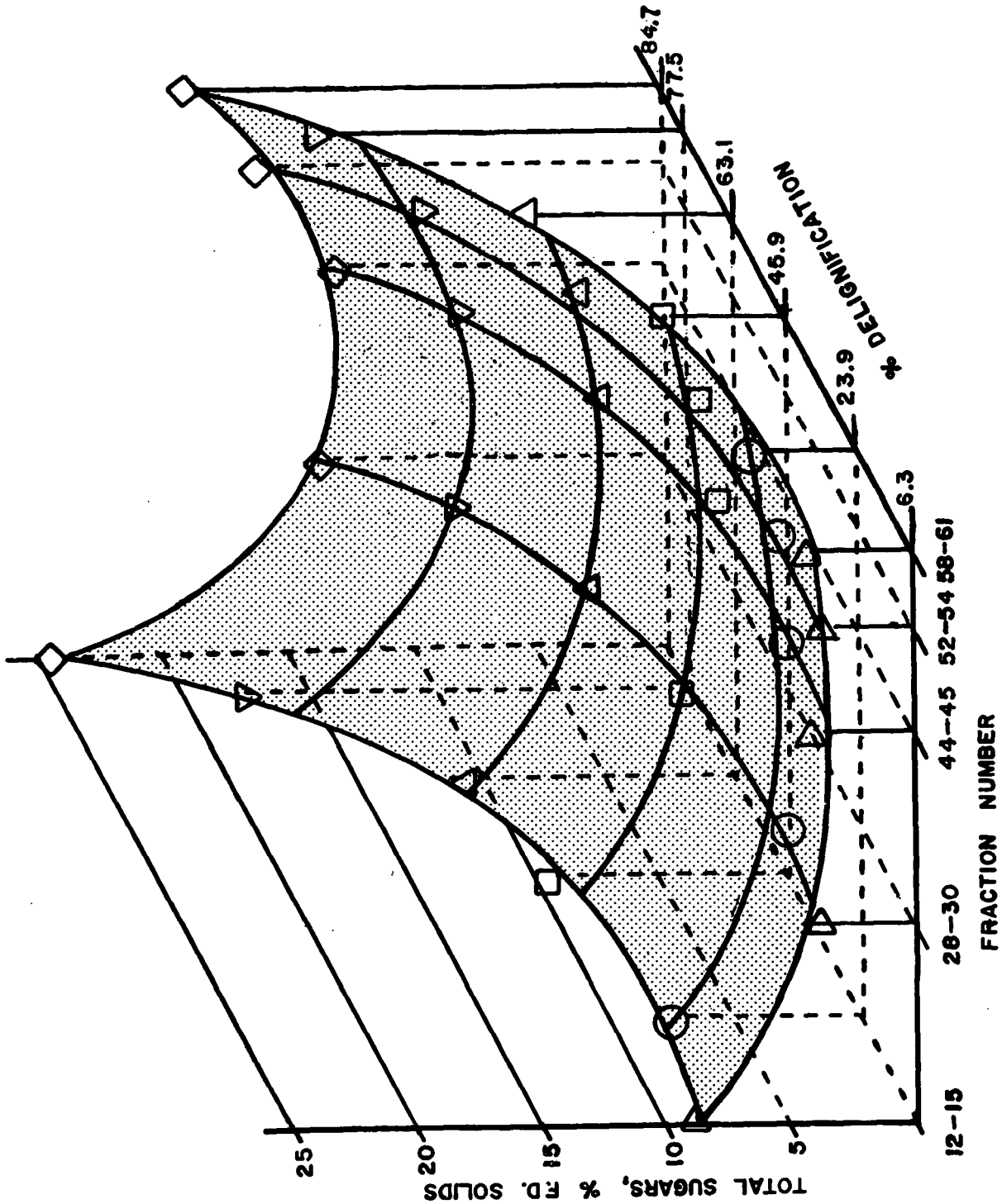

Figure 10. Total Sugars Versus % Delignification and Fraction Number

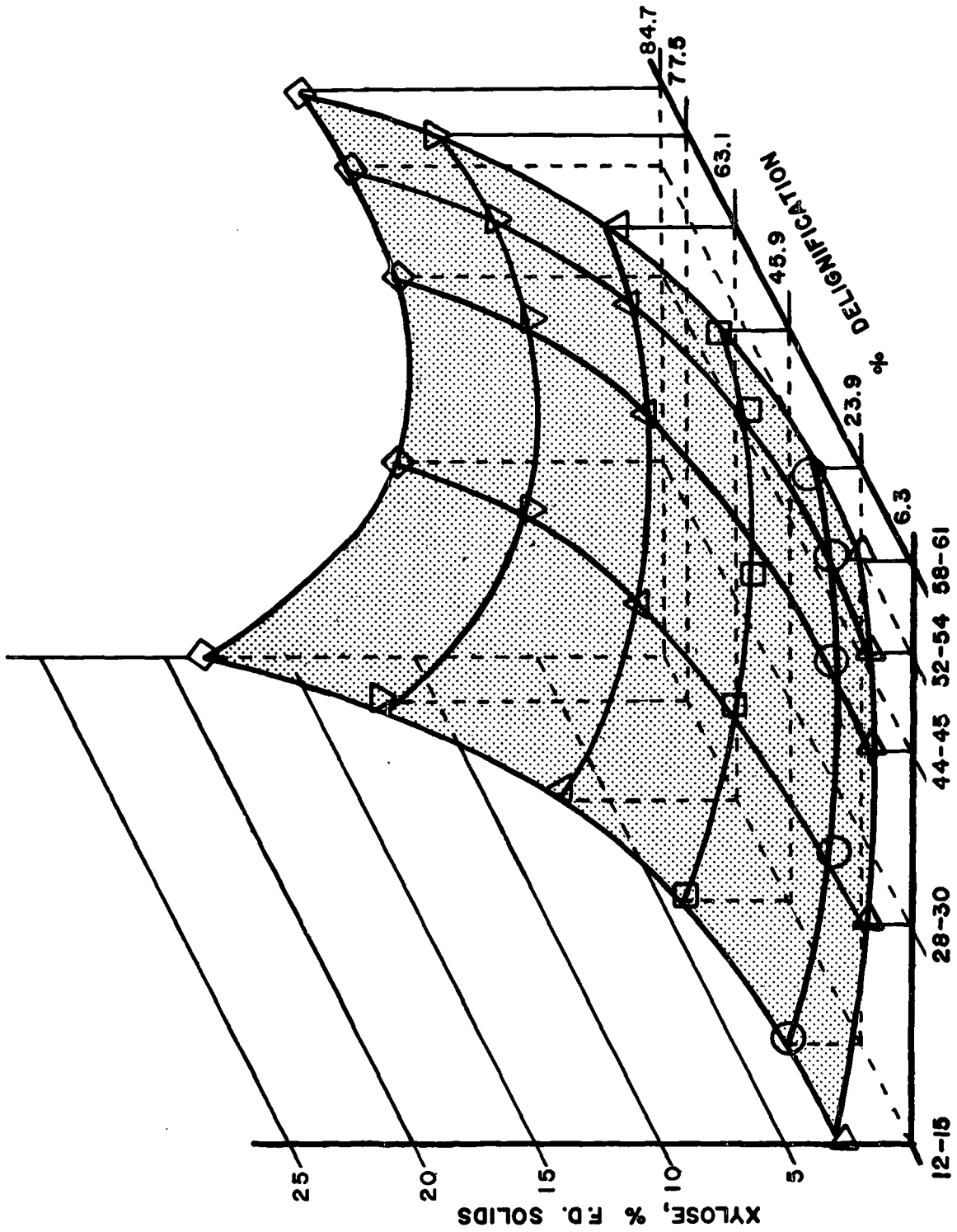

Figure 11. Xylose Versus % Delignification and Fraction Number

other hand, there is less similarity earlier in the delignification when there are significant amounts of glucose and galactose in addition to xylose.

TABLE III

MAJOR SACCHARIDES, % TOTAL SACCHARIDES

Fractions	Anhydro Sugar Units	% Delignification 6.3	23.9	45.9	63.1	77.5	84.7
12-15	Xylose (X)	31.1	43.7	44.7	68.6	72.9	76.7
	Glucose (D)	25.6	26.9	34.0	8.6	7.6	6.8
	Galactose (G)	23.3	14.9	10.6	10.5	10.6	8.8
28-30	X	42.5	48.7	56.0	64.0	69.1	79.3
	D	34.0	33.7	20.4	20.2	17.3	5.7
	G	14.2	11.2	12.7	6.7	5.4	7.3
44-45	X	42.2	53.6	55.8	69.7	77.5	83.7
	D	32.3	17.9	14.8	7.5	5.8	3.1
	G	14.9	17.9	14.8	9.4	5.8	4.6
52-54	X	45.2	59.1	55.4	76.8	79.0	80.1
	D	27.1	16.9	14.6	3.5	3.0	3.7
	G	13.6	8.4	14.6	5.2	6.0	5.6
58-61	X	40.7	51.9	64.7	61.0	70.5	79.9
	D	26.4	16.5	6.5	9.8	8.9	3.7
	G	14.2	4.7	8.6	8.5	5.5	4.8

The glucose, galactose, and arabinose contents, expressed as a percentage of the freeze-dried solids, are shown in Fig. 12. The absolute amounts of these sugars removed as delignification and column fractionation (from 1 to 65) proceeded remained relatively constant. Other sugars found by analyses were mannose and rhamnose which have only a minor influence over the total sugars and are listed in Table IV.

DISCUSSION OF RESULTS

The results of the polysaccharide analyses showed that polysaccharides were being removed with lignin during the PAA delignification of birch. A greater amount of total sugars was found as delignification proceeded for all fractions

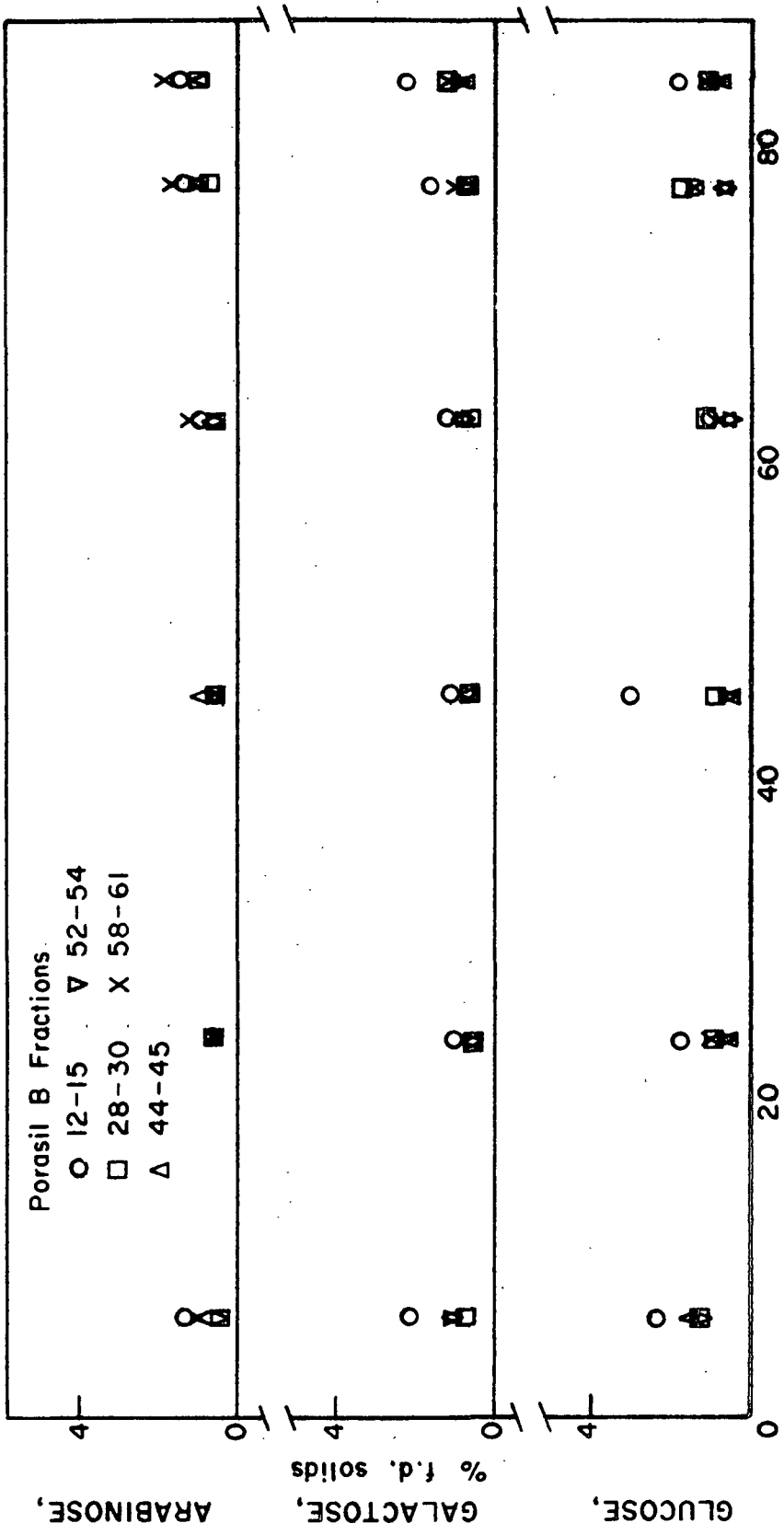

Figure 12. Glucose, Galactose, and Arabinose Content Versus % Delignification for Various Fractions

examined. This orderly trend in polysaccharide removal was analogous to the softwood case (84) described earlier. The early fractions (12-15) had the largest percentage (% freeze-dried solids) similar to the softwood case as shown in Fig. 8.

TABLE IV

MANNOSE AND RHAMNOSE, % FREEZE-DRIED SOLIDS

Fractions	Sugar	% Delignification					
		6.3	23.9	45.9	63.1	77.5	84.7
12-15	M	0.1	0.2	0.2	0.2	0.1	0.1
	R	0.5	0.3	0.3	0.3	0.3	0.5
28-30	M	0.07	0.05	0.2	0.1	0.1	0.2
	R	0.06	0.02	0.03	0.04	0.06	0.09
44-45	M	0.1	0.03	0.08	0.2	0.3	0.2
	R	0.03	0.01	0.01	0.01	0.04	0.1
52-54	M	0.2	0.06	0.1	0.2	0.3	0.6
	R	0.02	0.01	0.03	0.03	0.1	0.1
58-61	M	0.4	0.5	0.4	0.7	0.8	0.6
	R	0.02	0.04	0.04	0.1	0.2	0.2

Polysaccharide distribution as column fractionation proceeded was different for the hardwood case than the softwood. In the softwood case there was a trend toward more total sugars as the fractionation proceeded toward larger fraction numbers (smaller hydrodynamic size). The trends in hardwoods were consistent with the absorptivity data from Fractions 1 to 65. The greatest amount of total sugars was found for early fractions ex-Porasil B which had the lowest absorptivity values. The total sugars for the middle fractions drop to a lower value which corresponds to a higher absorptivity, and then begin to rise again for the late fractions with a corresponding absorptivity change.

Figure 9 showed that in the softwood case, xylose increased from less than 10% of the total sugars to just over 20% as the delignification proceeded to around 80% delignification. The early fractions (9-13) showed the greatest increase in xylose as a percentage of the total sugars.

At the same time, Fig. 9 showed an increase in mannose from around 25% of the total sugars to greater than 50% as the delignification proceeded. For mannose, the later fractions (47-51) showed the greatest increase and the early fractions the least. Since mannose had at least twice the influence as xylose over the percentage of total sugars, it was not surprising to find that the total sugars, when plotted as a function of column fraction number, increased as fraction number increased in the softwood case.

Table III showed that the xylose increased from 30 to 85% of the total sugars for the hardwood case as delignification proceeded. There was little difference between the trends in xylose as fractionation proceeded at the various stages in delignification. There was also little influence due to mannose as delignification proceeded because of the large xylose influence. Thus, due to differences in hemicellulose composition of the white birch in comparison with the loblolly pine, the polysaccharides being removed have a different influence over the hydrodynamic volume and, therefore, fractionation of the solubilized materials.

Hence, orderly trends in the composition of the polysaccharides being removed during PAA delignification of white birch were found. This was further evidence that there was organization of some type within the wood which may have an influence on the delignification mechanism.

Although only about 8% of the freeze-dried materials was saccharide material, the effect of the saccharides on the hydrodynamic size of the

solubilized materials can be quite influential, especially if the lignin and polysaccharides are bonded, because of the relatively small effective hydrodynamic specific volume of lignin as compared with polysaccharides (85).

From above results it is suggested that the composition of the hemicelluloses being removed with the lignin had an influence on the removal and subsequent fractionation of the solubilized materials. During delignification, the lignin must not only become soluble by the reactions described earlier, but it must also be small enough to be removed from the wood chip matrix. The large, bulky, and attached polysaccharides of varying amounts and compositions is likely to have a significant effect on the size and shape of the solubilized materials. These effects on the specific hydrodynamic volume can affect the ability of the solubilized materials to pass through the pores of the wood chip matrix. This agrees with the study of Kerr (87) in which a greater ease of lignin removal was found when the hemicelluloses were removed prior to delignification.

CARBOXYL CONTENT

Carboxyl groups were found in numerous studies on lignins (15,40,45,89). Under severe reaction conditions, Sarkanen and Suzuki (15) found 2.0 carboxyls per C_9 unit in their softwood PAA lignins. When milder conditions were used (40), lower values for the carboxyl content were found. A carboxyl content of the freeze-dried materials corresponding to 0.3 to 0.6 equivalent per C_9 unit was found by Albrecht and Nicholls (89) for loblolly pine PAA lignin removed under relatively mild reaction conditions. Those results compared well with 0.3 to 0.45 equivalent per C_9 unit for pine found by Ishikawa, et al. (40).

Albrecht's relatively low carboxyl content compared with that found by Sarkanen for softwoods led Albrecht to conclude that his loblolly PAA lignin

was less degraded. However, all carboxyl contents were above the 0.20 value found for solubilized pine and birch dioxane lignins (45).

The difference between 0.20 equivalent per C_9 unit and the larger values found in Albrecht's work probably relates to the differences in reaction systems. In the 0.2 case, an isolated dioxane lignin was being reacted which contrasts with the other case having lignin within the wood chip matrix. For the former, the isolated dioxane lignin only needs to undergo oxidation until it becomes water-soluble. Lignin as it exists in wood must not only become soluble but also have a hydrodynamic volume small enough to escape from the porous structure of the wood. Any bulky, attached group can hinder removal of the lignin from the wood matrix and thus result in further oxidation. This would result in either larger pores in the wood for the solubilized materials to pass out of or these materials becoming small enough to be removed from the wood structure.

In this study, carboxyl analyses were also done using the procedure given in the Experimental section. All samples were titrated as weak carboxylic acids with equivalence points found by use of the computer program in Appendix V around pH 7.5 as in the example shown in Fig. 13. Carboxyl determinations were expected to neutralize free carboxylic acids (15,20).

Results for the carboxyl analyses are presented in Table V. The carboxyl contents for the freeze-dried materials ranged from 0.5 to 0.8 equivalent per C_9 unit which corresponds with 11 to 18% of the freeze-dried materials.

These results indicate that aromatic ring degradation reactions have taken place during the delignification. Although the carboxyl contents were greater than those found in solubilized birch dioxane lignins (45), these values were lower than those noted by Sarkanen and Suzuki (15) in their PAA lignins.

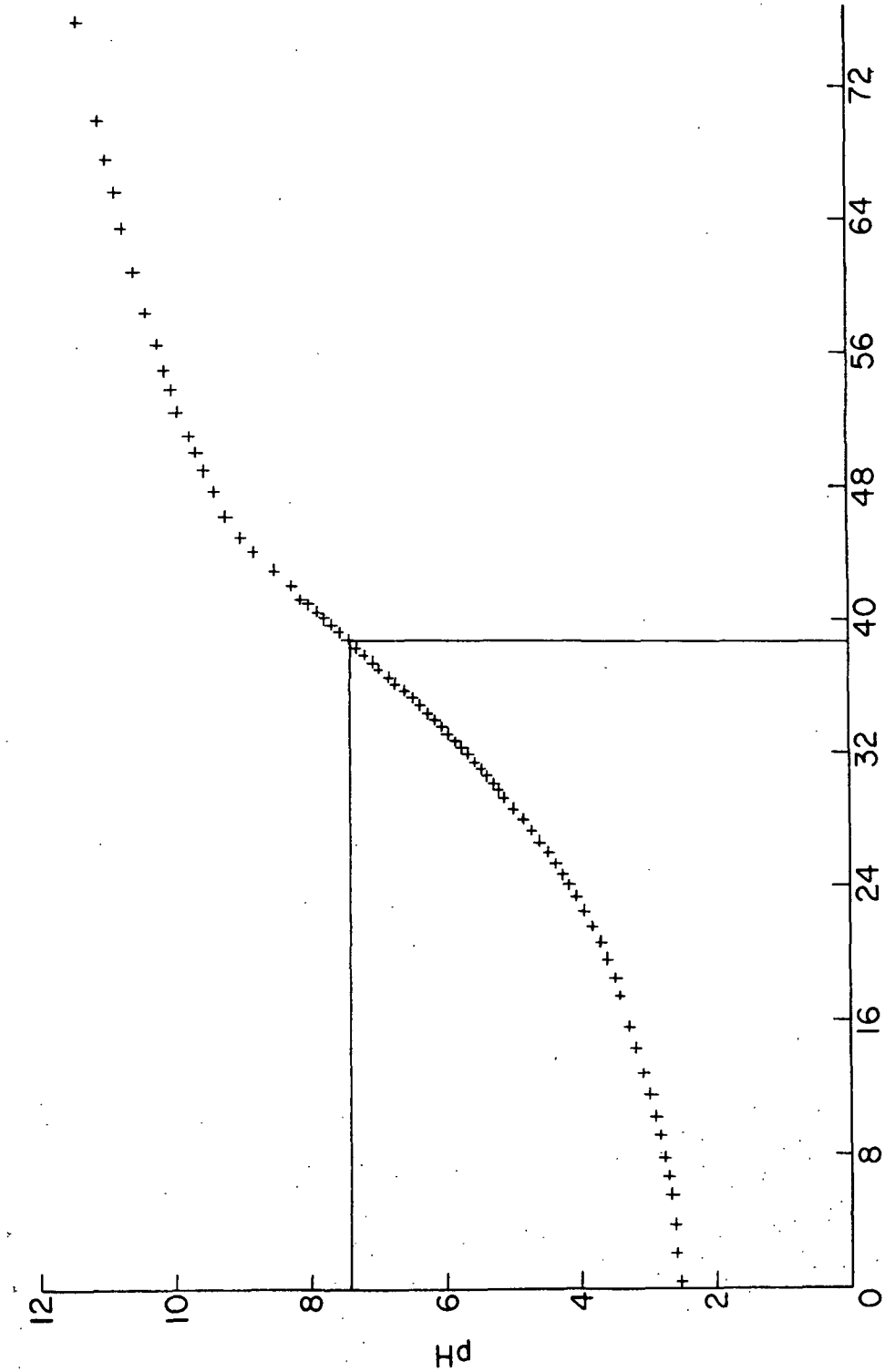

Figure 13. Potentiometric Titration Curve of Fractions 52-54 from Reaction Stage 2

TABLE V

CARBOXYL AND METHOXYL CONTENTS

Fractions	Methoxyl, OMe[b]/C9				Carboxyl, COOH/C9	
	1[a]	2	5	6	2	5
1-7	--	--	0.27	--	--	--
12-15	0.21	0.40	0.33	--	0.60	0.49
28-30	--	0.32	0.33	0.33	0.79	0.73
52-54	--	0.56	0.37	--	0.77	0.65
55-57	0.37	--	--	--	--	--

[a]Reaction stage.

[b]Assume eMW 200.

Table V shows that as delignification proceeded, a trend toward lower carboxyl contents was found for all three groups of fractions examined. As the fractionation proceeded from early (12-15) to late (52-54) fractions, the trend in carboxyl content correlated with the pattern of the absorptivities at 280 nm as shown on page 24. That is, the carboxyl content first increased and then decreased, with increasing fraction numbers, similar to the softwood case (89).

METHOXYL CONTENT

Results for the methoxyl analyses are presented in Table V. The methoxyl contents for the freeze-dried materials ranged from 3.3 to 8.7% of the freeze-dried materials. These values are considerably less than the 20 to 22% methoxyls for typical unmodified hardwood lignins (90). The middle reaction stages usually have the largest methoxyl values. This correlated with the absorptivity results. Similarly, the methoxyl results were consistent with the absorptivity results as fractionation proceeded.

INFRARED SPECTROSCOPY

INTRODUCTION

Insight into the difficult problem of identifying the molecular structure of lignin both as it exists in wood and in isolated lignin preparations was added through studies of lignin infrared spectra (91). The first complete studies of lignin infrared spectra were reported by Jones (92,93).

In studies of lignin, infrared spectra were useful in identifying the various functional groups as well as determining changes which occur in them during physical and/or chemical modifications of the lignin. Previous studies (94-135) on wood samples, pulps, model compounds, and isolated lignins have established assignments of the various bands in the infrared spectra (4000-600 cm^{-1}) of lignins as shown in Appendix VII.

Examples of studies in which various band assignments have been used are as follows: In one case, the bands assigned to p-hydroxyphenyl-, guaiacyl-, and syringyl-structural units were used to determine the relative amount of these three basic units present in natural lignins (128). In another case, lactone bands, usually found around 1730-1740 cm^{-1} in the spectra of certain lignin infrared spectra have been used to establish a possible mechanism of delignification (20,89,129). Also, there was evidence for a lignin-carbohydrate (xylan) bond in an infrared spectral study by Merewether (129). The 1510 cm^{-1} region, assigned to aromatic skeletal vibrations, has been used to follow species variations (80, 136). This band has also been used to determine the amount and nature of residual pulp lignin (100,120,125-128) and to observe the effects of PAA on the aromatic ring content of loblolly pine PAA freeze-dried lignin during delignification (89).

Infrared spectra of loblolly pine PAA lignins have shown some orderly structural differences (89). That finding, in addition to analytical data on the functional groups led to the conclusion that loblolly pine PAA lignin was not polydisperse.*

In this study, infrared spectra of white birch PAA solubilized materials have been examined to determine changes in structure as delignification and fractionation proceed.

OBSERVATIONS OF BIRCHWOOD

Two principal wood components of white birch are 4-O-methyl-glucuronoxylan and lignin. Characteristic absorption bands for xylans have been shown (94) to be located around 890 and 1735 cm^{-1} which can be observed in the infrared spectrum of O-acetyl-4-O-methyl-glucuronoxylan from white birch as indicated in Table VI and also in the infrared spectrum of white birch used in this study as shown in Fig. 14A. Characteristic absorption bands for lignins have been shown to be located around 1595 and 1505 cm^{-1} as also shown in Table VI and corresponding bands are observed in Fig. 14A.

After reaction with peroxyacetic acid to 80% yield, white birchwood gave the infrared spectrum shown in Fig. 14B which had two notable differences from the spectrum of the unreacted wood. The bands around 1595 and 1505 cm^{-1} were substantially reduced while changes in the remaining bands were less noticeable. This was consistent with significant removal of lignin by the PAA while the other wood components remained relatively unaffected.

*A polydisperse lignin as defined by Goring (85) is one in which there are rather small changes in physical or chemical properties with differences in molecular size.

TABLE VI

INFRARED ABSORPTION BANDS FOR PRINCIPAL WOOD COMPONENTS (94)

Polymer	Component Monomer	Characteristic Absorption, cm^{-1}
Cellulose I	β-D-glucose	1425; 663; 890
Xylan	Xylose	890; 1735
Glucomannan	β-D-mannose and β-D-glucose	805; 870
Lignin	Phenylpropane	1505; 1595

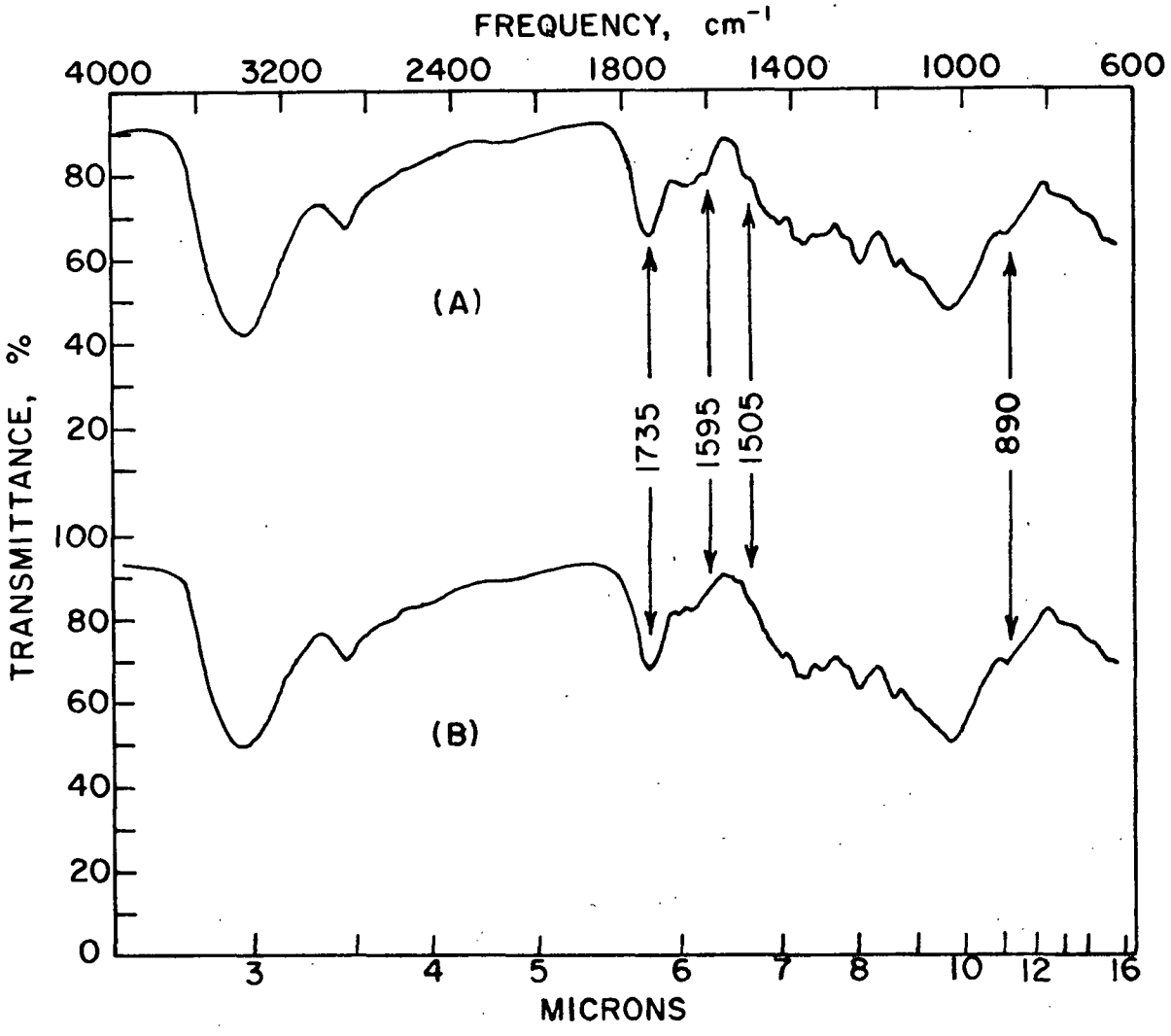

Figure 14. Infrared Spectra of Unreacted (A) and PAA Reacted (B) White Birchwood

SOLUBILIZED LIGNIN FRACTIONS EX-PORASIL B

A typical infrared spectrum of freeze-dried white birch PAA solubilized lignin is shown in Fig. 15A. All of the bands in this figure are included in the band assignments of lignins and carbohydrates found in Appendix VII. Note the band around 1510 cm^{-1} which indicates a significant amount of aromatic ring structures in the sample.

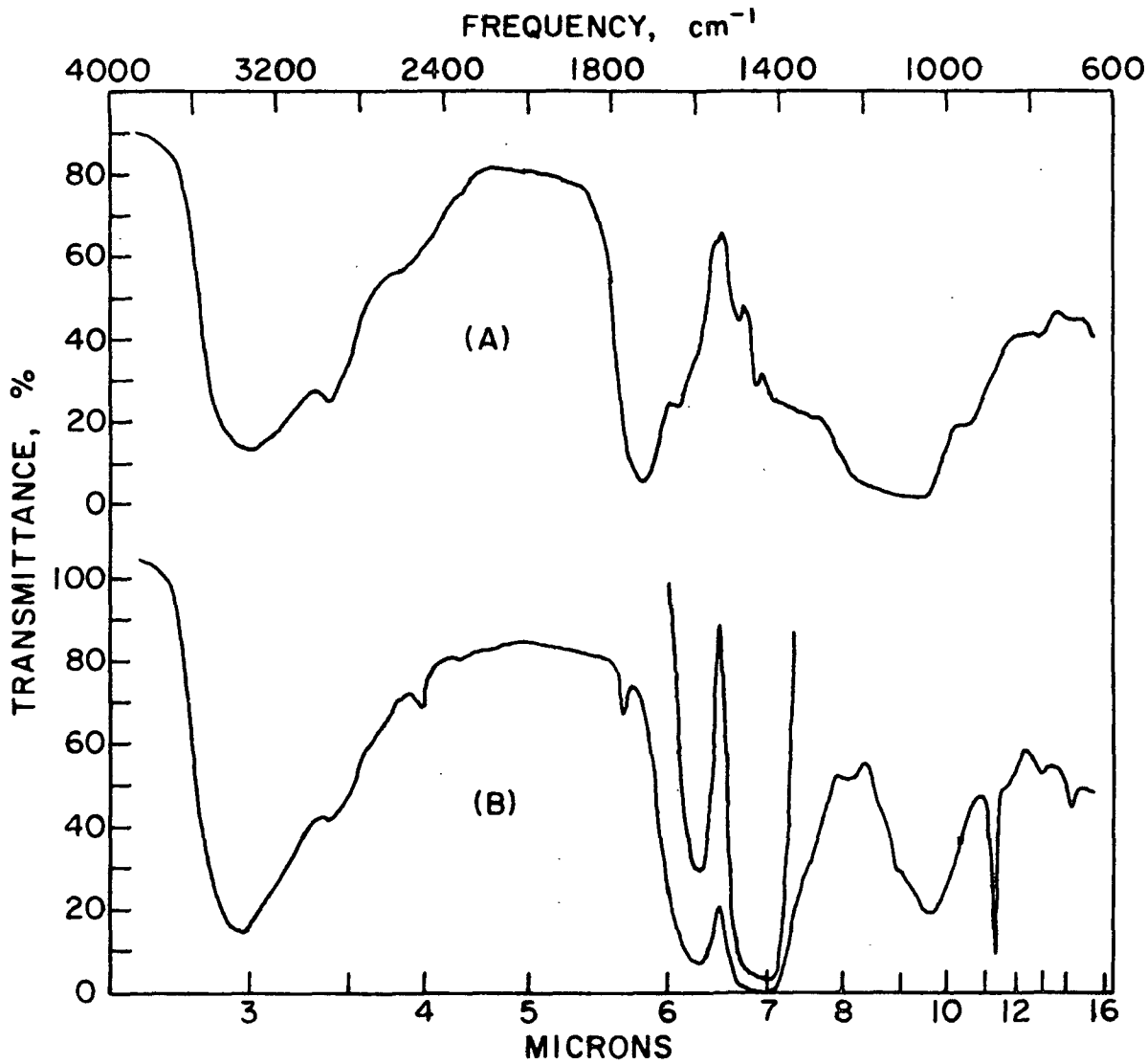

Figure 15. Infrared Spectra of PAA Freeze-Dried Fractions (12-15) from Reaction Stage 2 (A) and Its Sodium Salt (B)

One region which has received considerable study in the infrared spectra of lignins is the carbonyl region which stretches from 1780-1600 cm^{-1} (95,99,102, 106,108-111,133). For nonconjugated carboxyl groups, the carbonyl band is usually found around 1725 cm^{-1} (95,104,108,111) and larger values around 1780-1735 cm^{-1} for example can be the result of nonconjugated esters of 5-ring lactone groups (20,134).

The white birch PAA lignin has a large carbonyl band around 1725 cm^{-1} as compared to other lignins (91). A band near 1730 cm^{-1} has been assigned to the carbonyls of glucuronoxylan in previous studies (106,109). Bands in the 1730 or 1715 cm^{-1} regions may be present, but they would be covered by the large 1725 cm^{-1} band.

An infrared spectrum of the sodium salt of Fractions 12-15 from Reaction Stage 2 is shown in Fig. 15B. The carbonyl peak was considerably shifted with the appearance of two strong bands around 1590 and 1410 cm^{-1} which are characteristic of carboxylate ions (107). The 890 and 1775 cm^{-1} bands were due to sodium carbonate.

Two absorption bands at 855 and 815 cm^{-1} have been found (135) to be characteristic of guaiacyl units, while a peak around 835 cm^{-1} was characteristic of syringyl units. A dominant band around 815 cm^{-1} for white birch PAA lignin indicated the presence of more guaiacyl than syringyl units in this lignin sample probably as a result, in part, of the initial rapid removal of a methoxyl group from syringyl units as found in the sodium chlorite processes (87).

Representative infrared spectra of equal quantities of freeze-dried solubilized materials as delignification and fractionation proceeded are shown in Appendix VIII. Changes in structure which were observed both as delignification and fractionation proceeded were examined.

The 1510 cm^{-1} band which has been shown to be characteristic of the aromatic ring stretching vibrations in lignin (87,114) has been semiquantitatively used as a measure of the aromatic ring content by the approach of Marton and Sparks (120). This method gave a ΔT 1510 cm^{-1} value obtained by measuring the distance from the 1535 cm^{-1} minimum absorbance (arbitrarily set around 97% transmittance) and the 1510 cm^{-1} maximum absorbance.

Figure 16 shows this region for a number of representative freeze-dried fractions both as delignification and fractionation proceeded. A plot of the ΔT 1510 cm^{-1} values listed in Table VII as a function of percentage delignification and fraction number is shown in Fig. 17.

TABLE VII

INFRARED ΔT 1510 CM^{-1} VALUES FOR PAA FREEZE-DRIED FRACTIONS

Fractions	% Delignification					
	6.3	23.9	45.9	63.1	77.5	84.7
1-7	22.4[a]	--	--	61.6	--	39.6
12-15	28.0	56.0	66.0	66.6	65.6	58.2
28-30	39.2	60.6	59.6	62.4	66.4	59.0
48-49	37.5	68.8	64.0	--	62.8	60.0
52-54	43.0	81.0	71.2	72.0	68.4	60.2
58-61	47.6	--	73.0	--	--	55.6
62-65	31.8	--	--	59.2	--	46.0

[a]Distance in mm.

As delignification proceeded from Reaction Step 1 to 6, Fig. 17 shows there were structural changes which were observed in the 1510 cm^{-1} band. As delignification proceeded, there was an increase in aromatic ring content with a slight decrease at Reaction Step 6. The infrared results show that the greatest relative aromatic ring content was present around the middle reaction steps which was in

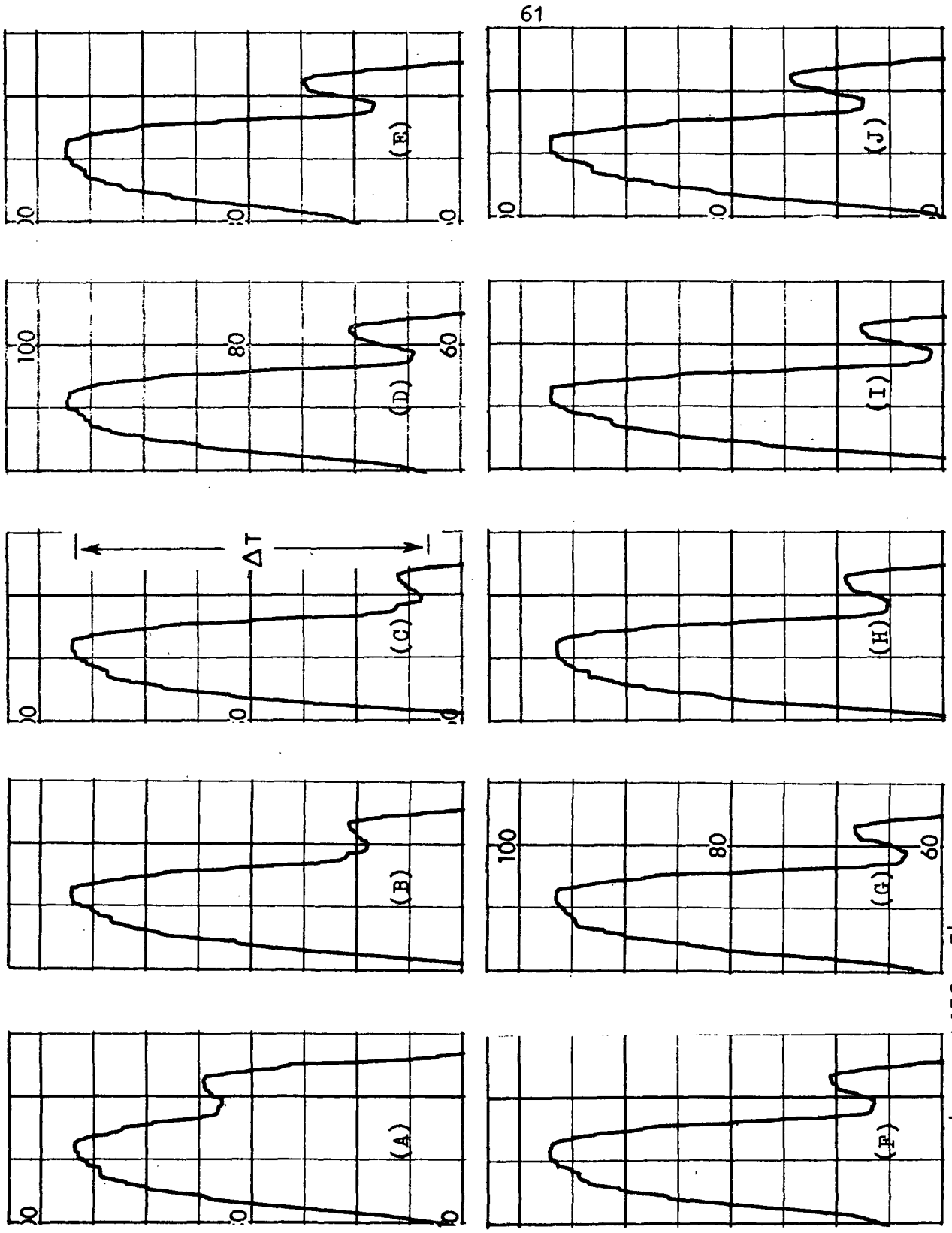

Figure 16. Infrared Spectra in the 1510 cm^{-1} Region for Fractions 12-15 from Reaction Stages 1(A), 2(B), 3(C), 5(D), and 6(E); and for Fractions 1-7(F), 12-15(G), 28-30(H), 42-43(I), and 62-65(J) from Reaction Stage 4

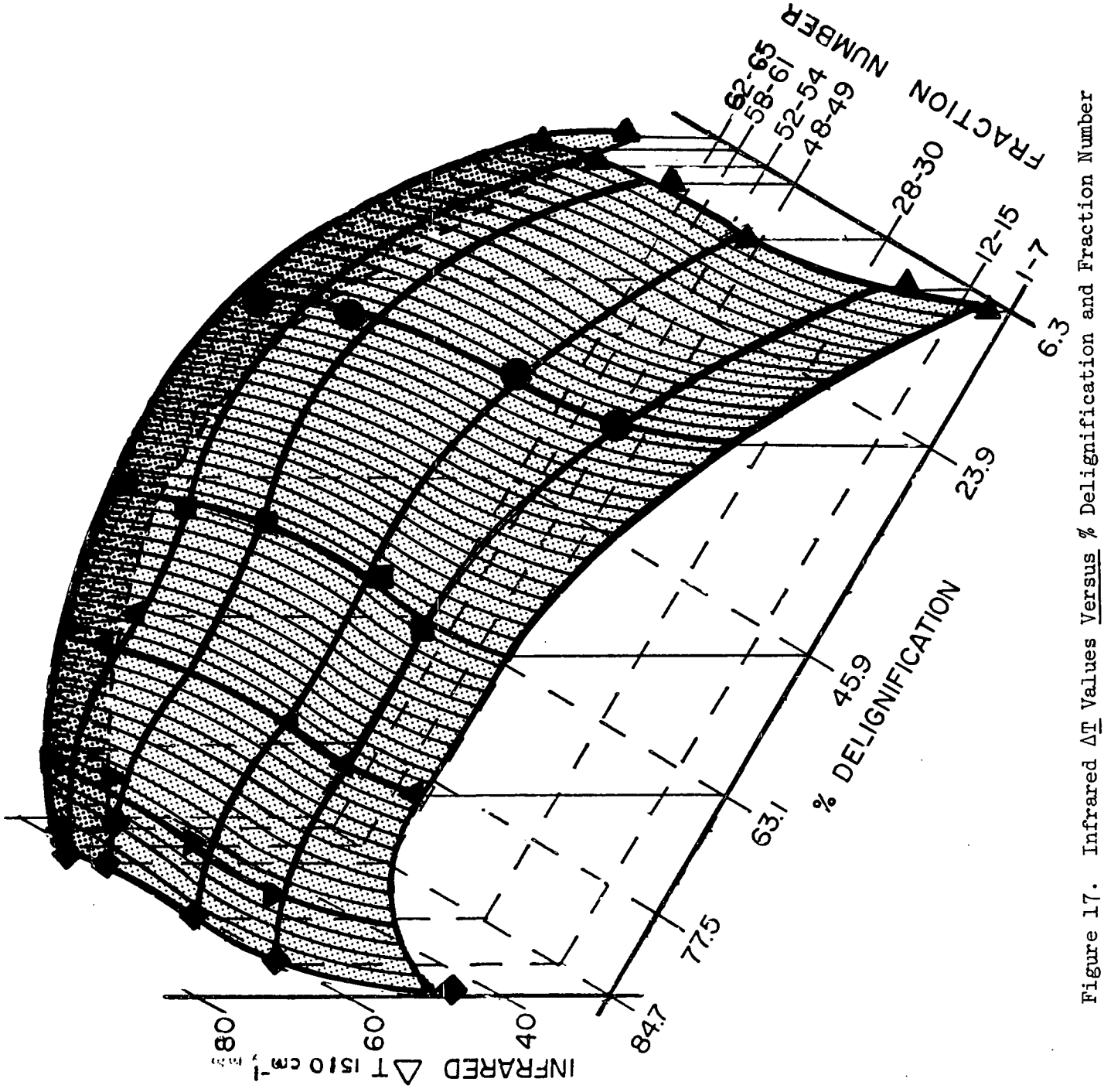

Figure 17. Infrared ΔT Values Versus % Delignification and Fraction Number

agreement with the absorptivity results presented earlier (see Normalized Absorbance Versus Fraction Number).

As fractionation proceeded from Fractions 1 to 65, Fig. 17 shows that the early fractions (1-7) had relatively less aromatic ring content than the mid-fractions. The late fractions (62-65) showed a small decrease in aromatic ring content. This result was similar to the softwood case (17) and again agreed with the absorptivity results presented earlier (p. 24). Although the method of Marton and Sparks (120) was used for determination of residual lignin in pulps and not isolated PAA lignins, the similarity of the results using their method to the absorptivity results indicated that both these methods were measuring aromatic ring content.

More distinct absorption bands were found in the 1500 to 1000 cm^{-1} region of the infrared spectra for the later reaction steps and for early fractions at any given reaction step as shown in Appendix VIII. These trends were similar to the xylose trends found in the carbohydrate results (p. 36). This increase in distinction within this region was believed to be possibly due to the xylose content of the fractions examined. A spectrum of O-acetyl-4-O-methyl-glucurono-xylan and a spectrum from Reaction Step 6, Fractions 12-15, with the greatest distinction in absorption bands in the 1500 to 1000 cm^{-1} region, as shown in Fig. 18A and 18B were found to be quite similar. Thus, the infrared results were consistent with the carbohydrate results and they showed how orderly trends in xylose content were reflected in orderly trends in the infrared spectra of those samples examined.

The infrared results indicate that the PAA freeze-dried fractions ex-Porasil were not all chemically uniform in structure. There were also orderly trends in the changes of chemical structure as delignification and fractionation proceeded which were in agreement with the previously found absorptivity data.

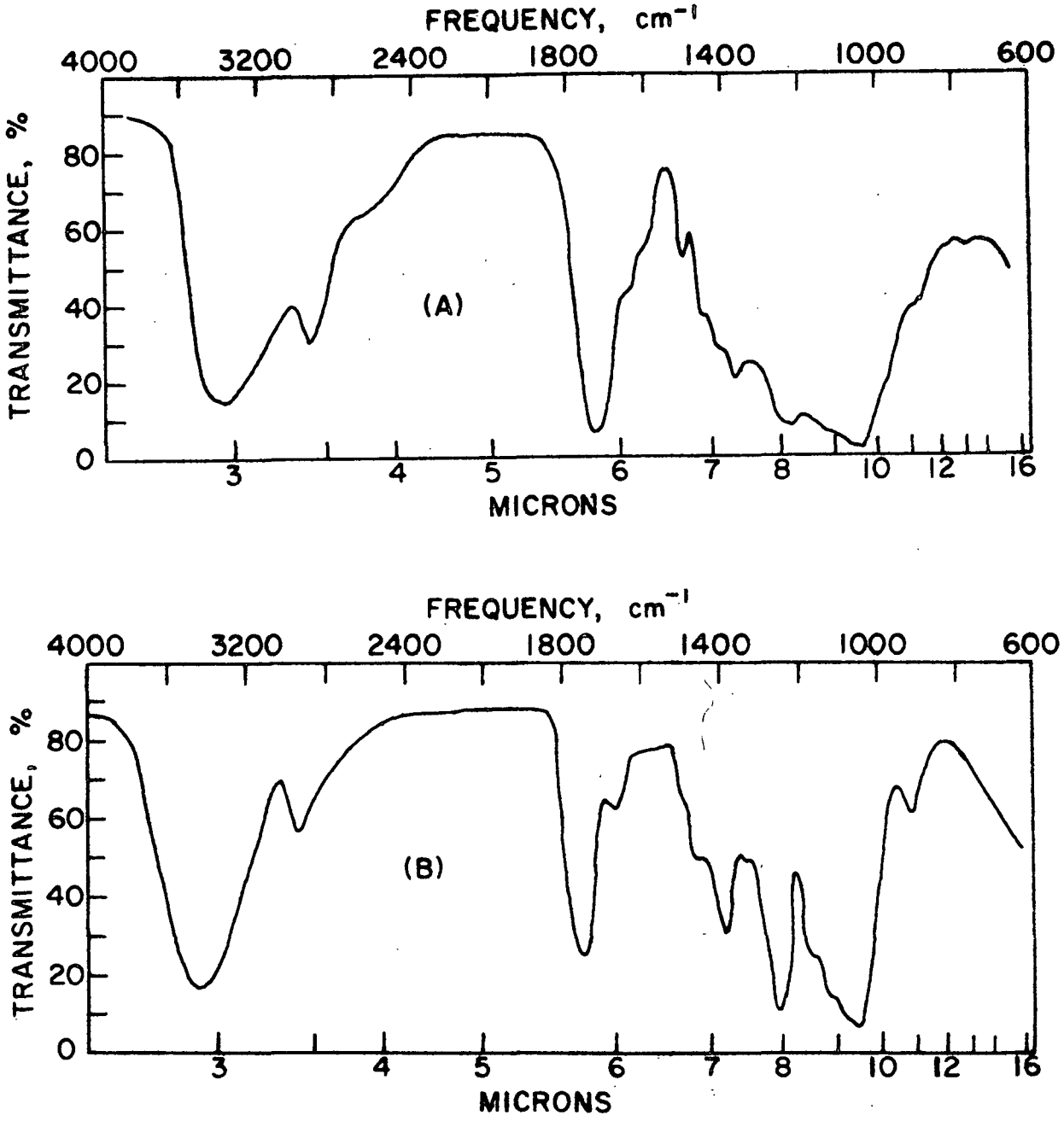

Figure 18. Infrared Spectra of Fractions 12-15 from Reaction Stage 6 (A); O-Acetyl-4-O-Methylglucuronoxylan from White Birch (B) (94)

PROTON MAGNETIC RESONANCE

INTRODUCTION

Proton magnetic resonance (PMR) spectra of lignins are difficult to examine because lignin is a heterogeneous mixture of many different molecules most of which have complex molecular structures. Despite the difficulties in examining the PMR spectra of lignins, the signals in lignin spectra have been interpreted in terms of known chemical shifts from protons in various known environments and model compound studies. PMR studies of lignins have been carried out by a number of workers (137) using those previous studies to obtain structural information about lignin.

PMR was first applied to lignin by Ludwig, et al. (138,139), who related the chemical shifts of lignin samples to the chemical shifts of a number of lignin model compounds. Although broad absorption bands were present in lignin PMR spectra, certain ranges of chemical shifts were assigned to certain structural portions of the lignin molecules as summarized in Appendix IX. Semiquantitative estimates of protons in certain chemical shift ranges were then used for structural determinations.

For example, in one study (140), the effect of ozonization on the aromatic rings was semiquantitatively studied by examining changes which occurred in the aromatic region of the PMR spectrum as ozonization proceeded. The decrease in percentage of aromatic protons can be seen in the results of that study presented in Fig. 19.

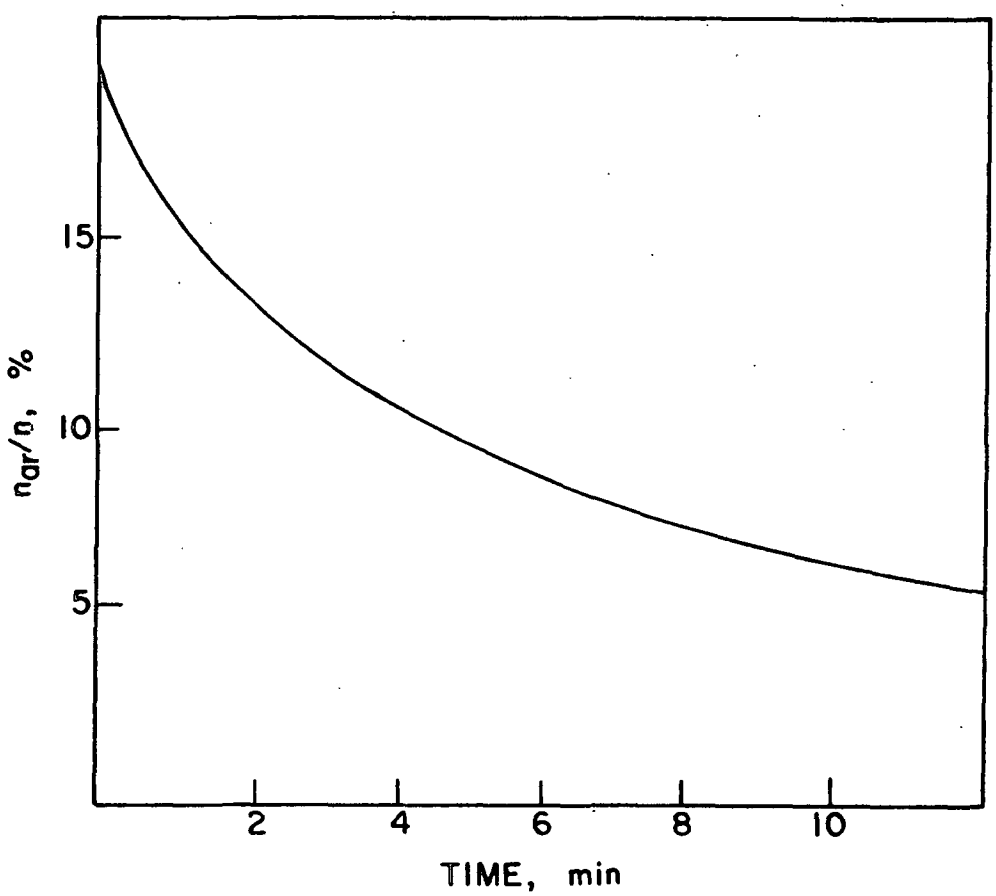

Figure 19. Percentage of Aromatic Protons on Ozonization (140)

WHITE BIRCH PAA SOLUBILIZED MATERIALS

In this study, the PMR spectra of white birch PAA solubilized materials were examined to determine what structural information could be gained from these spectra. A typical PMR spectrum for a sample of freeze-dried white birch PAA solubilized materials from Reaction Stage 4, Fractions 46-47, is shown in Fig. 20A. Structural interpretations deduced from the signals in this spectrum were based on studies of model compounds and isolated lignins as summarized in Appendix IX.

Absence of a signal in the region between δ = 9.75 and 12.00 indicated that there were no detectable free carboxylic or aldehydic protons. Aromatic protons were present in the sample as indicated by the signal around δ = 6.7. Vinyl

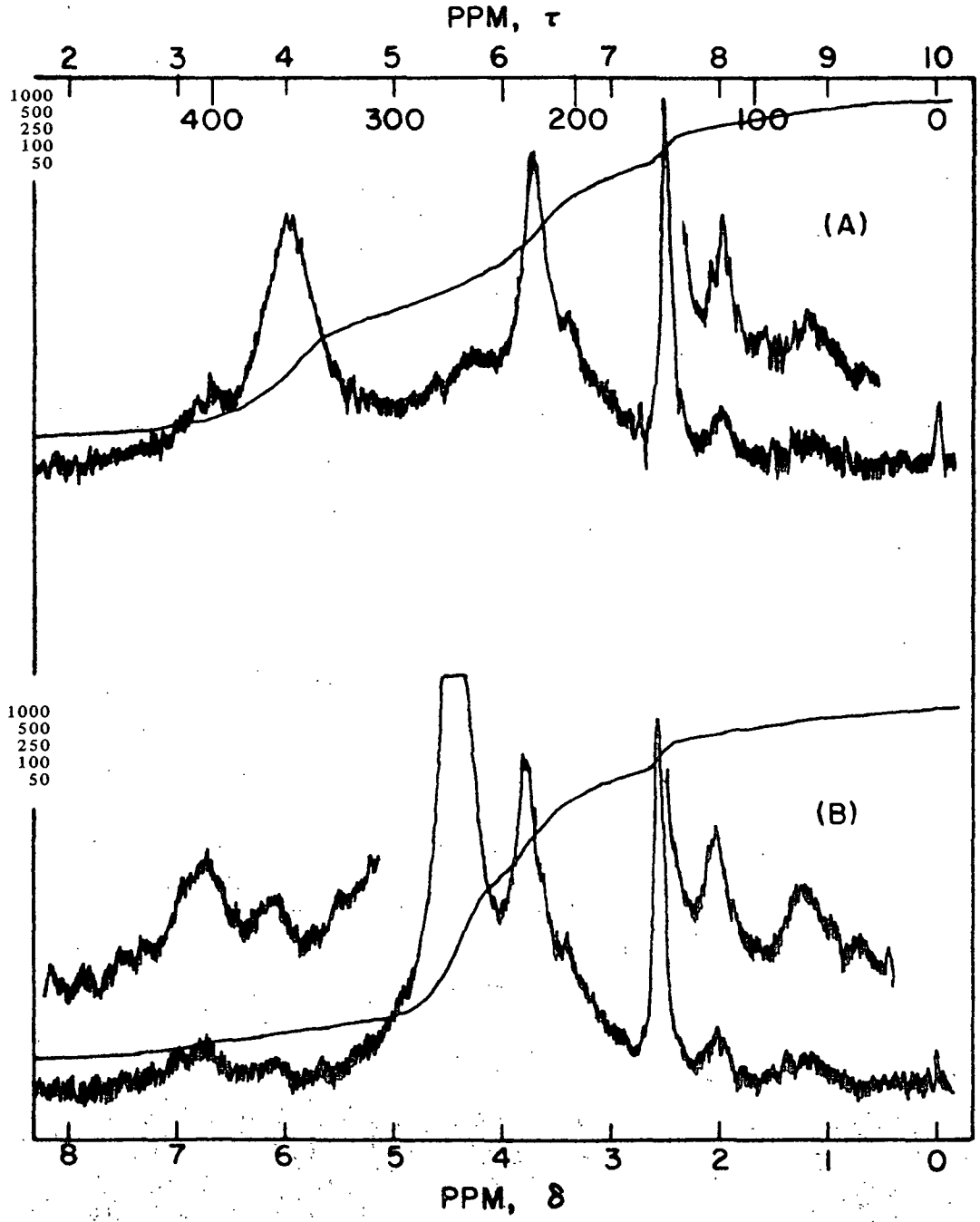

Figure 20. NMR Spectra of Fractions 46-47 from Reaction Stage 4, Before (A) and After (B) D_2O Addition

protons also could possibly contribute to this region. The signal around δ = 6.0 has been shown by deuterium exchange to be due mostly to hydroxyl protons.

Signals in the δ = 4.0 to 6.25 region have been attributed to benzylic protons, especially those with an oxygen attached to the α-carbon. Carbohydrate protons can also contribute in this region but their contribution in most cases would be minor because of their relatively small quantities. The signal around δ = 3.71 has been attributed to aromatic methoxyl protons. Signals in the δ = 2.7 to 3.6 region have been attributed to benzylic protons with no oxygen attached to the α-carbon. The solvent, DMSO-$\underline{d}_6$, has a signal around δ = 2.5. Aliphatic acetoxyl protons had a signal around δ = 2.0, and highly shielded aliphatic protons result in signals below δ = 1.75.

Aromatic hydroxyls for model compounds have signals which were located between δ = 4.94 and 6.87, but the large size of the hydroxyl signal in the PMR of the white birch PAA lignin indicated the presence of more than just aromatic hydroxyls. Aliphatic hydroxyl signals have been located between δ = 2.53 and 4.05 while carboxylic and aldehydic hydroxyl signals have been located between δ = 9.75 and 12.00. The actual location of the hydroxyl signal of a sample when several types of hydroxyls are present can be at an average of the individual signals in these systems. This averaging effect is aided by the presence of acid hydroxyls. Figure 21 shows some of the variation in the hydroxyl signal encountered in the freeze-dried samples. This variation indicated that these materials were not all chemically alike; however, this variability makes semiquantitative determinations, especially in the aromatic region, impossible.

A small amount of D_2O was added to the above samples in an attempt to move the hydroxyl signal out of the aromatic region. The broadness of the HDO signal, as shown in Fig. 20B, still made semiquantitative determinations in the aromatic region impossible.

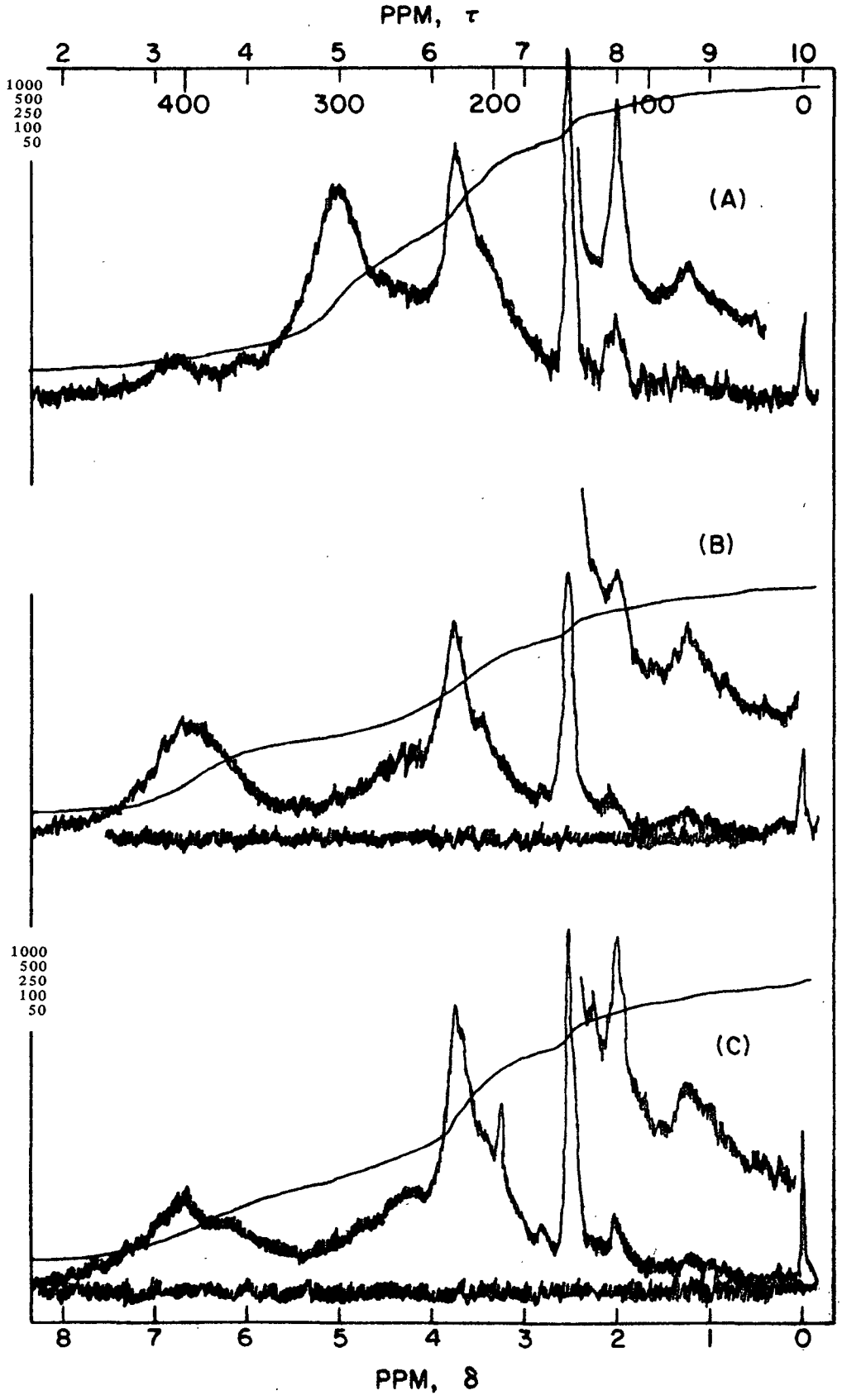

Figure 21. NMR Spectra of Fractions 8-11 (A), 37-39 (B), and 55-57 (C) from Reaction Stage 4

An attempt to isolate the aromatic signal by shifting the hydroxyl peak through variation in temperature was made. The effect of temperature was to either broaden or sharpen the spectral peaks, but little movement in peaks was observed. At cold temperatures (frozen) the signals were very broad and when the samples were heated to higher temperatures, the signals became more distinct as shown in Fig. 22. Aromatic signals at cold temperatures could hardly be observed, but at high temperatures they could easily be found. However, the broadness of the hydroxyl signal still extended into the aromatic region, making semiquantitative determinations in that region impossible.

Interference from the broad hydroxyl signal was minimized by replacing nearly all of the hydroxyl protons with deuterons as described in the Experimental section. Addition of D_2O now moved most of the HDO signal out of the aromatic region as shown in Fig. 23. Since not all of the hydroxyl protons were replaced by deuterons, the relative aromatic content determinations of the freeze-dried materials were at best inaccurate. Even if the hydroxyl signal could be removed from the spectrum, its variation in size and location would give inaccurate semiquantitative determinations of the relative aromatic content when absent. Thus, the complexity of the spectra, although indicating changes in chemical structure of the PAA solubilized materials, make semiquantitative determinations impossible.

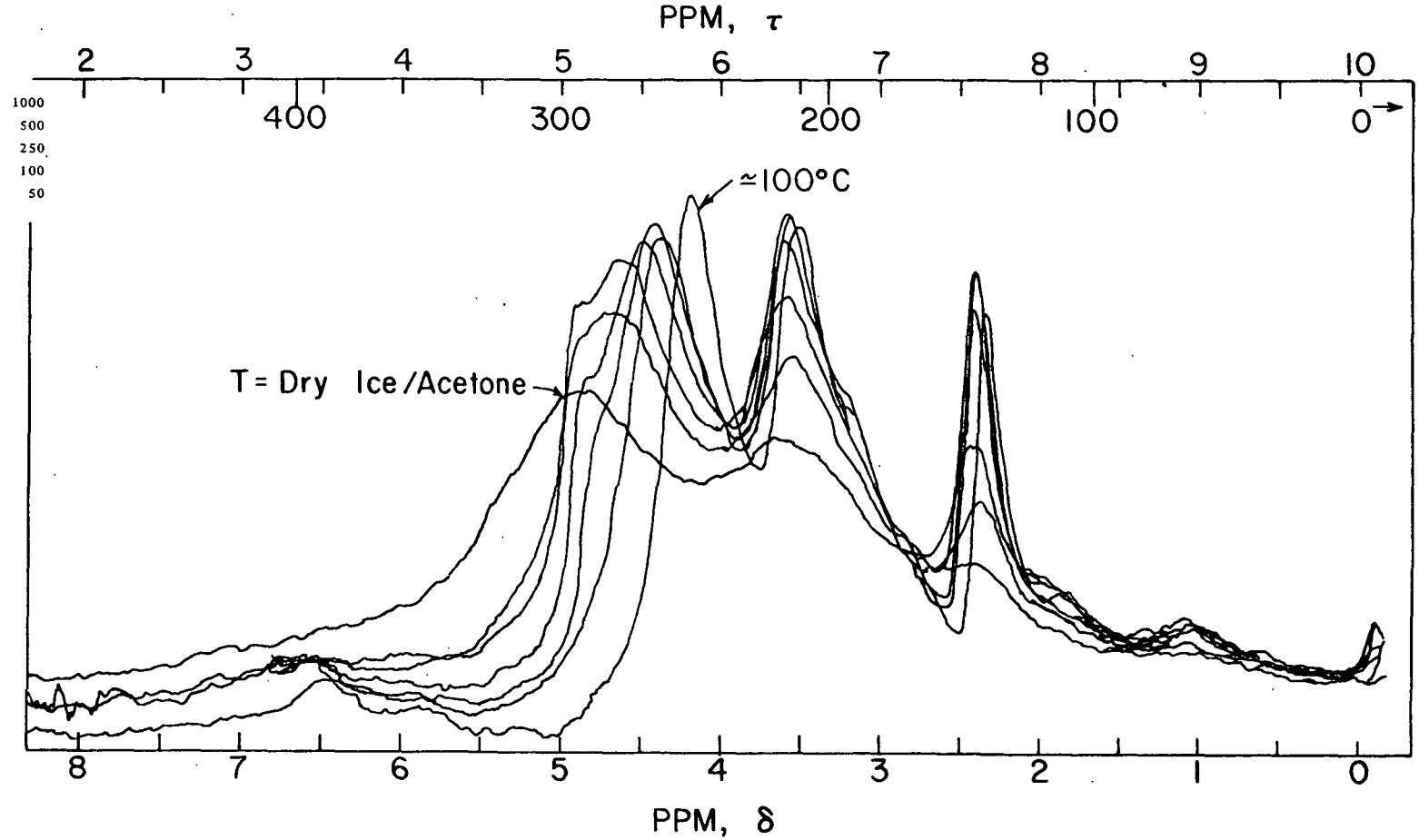

Figure 22. NMR Spectra of Fractions 55-57 from Reaction Stage 2 at Various Temperatures

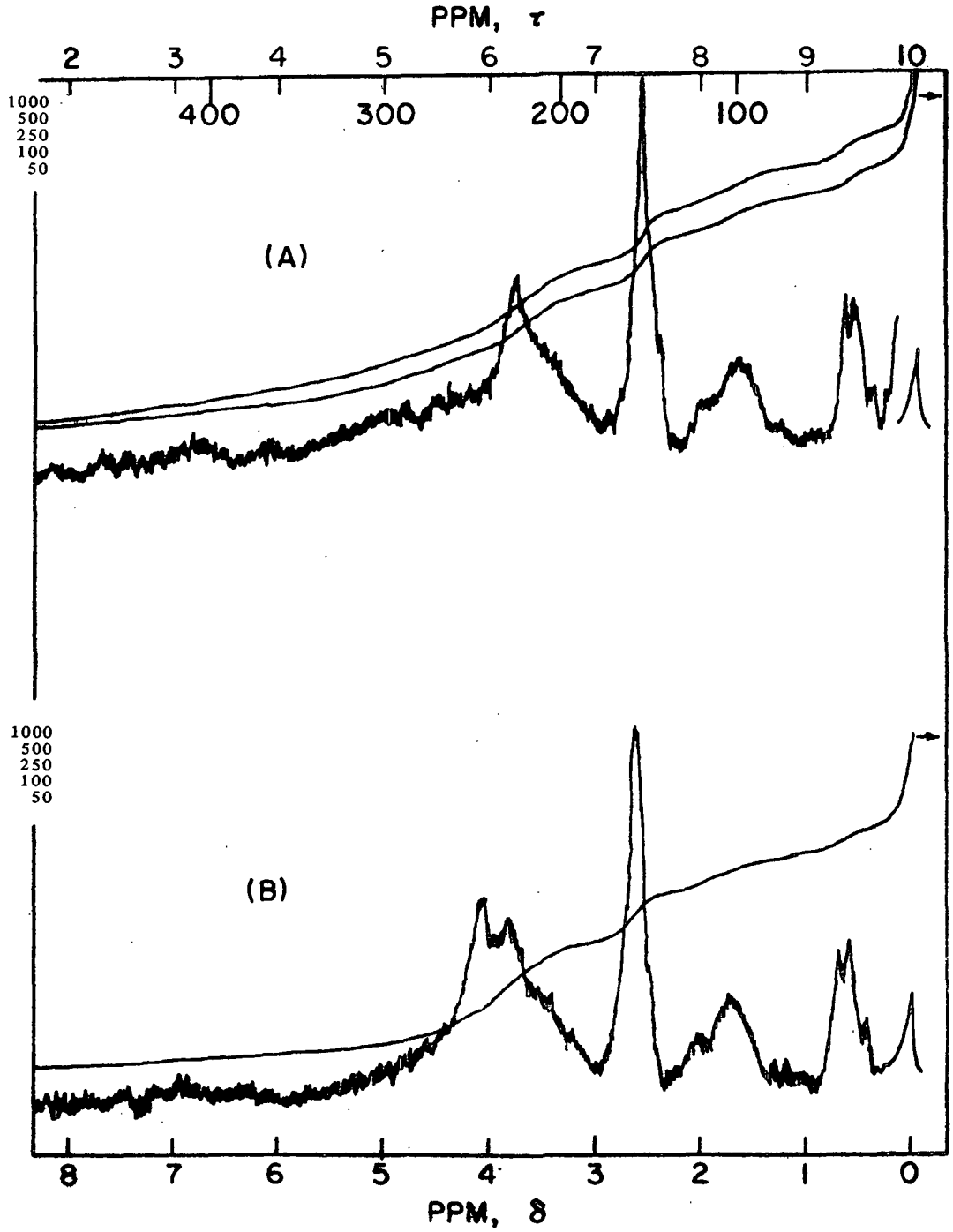

Figure 23. NMR Spectra of Fractions 8-11 from Reaction Stage 4 After the Hydroxyl Hydrogens were Replaced by Deuterons, Both Before (A) and After (B) D_2O Addition

EVIDENCE FOR A LIGNIN-CARBOHYDRATE BOND

PAPER ELECTROPHORESIS

It has been known since the 1940's that when some or all of the components of a mixture are ionizable, a separation of these components may be obtained when the mixture in solution is subjected to an electric field (141). In this process known as electrophoresis, the mixture is applied as a spot or as a streak of solution on a supporting medium. This can be filter paper, cellulose acetate membrane, starch gel, agar gel, glass fiber sheets, or other less commonly used supports.

When subjected to an electric field, each ion will migrate to one pole or the other, depending on the sign of the charge it carries. After separation, the components of the mixture are located by staining, chemical reactions, or optical means.

Two features which are most relevant to the electrophoretic mobility of an ion are the following:

(1) the characteristics of the ion itself, including the sign and the magnitude of its charge, its physical size (hydrodynamic volume), and its geometrical configuration, and

(2) the characteristics of the environment including pH, temperature, ionic strength, viscosity, pore size, weight ratio of paper, etc.

Since the environmental characteristics described above have been kept constant in this study, the characteristics of the ions themselves will determine their electrophoretic mobilities.

The freeze-dried PAA solubilized materials from Fractions 1-65 have been shown to contain both lignin and carbohydrate materials. For any given fraction ex-Porasil, the hydrodynamic volume of the lignin and carbohydrate materials

should be the same if the lignin and carbohydrate are not physically associated in some way. Thus, physical size differences between the lignin and carbohydrate materials are expected to have little effect on the electrophoretic separation of these materials.

Previous studies (142) have indicated that the lignin portion of the solubilized materials has been degraded, in part, to muconic acid systems and related lactones. The carbohydrate of wood is known (1,4,6,143-145) to be oxidized less readily by PAA than the lignin, since, for example, keto, aldehyde, and carboxyl contents of a PAA-reacted holocellulose (143) remained nearly unchanged during a reaction run under quite severe reaction conditions. Thus, the lignin in the freeze-dried materials is likely to have a different charge than the carbohydrate which would favor a separation by paper electrophoresis of any lignin and carbohydrate components of the PAA solubilized materials, if the lignin is not chemically associated with the carbohydrate in some way.

Past attempts (79,146-150) at this type of separation on different types of lignin-carbohydrate materials have been made, but a lignin component could not be isolated free of carbohydrates. Lindgren (146) was not able to isolate a spruce lignin free of carbohydrate by paper electrophoresis using glass-fiber sheets and NaOH buffer. Simonson (79,149) found the same result for birch lignin samples and thus assumed a lignin carbohydrate bond to be present in birch.

When Bolker and Wang (150) used the procedures of Lindgren given above in an attempt to separate white birch Bjorkman lignin samples, one spot resulted on their electrophoretograms. A control experiment showed that xylan separated clearly from birch dioxane lignin and gave two spots. On hydrolysis of the lignin-carbohydrate sample, they found two spots, and the original spot was no longer detectable. Thus, Bolker and Wang were more convinced that there was a lignin carbohydrate bond in white birch. An attempt in this study to separate

any carbohydrate from the lignin components in fractions ex-Porasil of white birch PAA solubilized materials by paper electrophoresis is described in the following section.

PAPER ELECTROPHORESIS OF FRACTIONS EX-PORASIL B

The result for the paper electrophoresis of freeze-dried Fractions 45-50 for the combined Reaction Stages 1-6 containing about 6% carbohydrate is shown in Fig. 24. The molecules remained as one spot which has been shown by staining with α-naphthol reagent and ultraviolet absorbance at 280 nm to contain both carbohydrate and lignin, respectively. Failure to separate any lignin and carbohydrate components implies that either these materials are chemically associated in some way or they have the same electrophoretic mobilities (charge), by coincidence.

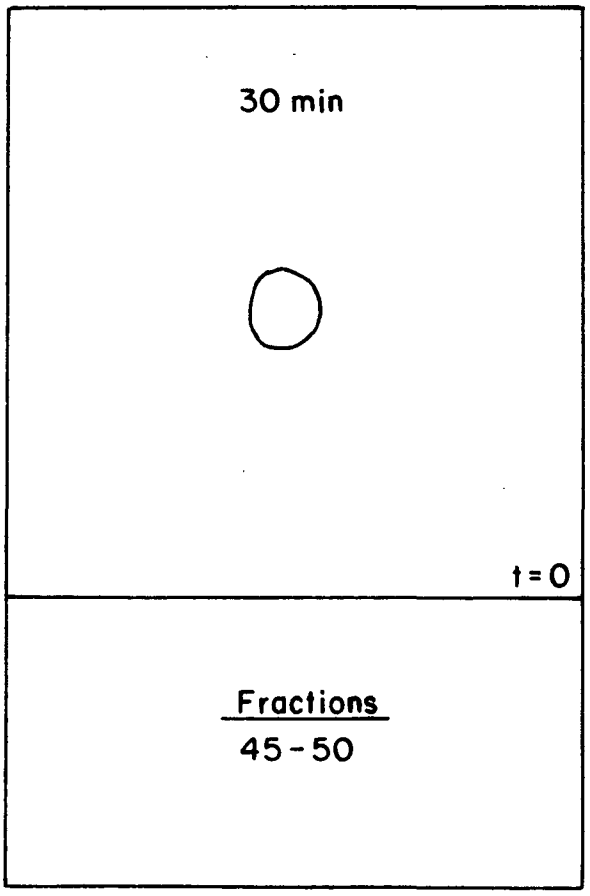

Figure 24. Electrophoretogram of Fractions 45-50 Ex-Porasil B

If the lignin and carbohydrate are separate components, and they came off the Porasil B column at the same time, they may be assumed to have the same hydrodynamic volume. The paper electrophoresis of these components was carried out at a much higher pH than for the column separation. Assuming the hydrodynamic volume change due to the change in pH is only small or in the same direction for both components, the conclusion drawn above remains unchanged.

This situation is also encountered in the results for the paper electrophoresis of two additional groups of fractions shown in Fig. 25. These groups of fractions represent late, mid, and early materials ex-Porasil. Upon paper electrophoresis the population in each of these cases remained as one spot containing lignin and carbohydrate. Failure to separate any lignin from carbohydrate again implies that either these materials are chemically associated or they have the same electrophoretic mobility for each case. As the number of cases is increased, the probability of the second argument being applicable decreases.

Since, as discussed above, the lignin portion of the solubilized materials has been shown to be degraded in part to muconic acids and lactones by PAA, while the carbohydrates do not change significantly, the lignin and carbohydrate parts probably do not have the same charge. The lignin is probably more charged and thus more mobile than the carbohydrate. If the charges are significantly different, the result of one spot thus indicates that the lignin and carbohydrate are likely to be chemically associated.

To determine whether this physical association between the lignin and carbohydrate materials is entanglement, electrophoretic separations of mixtures of hemicelluloses with the freeze-dried materials were examined. The results for the paper electrophoresis of a (50-50) mixture of the sample described

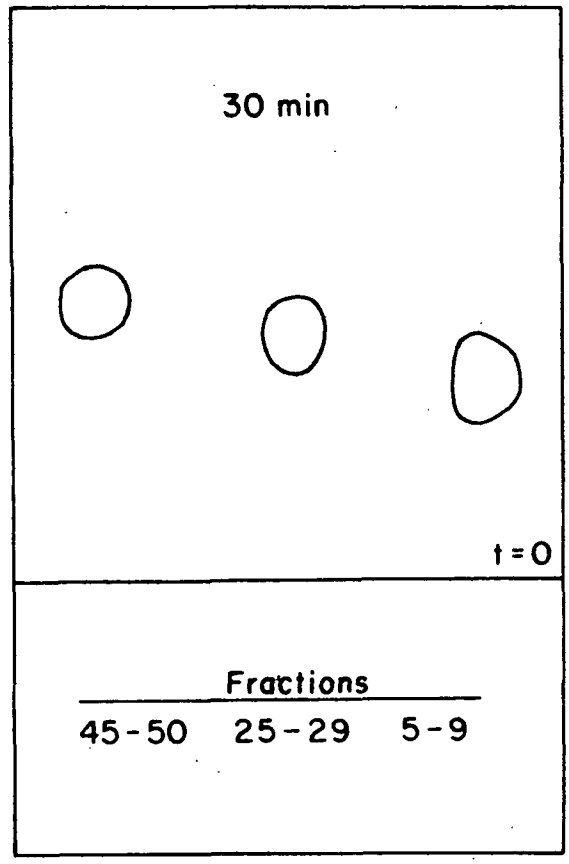

Figure 25. Electrophoretograms of Fractions Ex-Porasil B from Composite Liquor

above with sapote gum* in one case and with elm xylan in another are shown in Fig. 26. For the mixture with sapote gum (Fig. 26A) a separation can easily be obtained. This finding demonstrates that a hemicellulose can be separated from the freeze-dried materials ex-Porasil and that lignin and carbohydrate materials are certainly not always physically associated by entanglement, if ever. However, for the mixture with elm xylan (Fig. 26B) the separation is not quite as dramatic. The same trends occur, but the electrophoretic mobility of the elm xylan is so close to that of the fractions examined that the results for this test mixture are inconclusive. The differences in hydrodynamic size

*Sapote gum is a polysaccharide which consists of residues of uronic acid, D-xylose, and L-arabinose and of methyl groups in the approximate ratio of 1.0:2.2:1.0:0.58.

and in the amount of charge between the elm xylan hemicellulose and the PAA fractions is not known and could possibly lead to this inconclusive result.

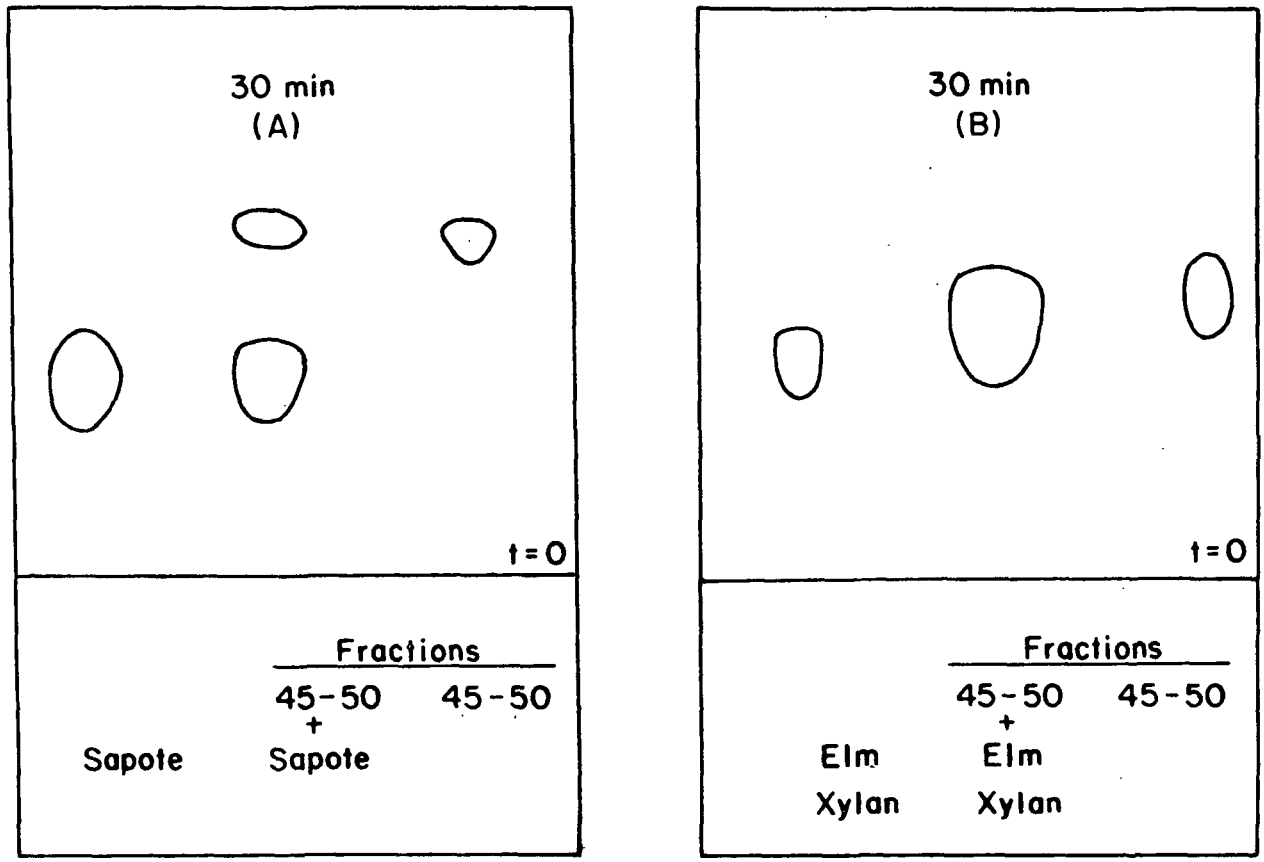

Figure 26. Electrophoretograms of Fractions 45-50 Ex-Porasil B Mixed with Sapote Gum in One Case (A) and Elm Xylan in the Other (B)

The result for the paper electrophoresis of freeze-dried Fractions 10-14 from the combined Reaction Steps 1-6 is shown in Fig. 27. This figure also shows the results of a paper electrophoretic separation of the above sample mixed with sapote gum in the presence of PAA under normal reaction conditions (see Preliminary Experiments and Selectivity). The separation of the sapote gum from the PAA solubilized materials remains unchanged when PAA is present under normal reaction conditions. This result indicates that the possibility of free-radical condensation reactions occurring during PAA delignification is not a significant factor in this work.

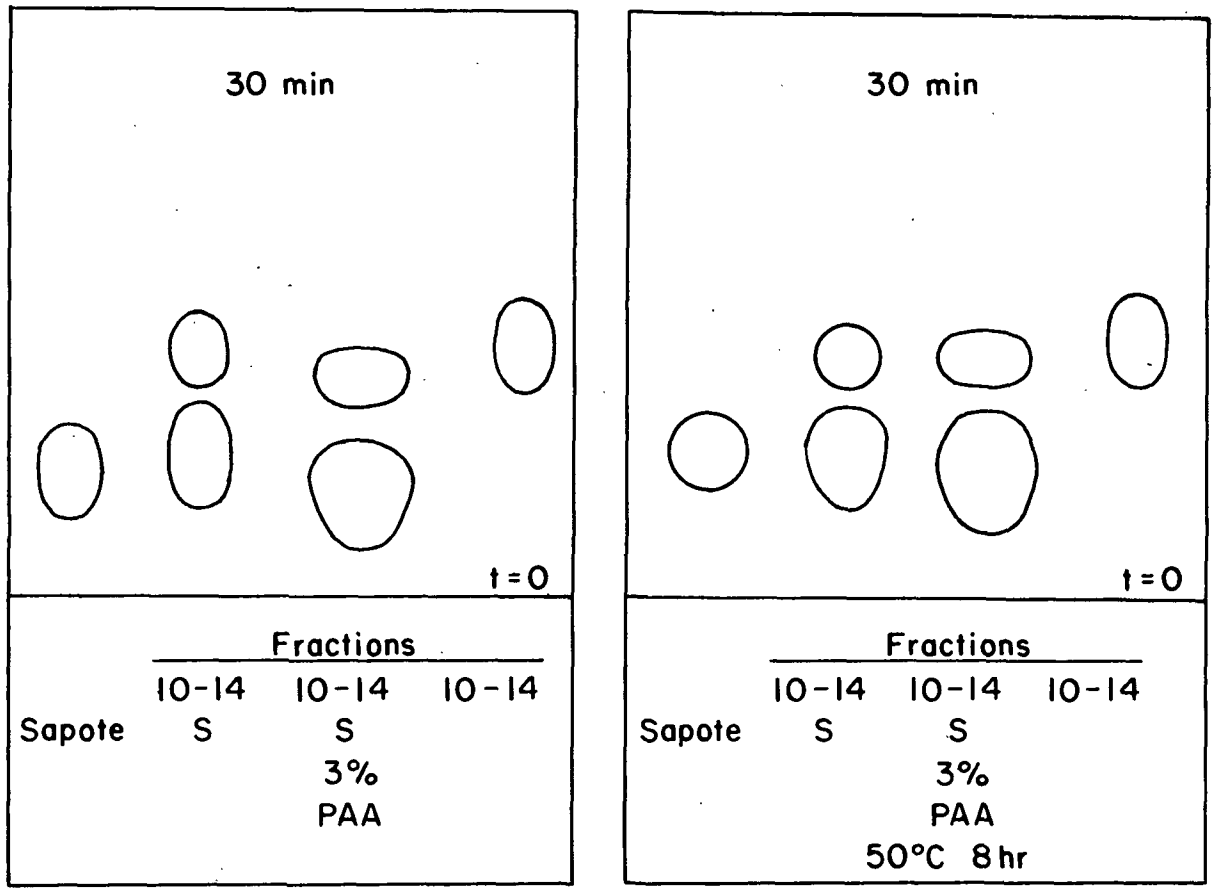

Figure 27. Electrophoretograms of Fractions 10-14 Ex-Porasil B Mixed with Sapote Gum in the Presence of PAA Under Normal Reaction Conditions

ENZYMATIC HYDROLYSIS

Removal of small amounts of "native" lignin* by Brauns with ethanol implied that lignin may be free in wood. However, when wood was extracted before the hydrolytic enzymes in the wood were allowed to react, very little "native" lignin was found (151). When allowed to react, the hydrolytic enzymes yielded 1.8 to 3.1% "native" lignin. Thus, the hypothesis of lignin free of carbohydrates in wood as the result of Brauns isolation studies was refuted.

*Native lignin is lignin free of carbohydrates.

An unusually high yield of "native" lignin was found in a sample of wood which had been decayed with brown-rot fungi (152,153). This lignin sample was shown to be identical with "native" lignin, thus supporting the hypothesis that lignin did not exist as free lignin in wood.

When a wood sample was exposed to various polysaccharide-splitting enzymes, some polysaccharides were still found to be associated with the isolated lignin (154). Other workers (148,155) used enzymes in an attempt to obtain carbohydrate-free lignin. In addition to finding that there were some remaining carbohydrates associated with their lignin samples, the size of the lignin sample was dramatically affected by the enzymatic degradation of the carbohydrates (148). Thus, from those results it was concluded that there was a lignin-carbohydrate bond.

Effect on Lignin Hydrodynamic Volume

In this study, an enzymatic hydrolysis reaction of a sample of PAA-solubilized materials containing about 20% carbohydrate from Reaction Stage 5 — Fractions 8-11 — was undertaken to determine what effect a change in the carbohydrate part of the solubilized materials would have on the hydrodynamic volume of the reacted lignin as measured by ultraviolet absorbance at 280 nm.

After 48 hours the enzymatic reaction was nearly complete as determined by a constant drainage time through a viscometer. The results of the fractionation of the hydrolyzed samples can be seen in Fig. 28. All materials came off the column between the void volume and the total liquid volume, thus indicating that the separation was by hydrodynamic volume.

Since spruce dioxane lignin has been shown to be unaffected by the enzyme (148), the elution volume of the lignin as measured by ultraviolet absorbance at 280 nm would be expected to remain unchanged if the lignin was not attached

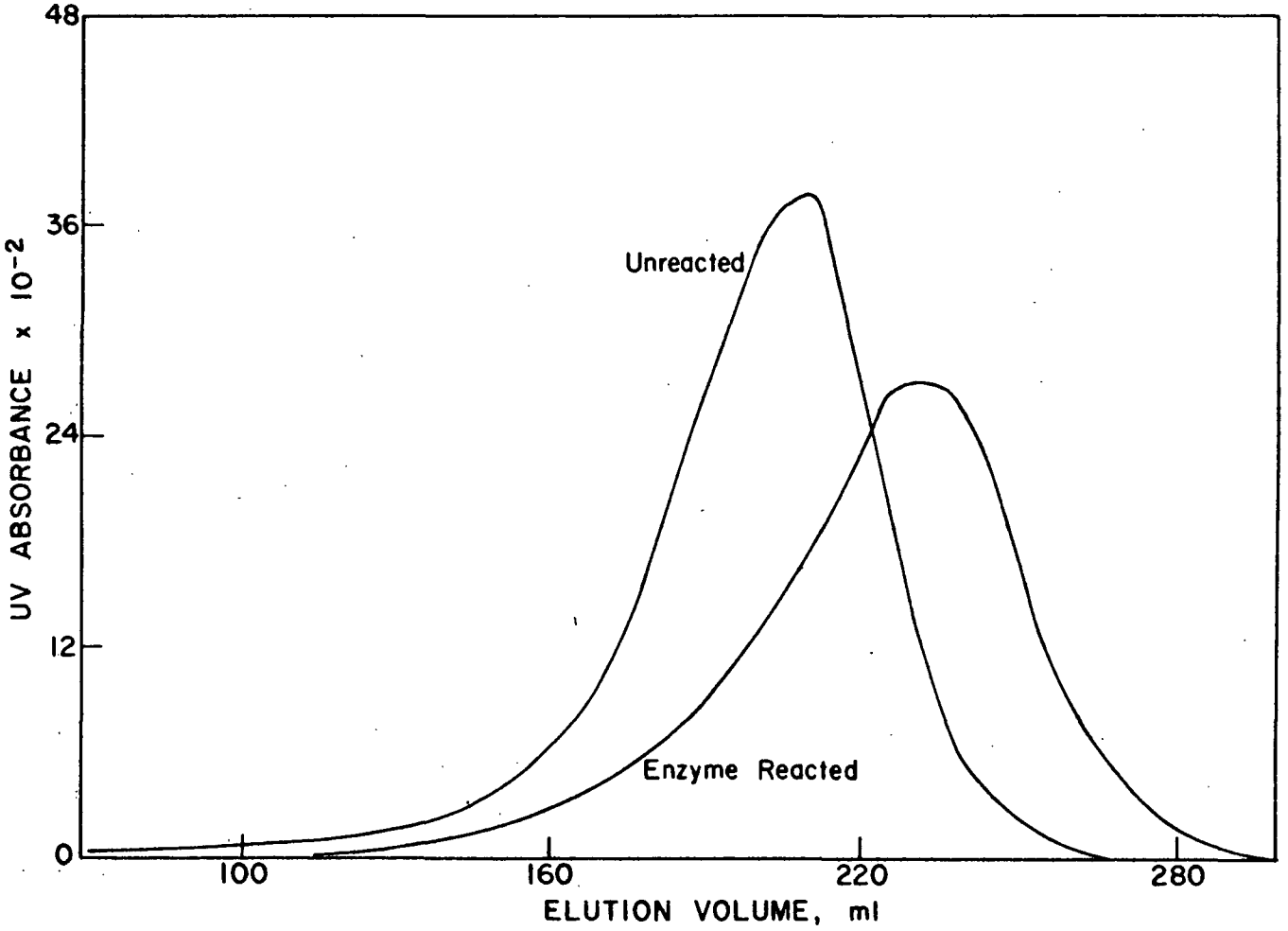

Figure 28. UV Absorbance at 280 nm Versus Elution Volume for Unreacted and Enzymatically Reacted Fractions Ex-Porasil B

to the carbohydrate component of the PAA solubilized materials. However, the reacted lignin came out at a larger elution volume than the unreacted.*

This result showed that as the enzyme hydrolyzed the carbohydrates, the overall system became smaller in hydrodynamic volume also. This again implied that the lignin and carbohydrate components of the solubilized materials were bonded.

OPTICAL MEASUREMENTS

A beam of plane-polarized light can be visualized as the vector-resultant of two oppositely rotating beams of circularly-polarized light. When circularly-polarized light travels through a medium containing asymmetric molecules, the refractive indices of the two directions of polarization will be different. These differences in refractive index correspond to differences in light velocity. The change in velocity of the two oppositely rotating beams experiencing the medium will cause a continual rotation of the plane of their resultant until they reach a medium in which they have equal velocities. This phenomenon is known as optical activity, and the change in rotation for this medium is known as its optical rotation for the wavelength of light being used.

The phenomenon of optical activity has been known since the 17th century. Changes in optical activity with wavelength were studied by Biot (156) in 1817. This phenomenon became known as optical rotatory dispersion (ORD). The field of ORD remained simple, with measurements being taken at only a few wavelengths, for many years until the invention of the photoelectric spectropolarimeter.

*Note that longer elution volume corresponds to smaller molecules.

There are two types of ORD values: plain and anomalous. A plain curve does not have an extremum (maximum or minimum) within the spectral region being investigated, as shown in Fig. 29 and 30. Sucrose exhibits a positive plain ORD curve as in Fig. 29 (157), while several methyl β-D-aldo-pyranosides exhibit negative plain ORD curves as in Fig. 30 (158).

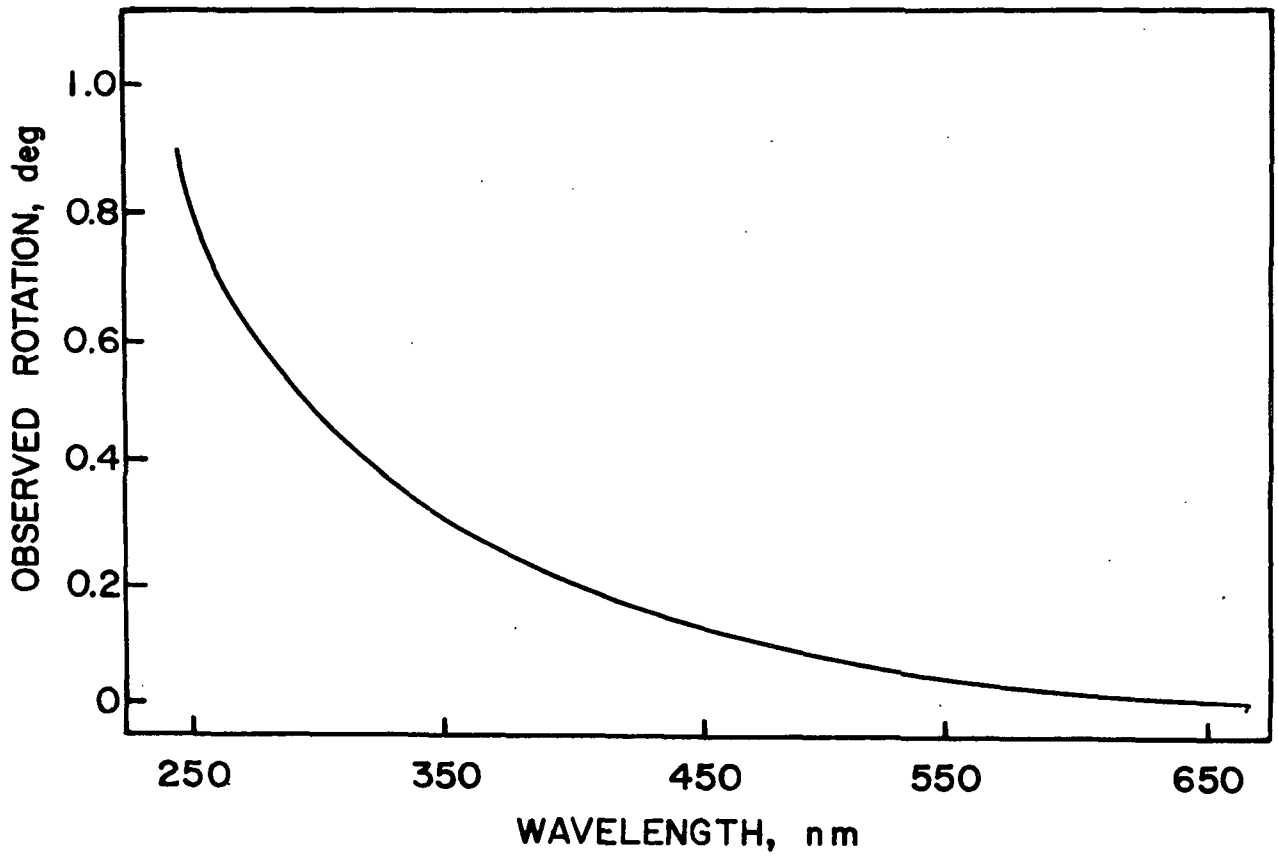

Figure 29. Optical Rotatory Dispersion Spectrum of Sucrose (157)

Anomalous curves occur when the molecule has a chromophore that absorbs light in the region under investigation which interacts with the optically active part of the molecule. These curves can have one or more extrema called Cotton effects as shown in Fig. 31 (159). An inflection point in an ORD curve usually corresponds to an absorbance maximum of the chromophore part of the molecule.

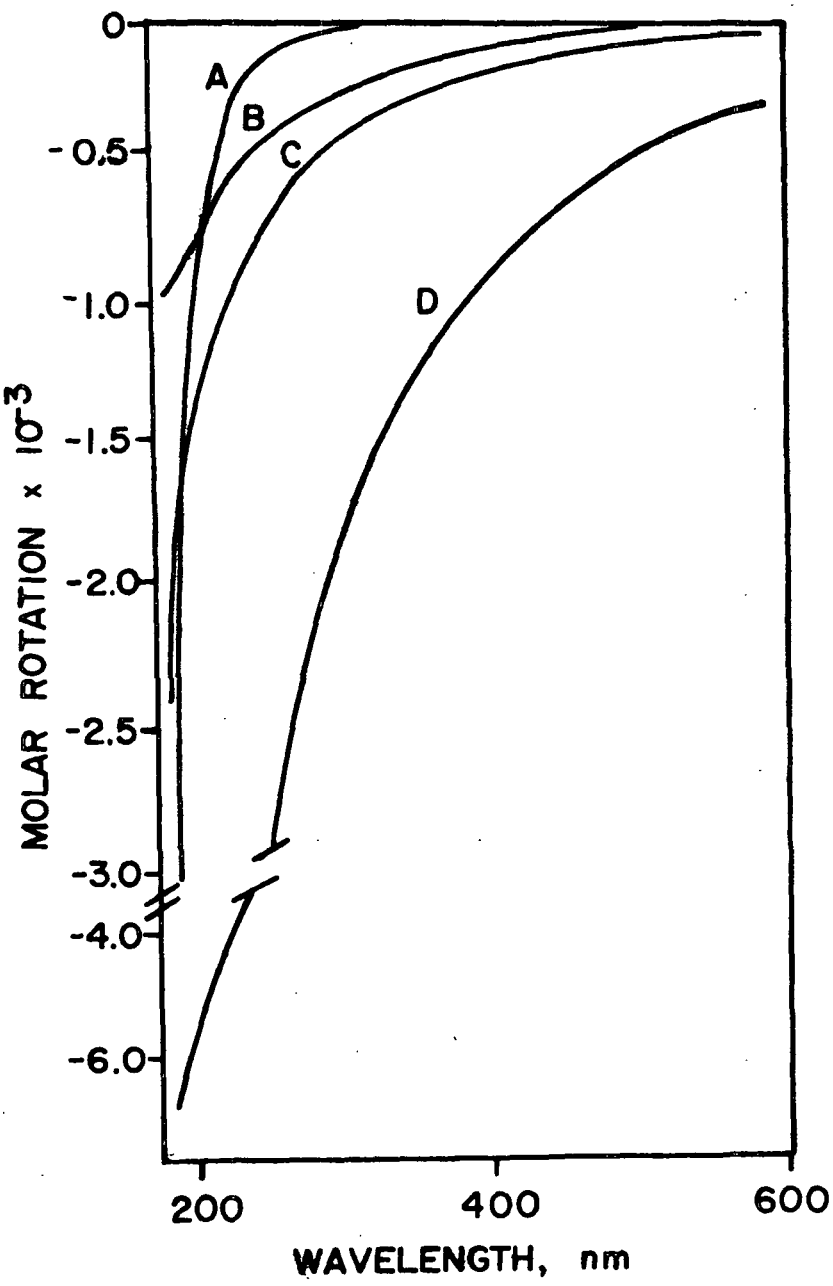

Figure 30. Optical Rotatory Dispersion Curves for Methyl β-D-Galacto- (A), Gluco- (B), Xylo- (C), and Arabino- (D) pyranosides (158)

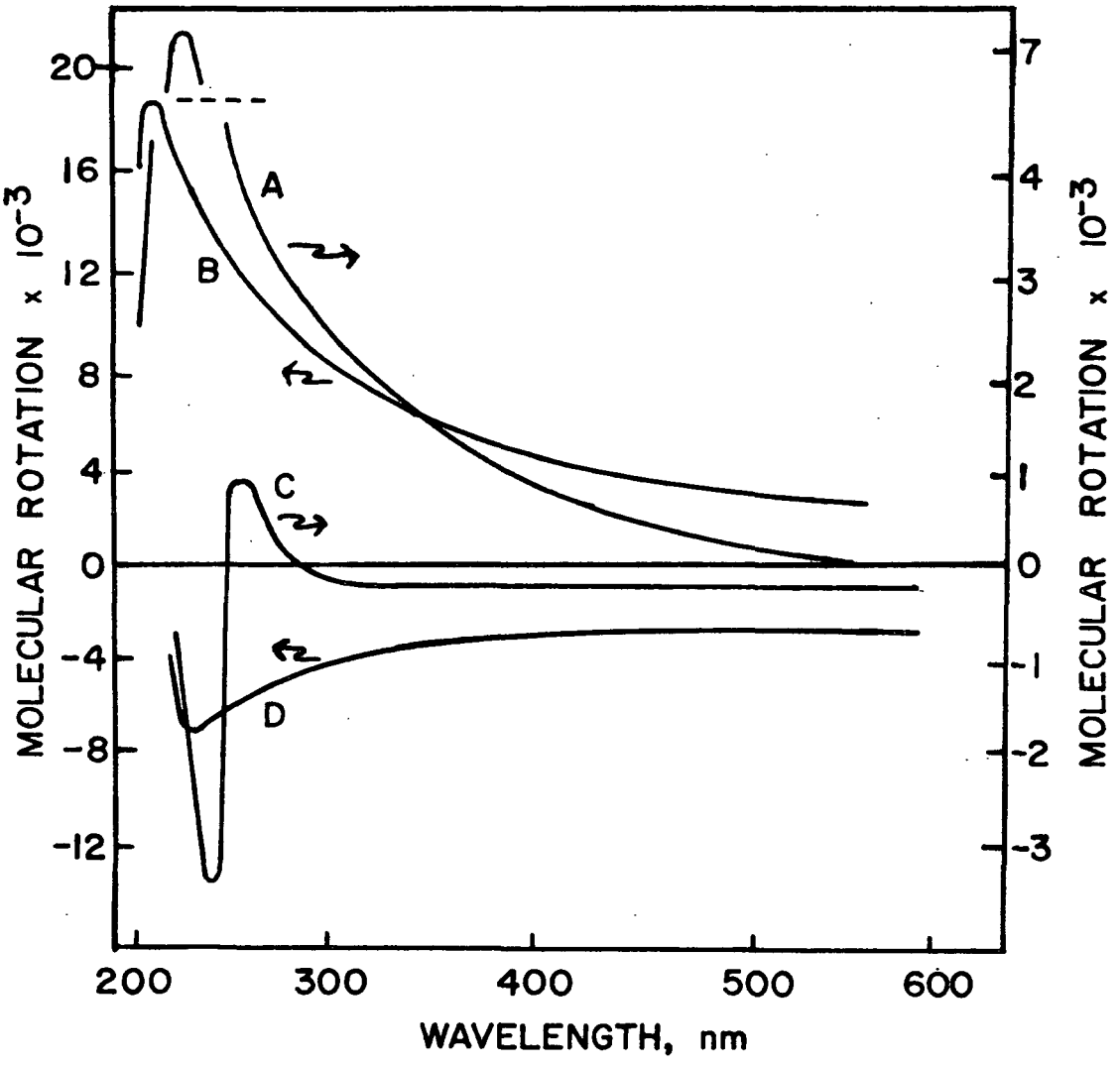

Figure 31. Optical Rotatory Dispersion Spectra of Methyl α-D-Xylothia- (A) and Xylo- (B) pyranosides and Methyl β-D-Xylothia- (C) and Xylo- (D) pyranosides (159)

Soon after the discovery of ORD, differences in absorption of the two components of polarized light were observed by Haidinger (160). This phenomenon became known as circular dichroism (CD). The wavelength of CD extrema corresponds to the wavelength of the absorption extrema in the ultraviolet spectrum and the inflection point in the ORD of the molecule as shown in Fig. 32 (161). The units commonly used in CD are molecular ellipticities [θ] which are related to the differences in absorption Δε by Equation (4):

$$[\theta] = 3300\ \Delta\varepsilon \qquad (4)$$

where $\Delta\varepsilon = \varepsilon_L - \varepsilon_R$ with ε_L and ε_R being the molecular extinction coefficients for the left and right rays.

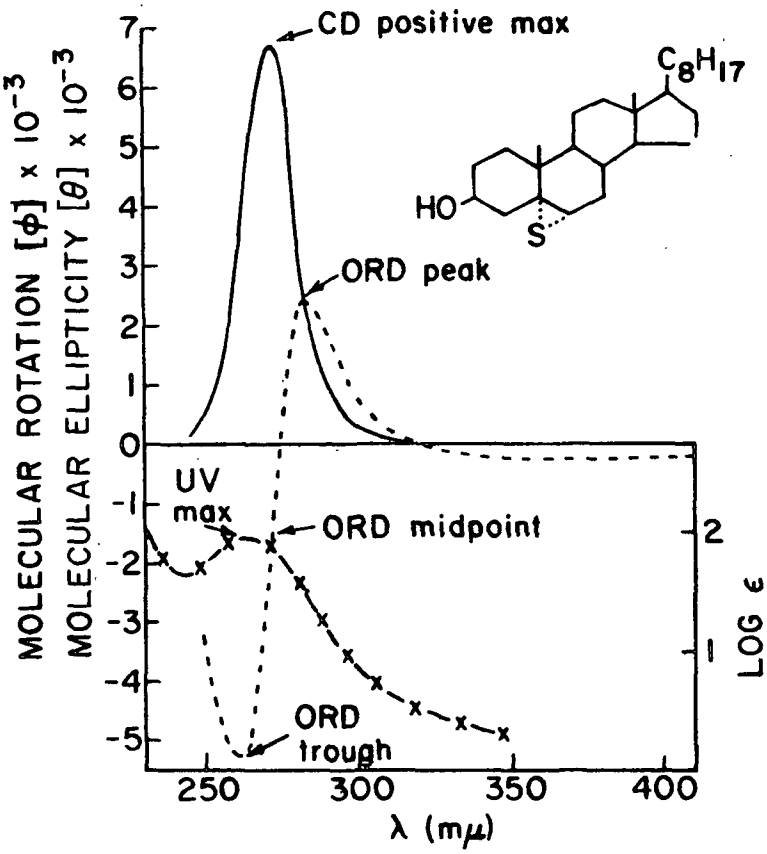

Figure 32. Interrelationships Between ORD, CD, and UV Spectra (161)

For many compounds the ORD and CD results can be used interchangeably. Despite their similarity in use, the two methods do have some differences. The most distinguishing feature of the ORD is the operation of background effects, i.e., the rotational contributions of more distant absorption bands of the same chromophore or other atoms in the same compound which may produce variations in shape that are not encountered in the CD. Thus, for fingerprinting purposes, the ORD would be the most useful.

The existence of background effects can add distinctness to the ORD of a given compound; however, this same effect makes quantitative determinations difficult and at times impossible. The CD spectrum of a given compound will usually clearly distinguish the various Cotton effects which are difficult to distinguish in the ORD.

Because of the complexity of the ORD and CD curves, theoretical studies have been limited to a number of specific groups of aromatic compounds. Empirical rules have been suggested for aromatics in rigid systems as well as phenyls and other aromatic systems (162). In some very specific cases the absolute configuration of asymmetric centers and the conformation of rings or conjugated systems could be deduced from the sign and magnitude of the Cotton effects. Quantum mechanics has been successfully used (163,164) to interpret some of the empirical findings in the ORD and CD fields.

When a chromophore within a molecule has considerable inherent symmetry (e.g., the phenyl group) and the remainder of the molecule is dissymmetrically disposed with respect to this chromophore, then the effect of the asymmetric environment is to induce a dissymmetry in the electron distribution within this chromophore (165). In this case the electronic transitions of the chromophore become optically active. The induced rotational strengths for the chromophores' electronic transitions is related to the interaction of the chromophore with its dissymmetric molecular environment. Variations in rotational strength of a particular transition of a chromophore from molecule to molecule as measured by optical rotatory dispersion (ORD) has been used in specific cases to determine structural information about these molecules (162).

Recent improvements in instrumentation have made it possible to examine the ORD Cotton effects associated with electronic transitions from chromophores

such as phenyl groups. Better inherent resolution of circular dichroism (CD) versus ORD has permitted the direct observations of the Cotton effects associated with these closely spaced electronic transitions. Three absorption bands (180-190, 200-220, and 260-280 nm) become optically active for simple aromatic compounds in dissymmetric surroundings (165-169).

The electronic transitions of a chromophoric group within an asymmetrical environment display Cotton effects whose sign and magnitude depend upon the nature and position of the asymmetrically located groups in the molecule. The influence of remote substituents on the Cotton effects of a given molecule have been examined (170,171). For the series of compounds related to A and B,

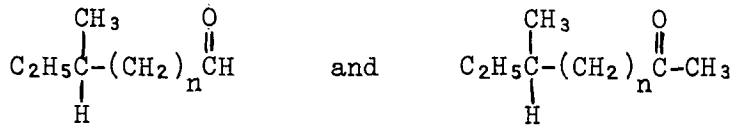

A and B

where n goes from 0 to 3, the effect of distance between the chromophore and the asymmetric environment on the Cotton effects is summarized in Table VIII. The reversal in sign for n = 0 and n = 1 has been attributed to free-rotational isomers in solution (166,170). Flexible side-chains result in Cotton effects which are small in themselves. The results of those studies indicate that when the distance between the chromophores and the asymmetric environment exceeds 4.5 A, the Cotton effects can no longer be reliably determined. It was also found that for substituents such as alkyl, hydroxyl, or even benzyl on a rigid skeleton at a distance greater than 4.5 A from the chromophore giving the Cotton effects, there was nearly no difference in the Cotton effects curves.

TABLE VIII

THE EFFECT OF DISTANCE BETWEEN THE CHROMOPHORE AND THE ASYMMETRIC ENVIRONMENT ON COTTON EFFECTS

n	Resulting Cotton Effect
0	Positive
1	Negative
2	Weak negative on a positive background
3	Plain dispersion curve (170)

For the phenyl absorption bands, distances less than this may be required to induce Cotton effects as shown in a study by Lyle (171). Compounds C and D, which have no CH_2 groups between the chromophore and the asymmetric carbon, have strong Cotton effects while Compounds E and F, which have only one CH_2 group between the chromophore and the asymmetric carbon, have plain dispersion curves. The study using compounds related to those above also showed that for

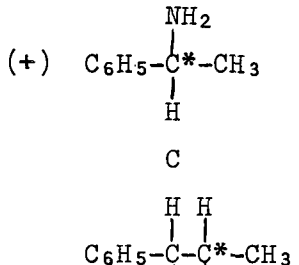

C

E

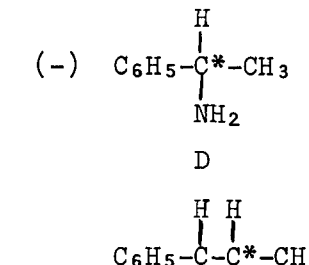

D

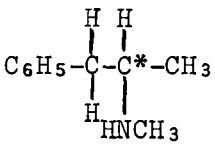

F

compounds with more than one asymmetric center, the resultant ORD curve was not completely the sum of the individual ORD curves.

Use of the ORD and CD spectra in the field of polysaccharides was limited because most chromophores associated with polysaccharides absorb light outside the ultraviolet range. Previous work in the 350-600 nm range stimulated little

interest because most spectra were positive plain or negative plain. Interest grew when various workers began to make derivatives of the polysaccharides which would absorb in the ultraviolet spectral range.

Cellulose and xylose acetates were prepared and analyzed for their ORD and CD characteristics by Marchessault, et al. (172). Conclusions about the stereochemistry and conformations were drawn in this study. It is of interest to look at the types of conclusions which can be drawn from the CD curves shown in Fig. 33 for the xylan acetates, especially the white birch and esparto acetates. The former consists of a linear backbone of β-1,4-linked D-xylopyranose residues of which approximately every tenth is substituted at the 2-position with a 4-O-methyl-D-glucuronic acid residue. The esparto has no such acid and, therefore, the difference in CD curves was attributed to the attached acid. Thus, ORD and CD techniques have become useful for natural products which are optically active and have an attached chromophore in the ultraviolet spectral region.

Cotton effects in ORD curves of carbohydrates have been attributed to at least two predominant asymmetric absorptions, the major one near 150 nm and another near 200 nm. The ring oxygen has been shown to contribute to the overall effect because when it was replaced by sulfur, a change in the ORD curve was observed as shown in Fig. 31. It can be noted that there are no Cotton effects for the xylan compounds in the aromatic transition region. Lactones have been shown (173,174) to give peaks and troughs between 225 and 230 nm with the other peak being beyond the lower limits of the instrument.

Optical rotatory dispersion studies on various phenyl glucosides have been made by Sticzay, et al. (175). Many Cotton effects for these compounds were observed by Sticzay and to provide a basis for experience in this study, the

ORD data of Sticzay on phenyl-β-D-glucopyranoside was compared to CD data obtained in this study and is shown in Fig. 34.

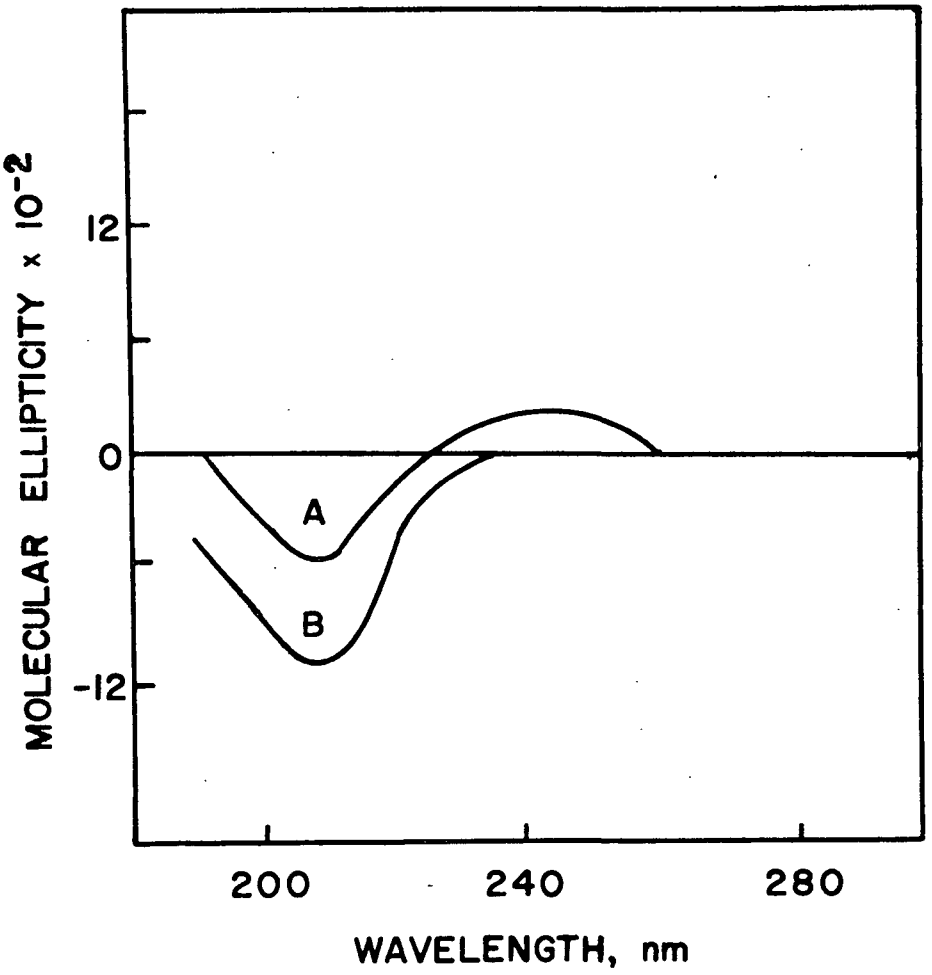

Figure 33. Circular Dichroism Spectra of White Birch (A) and Esparto Grass Xylan Diacetates (B) (172)

The CD curve has four negative minima corresponding to the four negative Cotton effects seen in the ORD curve. The similarity of shape of these two curves and the location of the minima corresponding to the inflection points in the ORD curve show the complementary nature of the two techniques.

Although metal complexes, which at times become so closely associated that they are nearly bonded, can give Cotton effects, a lignin-carbohydrate complex of this type in solution resulting in Cotton effects is unlikely for the PAA

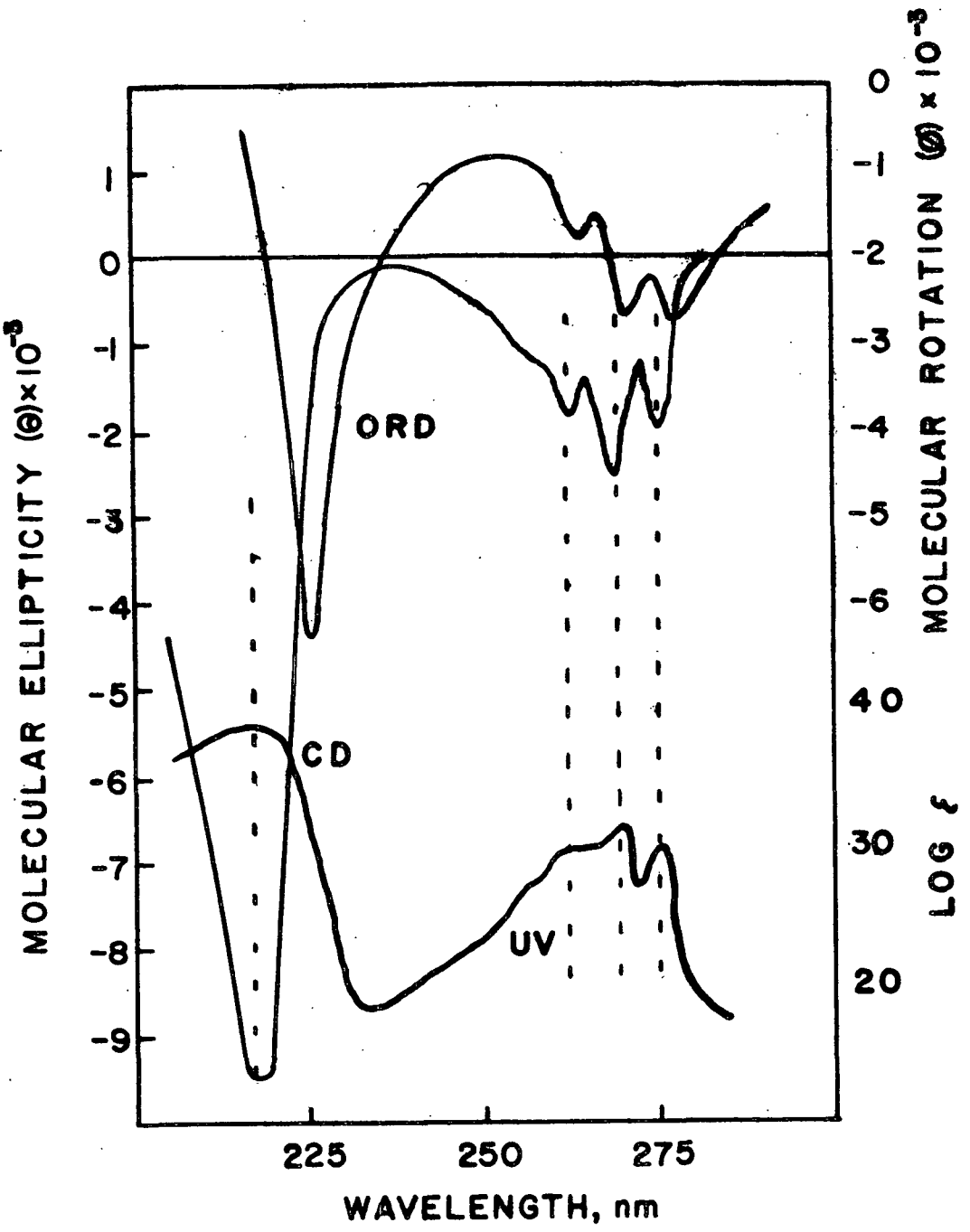

Figure 34. ORD (175), CD, and UV (This Work) of Phenyl-β-D-glucopyranoside

solubilized materials. Benzene substitute complexes formed when benzene was used as a solvent have been shown to be very weak ones (176). Changes in ORD Cotton effect curves when benzene was used as a solvent in place of the original solvent were insignificant. Benzene has a dielectric constant of 2.27 and behaves in the same way as dioxane, which is a common ORD solvent with dielectric constant 2.21. It has also been shown that in solvents where hydrogen bonding is taking place, the changes in the ORD curves are not significant enough to mistake them as additional Cotton effects (162).

A benzene-iodine complex is known to have an ionic distance of separation of about 5 A (177). Since this is a stronger association than would be expected for a lignin-carbohydrate association,* the ionic distance would be significantly greater than 5 A, which is greater than the 4.5 A beyond which electronic transitions cannot give rise to Cotton effects in the aromatic region. Thus, an association in solution of a complex of the lignin and carbohydrate materials from the PAA-solubilized materials is unlikely to give Cotton effects in the 280 nm region.

Presumably then, in order to observe Cotton effects from aromatic electronic transitions for the PAA solubilized materials, the carbohydrate and lignin components must be bonded. For some known phenyl glycosides where the aromatic and sugar parts are known to be bonded, the Cotton effects from transitions are clearly observed (175,178,179). Substituents in the ortho and para positions on the aromatic part of the molecule have been examined for their Cotton effects (178,179).

*If this is only an association between the lignin and carbohydrate it would be expected to be a weak donor-acceptor type of association as opposed to a bond such as an ether linkage.

OPTICAL MEASUREMENTS ON FRACTIONS EX-PORASIL B

Optical Rotation at 546 nm

In previous work by Albrecht and Nicholls (89), the optical rotations of freeze-dried samples of peroxyacetic acid (PAA) lignins were determined and are shown in Table IX which illustrates that for any given yield range the early fractions ex-Porasil had positive rotations. Those coming off later had negative rotations. In all cases, it can also be seen that as the reaction proceeded, the rotations tended to change, but insufficient data were obtained to firmly establish any particular trends. These rotations must be associated with the associated polysaccharides, because lignins are optically inactive. More extensive optical rotation data for white birch PAA lignins have been obtained in this work as shown in Table X. Again, for any given yield range the early fractions ex-Porasil have positive rotations and in addition those coming off later show a clear trend to more negative rotations. Also, as the reaction proceeds there is a clear trend toward more negative rotations as shown in Fig. 35.

TABLE IX

SPECIFIC ROTATION AT 546 NM FOR LOBLOLLY PINE PAA-SOLUBILIZED MATERIALS (84)

	Specific Rotation				
	Fractions Ex-Porasil B				
% Yield	4-8	19-23	28-32	38-42	52-56
98.4-91.2	+13.1	-17.7	-20.8	-18.4	-21.2
91.2-83.6	+18.2	-16.5	-16.5	-17.6	-19.0
83.6-77.0	+9.3	-15.3	-14.8	-15.0	-23.1

TABLE X

SPECIFIC ROTATION AT 546 NM FOR WHITE BIRCH PAA-SOLUBILIZED MATERIALS

	Specific Rotation Fractions Ex-Porasil B		
% Yield	16-19	42-43	55-57
100.0-98.6	+15.6	+1.5	-0.9
98.6-94.9	+3.5	+0.5	-1.7
94.9-90.2	+0.3	-1.0	-2.9
90.2-86.5	-4.2	-2.6	-5.5
86.5-83.6	-6.7	-5.5	-9.9
83.6-82.0	-8.3	-7.9	-13.6

From Fig. 35 it is apparent that trends in negative rotation essentially follow the trend toward more total sugars being present in the freeze-dried solids as delignification proceeds (Fig. 10). In addition, the trends in specific rotation follow the trends in polysaccharide composition as listed in Appendix V. An increase in the relative amount of xylose as delignification proceeds infers either an increase in the xylan polymer chain length or an increase in xylan content. The relationship between oligosaccharide chain length and specific rotation has been reviewed by Geczy (180). Xylan oligosaccharides have been shown to give more negative specific rotation with increase in chain length (181). Therefore, the trends in negative rotation in Fig. 35 reflect either an increase in xylan chain length or an increase in xylan content especially where xylan is by far the major saccharide component of the sample.

Similar reasoning can be applied to the trends in positive rotation at the initial reaction stages and at points where there is less xylan on a relative and absolute basis. In these cases there is more glucan and galactan in these samples. In addition to the loss in influence of the xylan, the trend toward

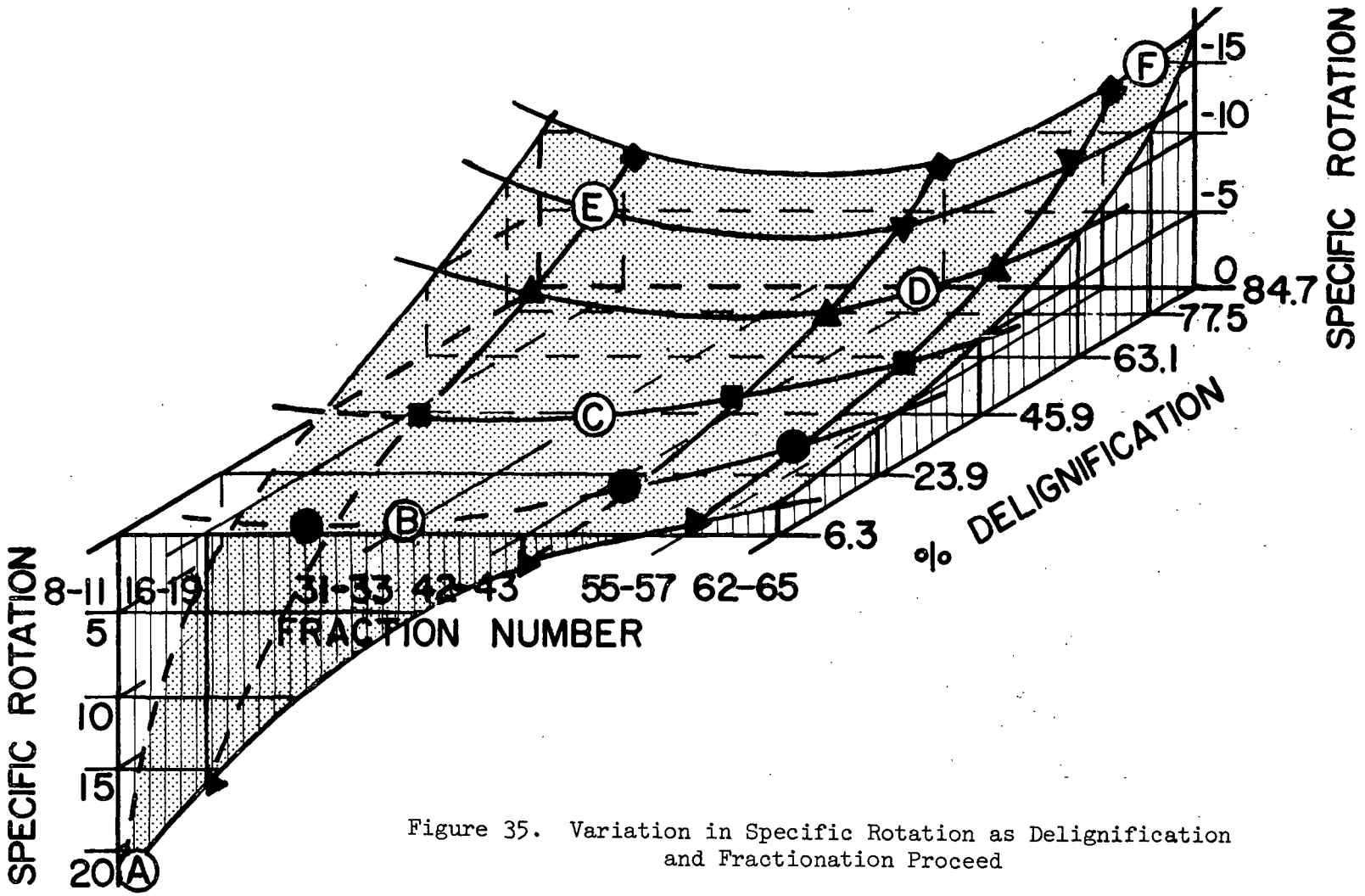

Figure 35. Variation in Specific Rotation as Delignification and Fractionation Proceed

more positive rotations would be contributed to by the glucan (182) and galactan from white birch (183) which have positive rotations.

Since the PAA freeze-dried samples have optical rotations and lignin-based chromophores (as indicated by infrared and ultraviolet earlier work), it would be expected that Cotton effects would be observed in the ultraviolet region or their ORD curves if the optically active portion is bonded to the lignin-derived chromophore. This would provide clear evidence for lignin-carbohydrate bonds which are implied by the results of electrophoresis experiments as described earlier in this work.

Preliminary Tests

An attempt was made to obtain an ORD curve for white birch freeze-dried PAA lignin samples in this work on a Perkin-Elmer 141MC spectropolarimeter. At longer wavelengths the specific rotations were obtainable, but as shorter wavelengths (33 nm) were approached, the chromophore absorbed too much of the incident light. Upon dilution to overcome this problem, the rotation diminished until it was undetectable. Thus, it became apparent that the instrument being used was not sensitive enough to obtain ORD curves for the samples being analyzed. This led to further data being obtained on the basis of using a JASCO J-20 instrument through the courtesy of Mr. Jacques Bambling, President of JASCO Inc. as detailed further in Appendix X.

Choice of samples for ORD determinations were made on the basis of data on optical rotations at 546 nm as shown in Fig. 35. The circles with a letter inside correspond to the samples run, and were these:

Reaction Step	Fractions	% Delignification
1 (A)	8-11	6.3
2 (B)	24-27	23.9
3 (C)	31-33	45.9
4 (D)	48-49	63.1
5 (E)	16-19	77.5
6 (F)	58-61	84.7

This selection of samples provided one sample with high positive, one with high negative, one with medium positive, two with medium negative, and one with nearly zero specific rotation at 546 nm. Also, in addition to the complete range of specific rotation, this selection represented samples ranging from early to late reaction steps and from early to late fraction numbers.

Optical Rotatory Dispersion and Circular Dichroism Curves

Specific rotations obtained from the converted raw data were first plotted as shown in Appendix XI. Later, on the basis of the above experience, the converted data were readjusted by averaging the points at which there was a high signal to noise ratio and replotted as seen in Fig. 36(A-F). The ORD and ultraviolet spectra are shown in all cases. The two CD curves run are shown for Samples A and F.

The ultraviolet spectra resemble each other in shape, but the amplitudes of the various peaks are variable. These spectra have a large peak around 200 nm and two shoulders around 235 and 275 nm.

Three distinct types of ORD curves can be observed. Fig. 36A, 36B, and 36E have ORD curves with a maximum preceding the remainder of the curve as shorter wavelengths are approached. Thus, these three curves have positive Cotton effects.

Figure 36C has no easily seen maximum or minimum. Thus, a positive plain curve is observed in this case.

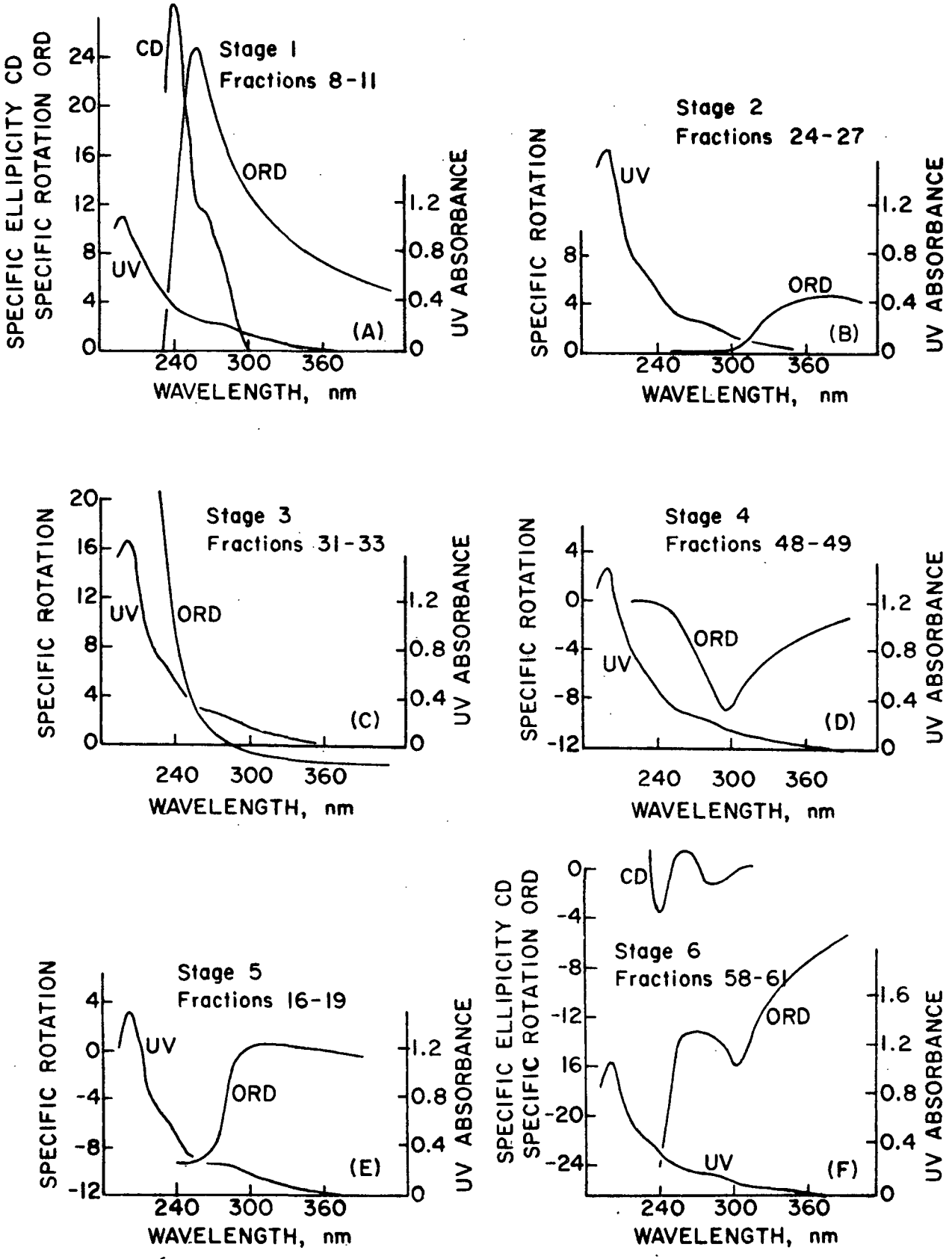

Figure 36. ORD, CD, and UV Spectra of Certain PAA Freeze-Dried Fractions Ex-Porasil at Various Reaction Stages

Figures 36D and 36F have ORD curves with a minimum preceding the remainder of the curve as shorter wavelengths are approached. Thus, these two curves have negative Cotton effects. Locations of the inflection points in the ORD curves were difficult to see probably because of overlapping of bands in the ORD.

Positive Cotton effects appear to be present in ORD curves for samples with fraction numbers less than 30 for any reaction stage. Negative Cotton effects appear to be present in ORD curves for samples with fraction number greater than 48. It is necessary to recognize that the material from the fractions ex-Porasil could be more heterogeneous than homogeneous from a molecular structure viewpoint. The specific rotations in Fig. 35 reflect trends in populations of molecules which probably have more similarity in hydrodynamic volume than in all specifics of chemical structures. Furthermore, if a material has molecules with different structures, a positive Cotton effect could cancel a negative effect and no effect may result as in Fig. 36C.

Two distinct CD curves can also be observed. Figure 36A has a CD curve with two positive maxima around 240 and 280 nm. These two maxima correspond very nearly to the locations of the shoulders in the ultraviolet as expected from the theory. Positive maxima verify that the ORD curve has positive Cotton effects with inflection points around 240 and 280 nm.

Figure 36F has a CD curve with two negative minima around 235 and 275 nm which again correspond well with the ultraviolet curves for these samples. Negative minima verify that the ORD curve has negative Cotton effect with inflection points around 235 and 275 nm.

Although the ORD and CD have been used in the study of naturally occurring polymers such as proteins, polypeptides, and polysaccharides (184), it is believed that this is the first study involving lignin. It is particularly interesting

that fractionation ex-Porasil, which is considered to proceed mainly on the basis of hydrodynamic size, has resulted in some fractions having sufficiently specific molecular structures to show the observed Cotton effects. This seems likely to have occurred because hydrodynamic size relates systematically to the composition and specific rotation of the carbohydrate moiety in such a way that there is a significant ordering of molecular structures capable of giving Cotton effects.

The Cotton effects in the ORD curves in conjunction with ultraviolet and CD results corroborates the implications made earlier in the electrophoresis and enzyme work that the lignin portion of the PAA solubilized materials from a white birch is bonded to the carbohydrate portions. Since these two components are linked outside the wood and there is no evidence for any bond formation during delignification, they must be bonded in the wood. Thus, the mechanism of lignin removal must also include the removal of the attached carbohydrate.

EXPERIMENTAL PROCEDURES

ISOLATION OF WHITE BIRCH PEROXYACETIC ACID LIGNIN

PREPARATION OF WOOD CHIPS

Blocks of sapwood from a 30-year-old white birch (Betula papyrifera) were obtained by cutting a 9-foot log into 2-inch disks and then cutting the disks into blocks as shown in Fig. 37. These blocks were then shaved by a special cutting tool borrowed from the Forest Products Laboratory in Madison into 0.5-mm thick wafers along the tangential face of the block as shown in Fig. 37. The wafers were then cut into chips with approximate final dimensions 12 x 8 x 0.5 mm in the longitudinal, tangential, and radical directions with respect to the pith.

These chips were extracted with acetone for 32 hours in a large Soxhlet extractor supplied with acetone from a 12-liter flask. Further extraction gave less than 0.1% extractives on an oven-dried wood basis. Extracted chips were stored at 5°C in the dark.

PREPARATION OF PEROXYACETIC ACID

All glassware coming into contact with PAA was passivated according to the procedure presented in Appendix I. Peroxyacetic acid was generated from the hydrogen peroxide oxidation of acetic acid with sulfuric acid as catalyst, using the procedure detailed by the FMC Corporation (22) presented in Appendix I. For safety and convenience, the generator was enclosed in a hood-vented, shatterproof, Plexiglas wire-mesh cage, as shown in Fig. 38. Peroxyacetic acid concentrations were determined according to the procedure of Sully and Williams (185) presented in Appendix I. The generator PAA was then quantitatively diluted with distilled water to make 3% PAA for ensuing reactions.

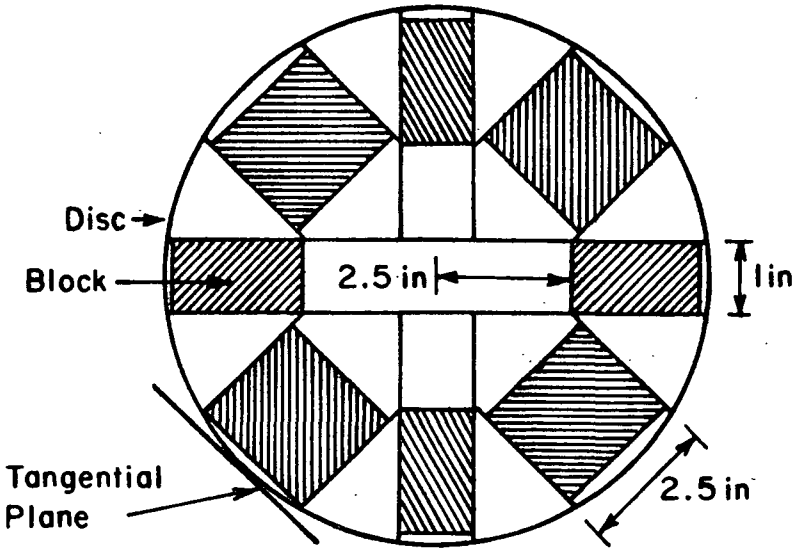

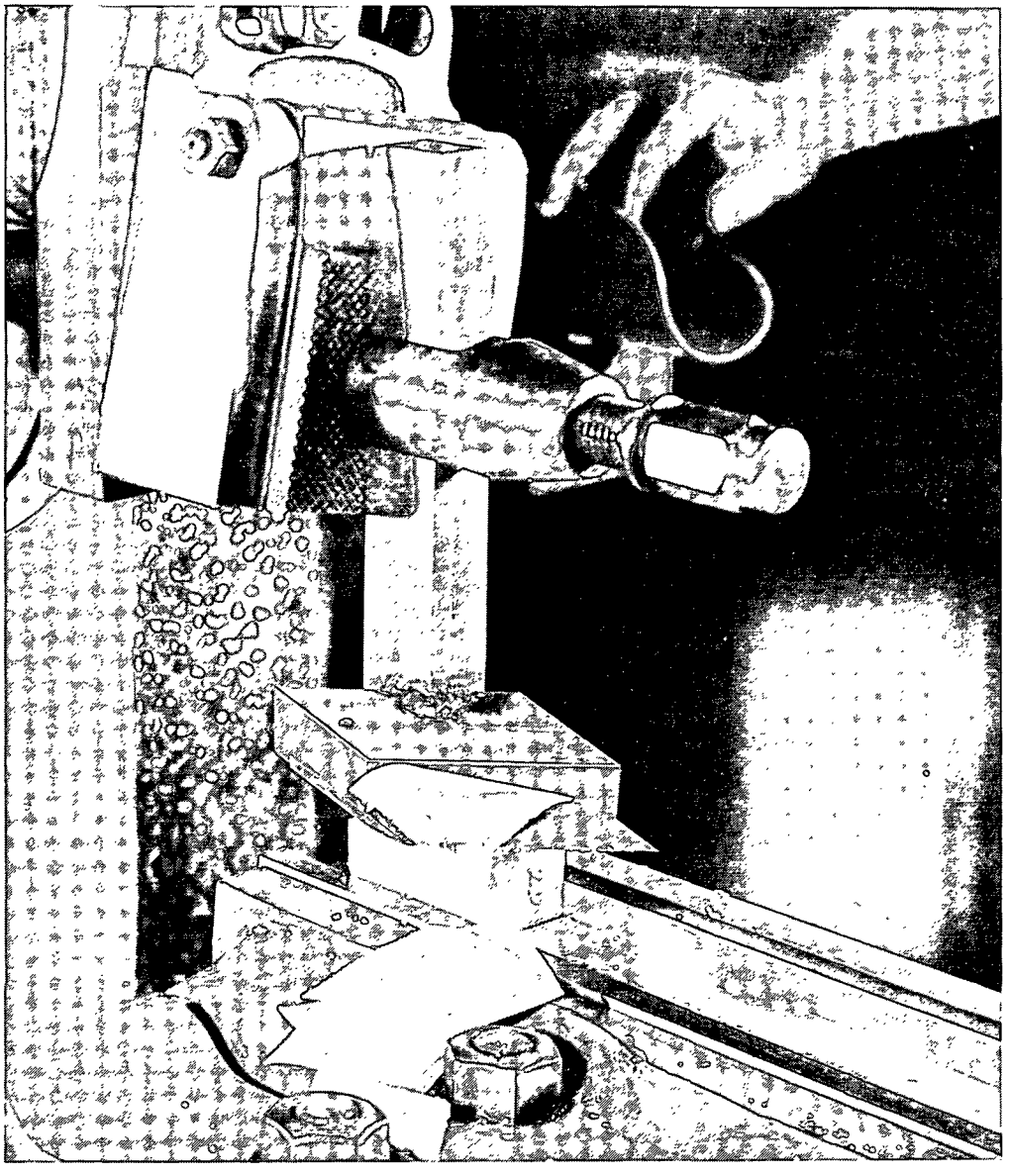

Figure 37. Cutting Pattern of a Typical Disk (Above) and Cutting Technique for Wafers (Below)

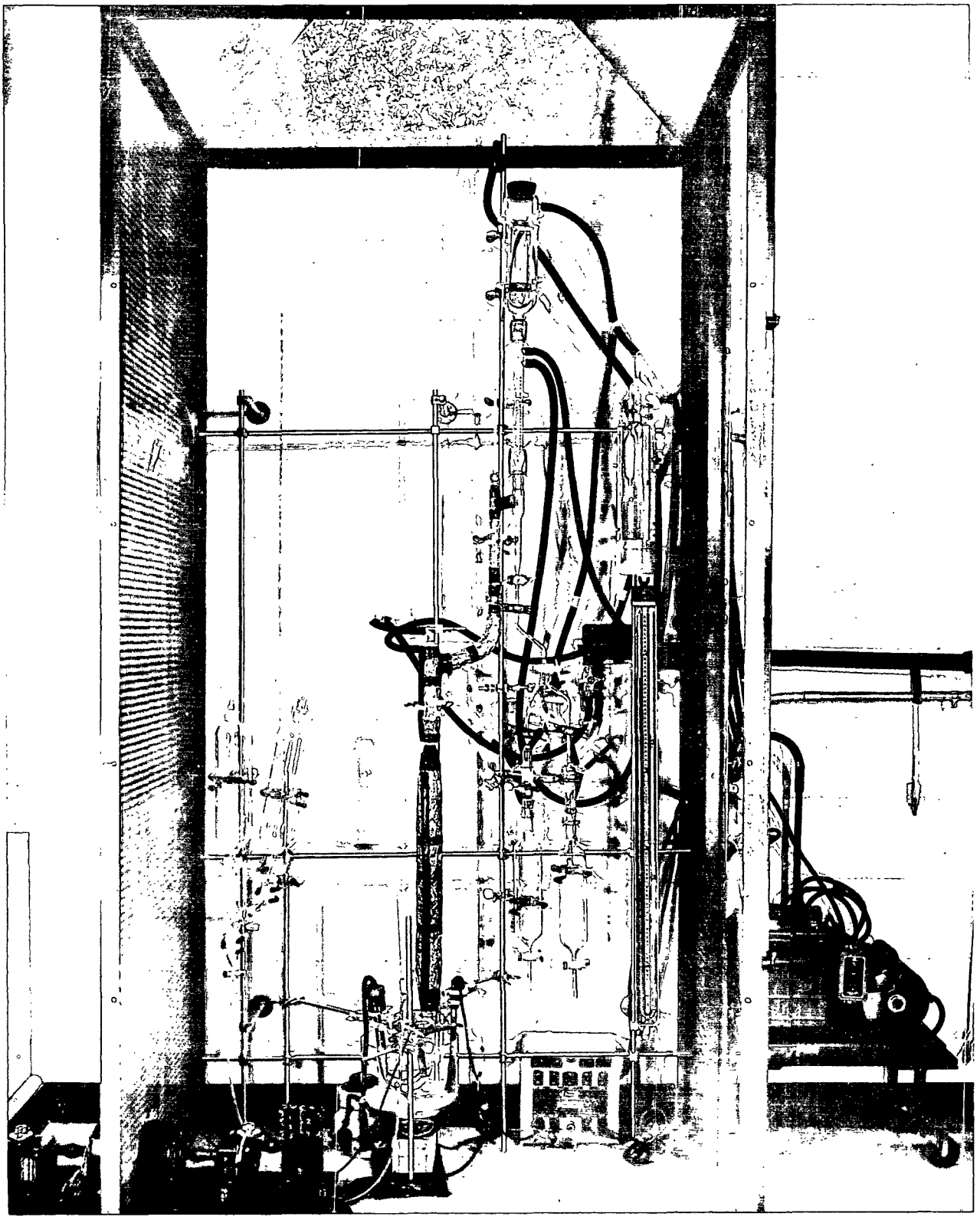

Figure 38. Peroxyacetic Acid Generator

CONTINUOUS FLOW REACTIONS

White birch chips (approximately 50 g OD) were water saturated and degassed prior to reaction by using vacuum with occasional releases for 3 hours to submerge the chips in 500 ml of distilled water. The water-soaked chips were packed into the reaction vessel between two perforated plates held together at the ends of a double 71/60 tapered glass joint by a stainless steel rod as shown in Fig. 39. The reaction vessel was then set into place within the continuous flow apparatus shown in Fig. 40 which was constructed from Pyrex glass, Teflon, and polyethylene. The established reaction procedure was based on the results of preliminary reactions shown in Table I and the results of preliminary reactions of Albrecht (17). Delignification occurred as PAA solution was continuously passed through the chip-filled reaction vessel which was submerged in an adjustable constant-temperature bath at 50°C. Peroxyacetic acid was furnished to the reaction vessel by the gravity feed of a 3-foot head via a 35-foot coil also located in the constant-temperature bath at 50°C and fed at a uniform rate of 25 ml/min by a constant level device supplied by a PAA reservoir.

The reaction vessel effluent containing the solubilized materials from the wood was rapidly cooled, and excess PAA was quenched by acetaldehyde (2:1 molar ratio) and collected in 2,000 ml aliquots representing 6 reaction steps. Solubilized materials were stored in amber bottles at 5°C in the dark until the quenching reaction was complete. These 6 samples were then concentrated to equal concentration (approximately 12 g/liter) prior to fractionation on Porasil B.

WOOD YIELD AFTER PEROXYACETIC ACID REACTION

Reacted wood chips were air dried on a fine sintered glass filter until all excess water had been removed from their outside surfaces. After the total yield of wet chips was measured, three weighed aliquots of these chips were

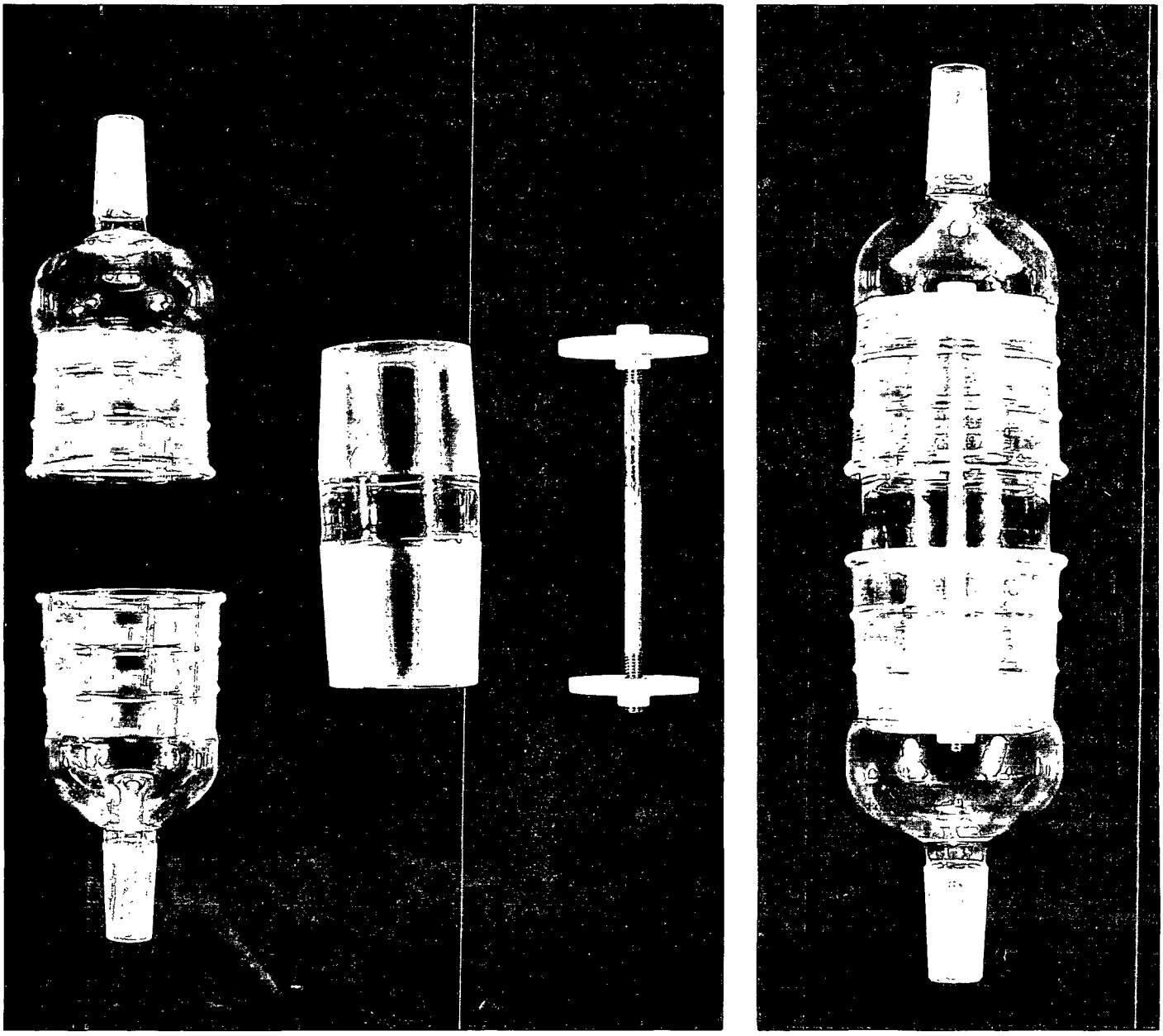

Figure 39. Peroxyacetic Acid Reaction Vessel

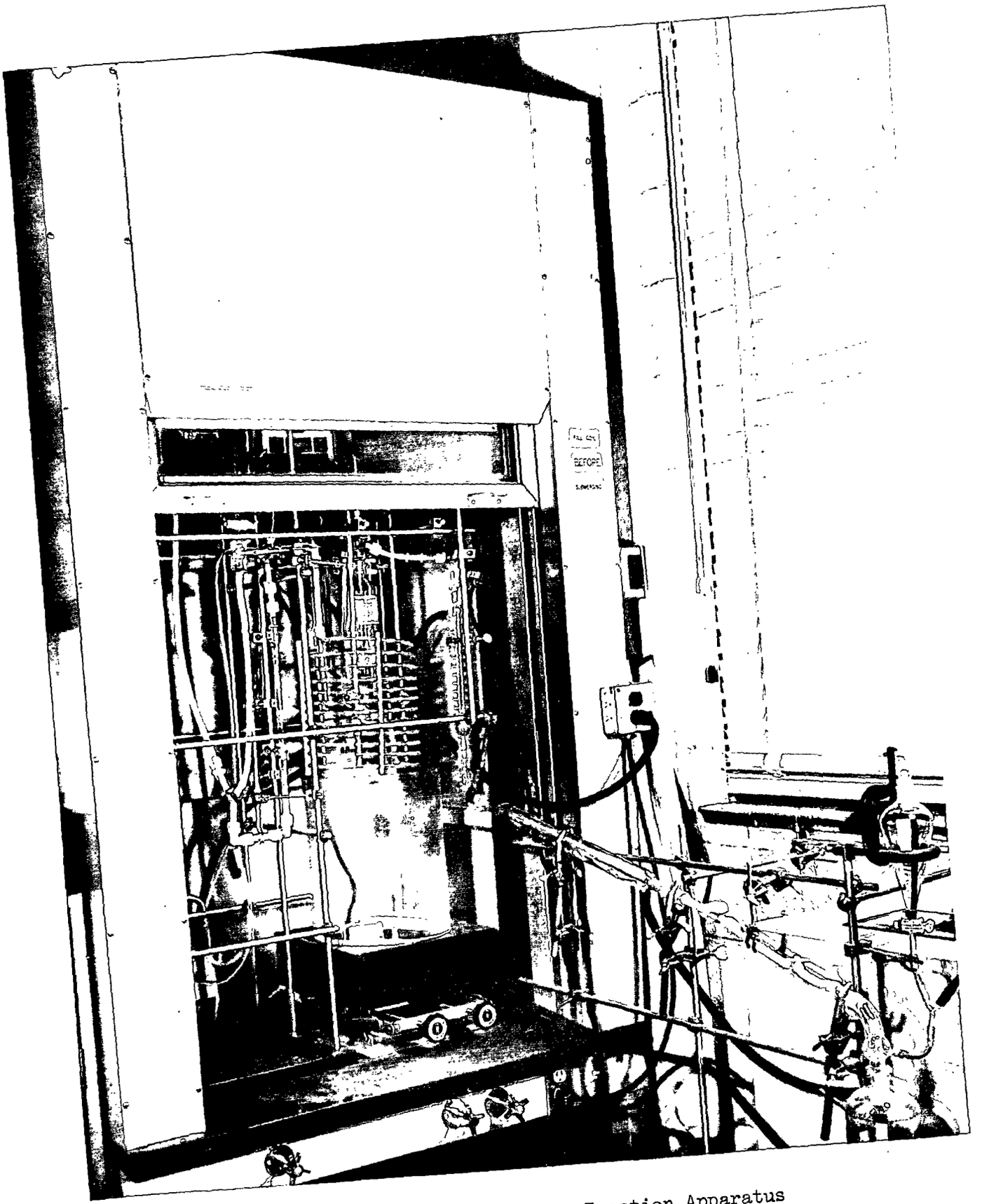

Figure 40. Continuous Flow Reaction Apparatus

oven-dried (186) to obtain the dry fraction of the wet chips. From this, the total dry yield and percentage yield were then calculated. Percent delignification was determined for three reaction stages (2,3,6) by stopping an individual reaction at each of these stages and determining yield and lignin content.

UNIFORMITY OF PEROXYACETIC ACID REACTION

A reaction following the procedures described above was stopped after 1.3 hours and the chips were rapidly removed. Any remaining PAA was quenched with excess acetaldehyde followed by washing and air drying of the chips.

Samples of reacted and unreacted chips were sent to John D. Hankey for staining. Microtome cross sections, 15 μm in thickness, of the submitted wood chips were prepared as shown in Fig. 41. Reacted and unreacted sections were mounted together on a glass slide and stained with phloroglucinol solution (1 g of phoroglucinol dissolved in a mixture of 50 ml of methyl alcohol, 50 ml of concentrated HCl and 50 ml of water).

FRACTIONATION OF WHITE BIRCH PEROXYACETIC ACID LIGNIN

PRELIMINARY EXPERIMENTS

Beer's Law

Five samples of varied concentrations were prepared by volumetrically diluting a portion of the PAA solubilized materials. Ultraviolet absorbance values at 277 nm were obtained for these samples using matching 0.1 cm path length Quarasil silica cells with distilled water in the reference cell.

Porasil B Packing

A small column (1-cm radius, 1-m length) packed to 90 cm with deaerated (4 hr), muffled (500°C for 12 hr) Porasil B was used for preliminary fractionations.

The void volume was determined by elution with Pharmacia Blue Dextran 2000. The total liquid volume of the column was determined by subtracting the dry volume of Porasil B, based on pycnometric measurements of Swenson (187) giving a specific volume of 0.448 ml/g, from the total empty volume ($\pi r^2 h$) of the column.

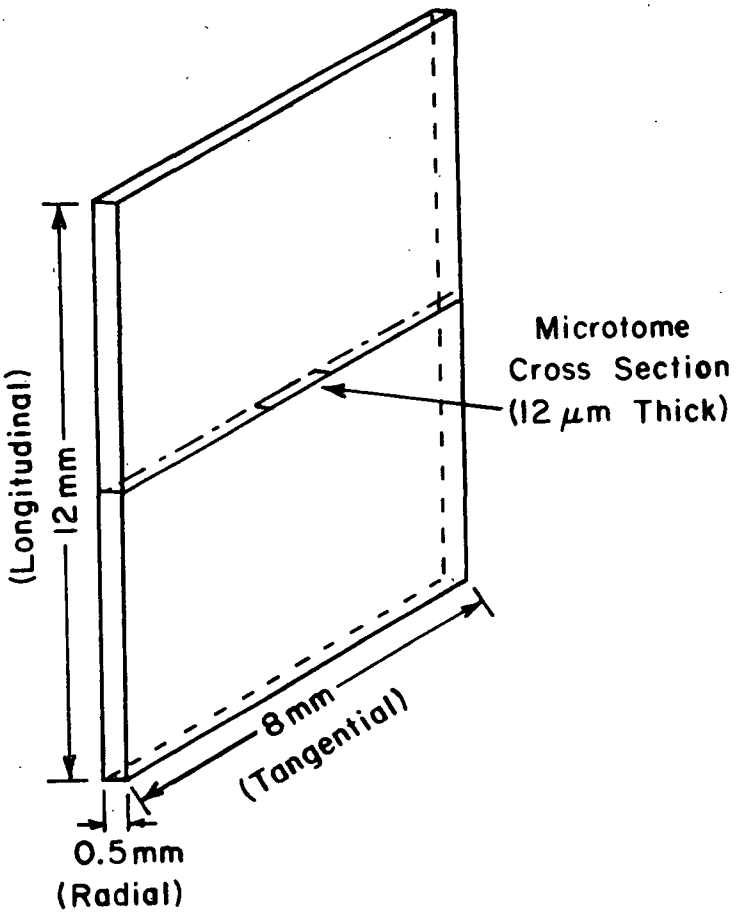

Figure 41. Sketch of Wood Wafer and Microtome Cross Section Stained

A sample (2.00 ml) of white birch PAA solubilized materials (c = 10 g/liter) was eluted through the small Porasil B column, and dried to constant weight. Another sample (2.00 ml) which did not go over the column, was similarly dried to constant weight. During elution the eluant was also monitored by ultraviolet absorbance at 280 nm.

Porasil B (2.5 g) was placed in contact with the PAA solubilized materials (5 ml) at a concentration (10 g/liter) comparable to those during fractionation. At designated times (10 min to 1 week) a portion of the solubilized materials was removed and diluted by a factor of fifty. Ultraviolet absorbance spectra were obtained for the sample which had been in contact with the Porasil B packing, and an identical sample which had not been in contact with the Porasil B packing. Also, infrared spectra of Porasil B and Porasil B which had been in contact with the solubilized materials were run. Both Porasil samples were washed with 2 liters of distilled water, dried (60°C, 30 psig), and made into pellets (2.50 mg Porasil to 500,000 mg KBr). An infrared difference spectrum, with the two different Porasils in the reference and sample beam, was obtained.

FRACTIONATION OF PEROXYACETIC ACID SOLUBILIZED MATERIALS

The fractionation of the PAA solubilized materials was accomplished on a large glass column (5.0-cm I.D., 160-cm length) located in a 72°F constant-temperature room. The eluate was continuously monitored by a Cary Model 15 spectrometer equipped with matching 0.1-cm path length Quarasil silica flow cells with distilled water in the reference cell. A siphon-manometer assembly connected to a Rinco Model VE-2002-B24 fraction collector as shown in Fig. 42 was used to collect 20-ml fractions.

Porasil B (100-200 A pore diameter) was used as the packing. The packing had been pretreated and packed as described previously (17). Glass wool was placed on top of the porasil to prevent disruption of the porasil upon sample addition. The void volume, total volume, and total liquid volume of the column were determined as described previously for the small column.

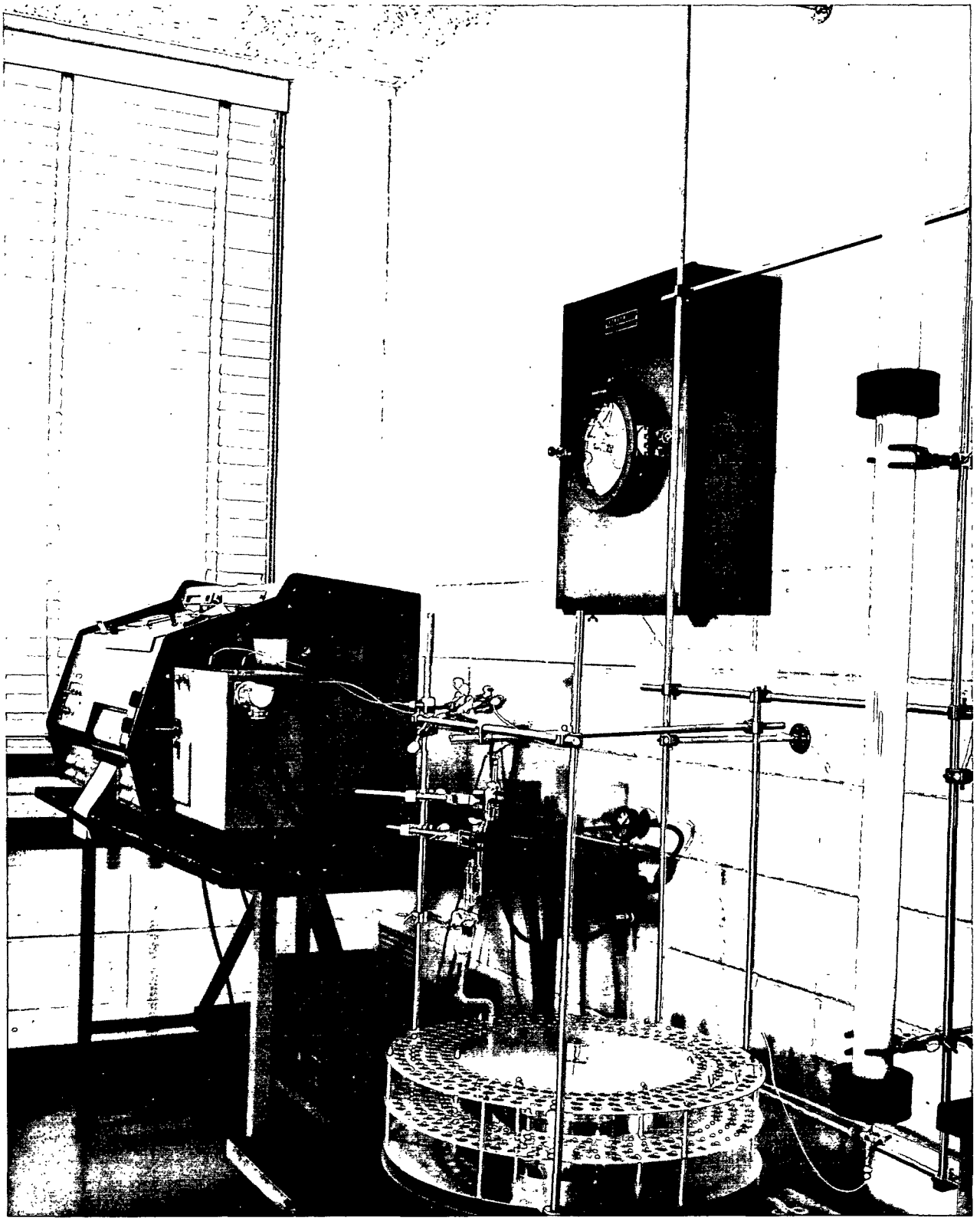

Figure 42. Fractionation Apparatus

Prior to application to the column, the PAA solubilized materials from each of the six reaction steps were concentrated to 12 g/liter. Prior to loading the column, 100-ml samples were filtered, and deaerated under vacuum for 4 hours. Deaerated, distilled water, gravity-fed at approximately 75 ml/hr was used as the elutant. The eluate was monitored by ultraviolet absorbance at 280 nm and automatically collected in 20-ml fractions until the absorbance was zero, about 160 fractions after the void volume had been reached.

All fractions were freeze-dried, with fractions prior to 66 resulting in pale-colored powders and, fractions after 66 resulting in sticky gums. The first 65 fractions were then oven-dried at 30 psig and 40°C for all reaction steps in one case. Later samples were only freeze-dried prior to collection.

To a 1000-ml sample of 3.0% PAA was added 44 ml of acetaldehyde. After addition, the sample was placed in a refrigerator until the PAA was quenched. This solution was concentrated to 100 ml, similar to the reaction steps, and fractionated.

FRACTIONATION AFTER METHYLATION (188)

Methanol was purified by adding methanol (125 ml) to iodine (0.9 g) and magnesium (9 g) with additional methanol (1575 ml) being added after the initial mixture stopped bumping. This mixture was refluxed (10 hr) and collected by distillation.

To 3.6 g of combined Fractions 1-65 for Reaction Steps 3-6 in 180 ml of methanol was added ion exchange resin (4.8 g) Amberlite IR-120. This mixture was refluxed overnight, after which the resin was removed and the methanol replaced by water. Potentiometric titrations were obtained for both methylated and unmethylated samples with (0.1N) NaOH.

Methylated and unmethylated samples (c = 12 g/liter) were fractionated as described before on the large column. Their eluates were monitored continuously by ultraviolet absorbance at 280 nm as described previously.

CHARACTERISTICS OF THE PEROXYACETIC ACID SOLUBILIZED MATERIALS

POLYSACCHARIDE CONTENT

Sugar determinations on certain freeze-dried fractions ex-Porasil B of white birch PAA solubilized materials at 5 stages of stepwise delignification were obtained using the method of Borchardt and Piper (189).

CARBOXYL CONTENT BY POTENTIOMETRIC TITRATION

The six samples of freeze-dried fractions ex-Porasil B were dried to constant weight over P_2O_5. Sixty milligrams of each were dissolved by 5.0 ml of distilled water in a 30-mm porcelain crucible. These samples were then titrated with 0.100_ NaOH. The pH of the solution was monitored by a glass-KCl/AgCl electrode, coupled to a Corning Model 12 pH meter capable of reading 0.01 pH units. The first derivative of the titration curve was used to obtain the inflection (equivalence) point.

METHOXYL DETERMINATIONS

Methoxyl contents were determined by the TAPPI T 209 sw-69 method.

INFRARED ABSORPTION BY PRESSED DISK METHOD

Freeze-dried fractions of white birch PAA solubilized materials representing early, mid, and late reaction steps as well as early, mid, and late fractions ex-Porasil B were placed in a vacuum dessicator and dried to constant weight. Samples of original wood (OW) and reacted wood (RW) (8 hr, 50°C, PAA)

were dried in a similar manner. Exactly 2.50 mg of each sample and 500.00 mg of pure KCl were mixed for one minute in a capsule vibrator. The mixed samples were dried to constant weight as before.

A sample (402.0 mg) of each mixture and 400.0 mg of pure KCl were weighed out and dried to constant weight. Pellets were made of each mixture by quantitatively transferring each mixture into the barrel chamber of the pellet dye. In the press, each pellet was evaculated for 2 minutes, pressed at 1000 psi for 3 minutes, and pressed at 22,000 psi for 10 minutes.

Regular infrared spectra were obtained with the pure KCl pellet in the reference beam to compensate for disk absorption and/or scattering. Differential spectra were obtained by placing one pellet in the sample beam and a different pellet in the reference beam. The two were then reversed to obtain the complementary differential spectra.

All regular spectra were obtained on the day on which they were made, using a Perkin-Elmer Model 700 infrared spectrometer. Differential spectra were all obtained within 2 days of when the pellets were made. Pellets were stored over P_2O_5 when not being used. ΔT 1510 cm^{-1} values were determined from spectra obtained on a Perkin-Elmer Model 621 infrared spectrometer.

PROTON MAGNETIC RESONANCE METHODS

Nine groups of freeze-dried fractions representing early, mid, and late reaction steps as well as early, mid, and late fractions ex-Porasil were placed in a vacuum desiccator and dried to constant weight over P_2O_5. Approximately 80 mg of these dried lignin fractions were dissolved in 0.4 ml of DMSO-d_6. PMR spectra of these samples were then obtained using a Varian A60A NMR spectrometer.

The 9 samples described above were also dissolved in D_2O. HDO was then removed by freeze-drying. This procedure was repeated six times under dry nitrogen atmosphere until the hydroxyl region of the PMR remained constant. PMR spectra of these samples were then obtained as described above taking care to avoid water contamination.

A sample (Reaction Step 2, Fractions 55-57) was examined by PMR at various temperatures. This sample was frozen in dry ice-acetone. PMR spectra were rapidly obtained as the solution approached room temperature. The sample was then heated in a steam bath. PMR spectra were again rapidly obtained as the solution approached room temperature.

The relative intensities of the various groups of resonances were determined by electronic integration. Integration was accomplished by zeroing the integrator between 1000 and 750 Hz and then integrating the 500 to 0 Hz region.

EVIDENCE FOR A LIGNIN-CARBOHYDRATE BOND

PAPER ELECTROPHORESIS OF FRACTIONS EX-PORASIL B

Procedures

Glass fiber* chromatography sheets (5 x 6 inches) were used as supports for the electrophoresis runs. These sheets were presoaked in buffer for at least 10 minutes prior to being used. After soaking, they were well blotted and placed in a Gelman (191) electrophoresis chamber. Magnetic grips were attached to each end of the sheets to keep them taut and in physical contact with buffer.

*The advantage of using the glass-fiber paper rather than cellulose paper is that complexes between the carbohydrates and the fiber are avoided and the location of the carbohydrates of all types is no longer a problem (190).

Once in place, the sheets were spotted (≈1 inch from the anode) with the solution (c = 1.5% in buffer) to be chromatographed. The spots contained between 30 and 40 µl of solution and were between 3 and 5 mm in diameter. The power (250 v and 40-60 ma) was then turned on and the electrophoresis allowed to proceed.*

After the desired amount of time had elapsed, the glass fiber sheets were removed horizontally from the chamber and set aside to dry. The location of the carbohydrates was determined by staining the paper with α-naphthol and sulfuric acid. The location of the lignin was determined by cutting certain sheets across the direction of current flow into 1-cm strips throughout the entire length of the sheet. The 1-cm strips were placed in distilled water and after several hours, the water was examined for its ultraviolet absorbance (lignin) at 280 nm. This location was supported by staining the paper with ρ-anisidine and sulfuric acid. The α-naphthol reagent was used for spotting the electrophoreograms shown in Fig. 24-27.

Buffer and Samples Tested

Stock (0.050N) sodium hydroxide solution was used as the buffer in the electrophoresis runs. All materials analyzed by paper electrophoresis were made up to ≈2% solids using buffer for dilution. Also, a mixture (≈2% solids) of sapote gum, freeze-dried Fractions 10-14, and 3% PAA were made up for electrophoretic measurements. This mixture was placed in a water bath at 50°C for 8 hours. Electrophoretic measurements were made both after initial mixing and after 8 hours at 50°C.

*The voltage chosen was as high as practical to bring about the maximum separation in the shortest acceptable time and yet not produce excessive heat in, and thus evaporation from, the sheet.

Staining Methods

To a solution of (1 g) α-naphthol in (5 ml) concentrated sulfuric acid was added 100-ml n-butanol. The sheets were sprayed and then heated in an oven at 110°C for 10-30 minutes. Lignin material with a small amount of carbohydrate has been shown to give a color reaction with α-naphthol, but its sensitivity is low. The associated carbohydrates in this case have not been ruled out as being responsible for the color reaction of this lignin with α-naphthol. Carbohydrates give purple spots [sensitivity, 0.04% for spruce xylan (146)]. Elm xylan and sapote gave similar colors in this study.

To a solution of (3 g) ρ-anisidine and concentrated sulfuric acid (8 ml), ethanol (100 ml) was added. The sheets were sprayed and left at room temperature for at least 5 minutes. Lignin gives light yellow spots. Xylan is known to give no color up to 1% solution (146). Upon heating at 110°C for at least 30 minutes, carbohydrate spots were observed for the ρ-anisidine spray as in other studies.

ENZYMATIC HYDROLYSIS OF FRACTIONS EX-PORASIL B (148)

A sample (133 mg) from Reaction Step 5, Fractions 8-11, was dissolved in 10 ml of a mixture of 75 parts by volume of 0.5M sodium acetate buffer at pH 5 and 25 parts of dioxane. To 5 ml of the above solution was added Onozoka SS* (1.65 ml, c = 0.25 mg/ml) which is a polysaccharidase consisting of a mixture of several polysaccharidases, including cellulase, mannanase, and xylanase.

The total mixture was placed in a 40°C constant temperature bath. Measurements of drainage times through a Cannon 50 viscometer were obtained for both blank and the solution with the enzyme. Drainage times decreased from about 590 sec initially to a nearly constant 530 sec after two days.

*This enzyme from Professor Hou-Min Chang, North Carolina State University, has been shown (148) to be inactive toward spruce dioxane lignin.

The enzyme hydrolyzate was then fractionated by gel chromatography using Sephadex G-75 as a packing in a column (52-cm length, 2-cm I.D.) with the eluant being the buffer described above. The eluant was constantly monitored for lignin by ultraviolet absorbance at 280 nm.

OPTICAL MEASUREMENTS AT DIFFERENT WAVELENGTHS OF LIGHT

Optical Rotation at 546 nm

Optical rotation determinations at 546 nm were made for samples from Reaction Steps 1-6 and groups of fractions (16-19, 42-43, 55-57). Approximately 5 ml of these samples at known concentrations between 3 and 5 mg/ml were added to a quartz 1-dm cell. Rotations were determined using a Perkin-Elmer 141 MC polarimeter. The entire system was kept at a constant 20°C. Ten individual readings were averaged to obtain the observed rotation of each sample.

Preliminary Optical Rotatory Dispersion Tests

A sample of recrystallized phenyl-β-D-glucopyranoside (c 2.50 H_2O) was prepared for an ORD determination. The rotations of this and a diluted mixture were determined at various wavelengths between 250 and 350 nm. A deuterium light source was used to second check the deuterium rotations.

Optical rotatory dispersion determinations of several of the freeze-dried fractions were attempted on the Perkin-Elmer 141 MC polarimeter. The optical rotation measurements were made until the sample absorbed all of the incident beam. Samples were then diluted until the beam could again pass through. This procedure was followed until the rotations could no longer be determined.

Optical Rotatory Dispersion and Circular Dichroism Measurements

Optical rotatory dispersion data for six representative freeze-dried fractions were obtained from the JASCO Corporation. An ORD/UV-5 instrument with

a 350 w xenon light source was used. The concentration used was approximately 1 mg/ml. Several cells were used including a 10 cm, 2 mm, and 1 mm path length. All spectra were obtained at room temperature. In addition to the six ORD curves, two circular dichroism (CD) curves were also obtained under similar conditions. A known sample of phenyl-β-D-glucopyranoside was also examined for reference purposes.

CONCLUSIONS

An experimental program was designed to isolate, fractionate, and analyze the peroxyacetic acid (PAA) solubilized materials from white birch. These materials were collected at six consecutive reaction stages and fractionated at each of these stages. From the fractionation results, it is concluded that a greater proportion of larger molecules was removed from the wood as the delignification proceeded.

Physical and chemical analyses showed that there were significant differences between the various fractions. These analyses showed that aromatic degradation occurred during delignification. Significant and orderly trends in aromatic and carbohydrate contents of the fractions were observed as a function of fraction number and percent delignification.

The lignin and carbohydrate in the fractions could not be separated by paper electrophoresis. Degradation of the carbohydrate part of the solubilized materials by an enzyme resulted in a loss of hydrodynamic size of the lignin remaining after hydrolysis. From these two results it is inductively concluded that the lignin and carbohydrate are bonded.

Variation in specific rotation as a function of fraction number and percent delignification reflected trends in polysaccharide amounts and compositions. Cotton effects in the optical rotatory dispersion (ORD) and circular dichroism (CD) curves for several of these samples provides positive evidence for a lignin-carbohydrate bond.

If the lignin and the carbohydrate are bonded, they must be removed from the wood together. Since the carbohydrate is many times larger than lignin of equivalent molecular weight, it is concluded that the bonded carbohydrates can be a significant influence in the removal of lignin from the microporous structure of wood.

ACKNOWLEDGMENTS

The author would like to express his sincere gratitude to his Thesis Advisory Committee: Drs. G. A. Nicholls (Chairman), R. H. Atalla, and D. C. Johnson, for their guidance, assistance, and many helpful discussions. The author is especially grateful to Dr. Nicholls for his advice in writing the manuscript.

The author would like to thank all of the faculty and staff members for their help in this work: especially L. G. Borchardt and J. P. Rademacher for sugar and lignin determinations, N. S. Thompson, E. E. Dickey, and I. A. Pearl for extractives of various types, J. D. Hankey for his staining work, and to the Photography Department for their many reproductions.

The author would like to thank the Forest Products Laboratory in Madison, Wisconsin, for the use of the special cutting tool. Mr. Jacques Bambling and JASCO Corporation are appreciated for their ORD and CD curves.

The Institute is wholeheartedly thanked for its financial support.

However, I am most grateful to my wife, Susan, for her lab assistance, proofreading, and typing of the complete manuscript, but mostly she is appreciated for her loving encouragement throughout.

LITERATURE CITED

1. Poljak, A., Angew. Chem. 60A(2):45(1948); ABIPC 19:389.

2. Poljak, A., Holzforschung 5(2):31(1951); ABIPC 21:839.

3. Poljak, A., Angew. Chem. 66:302(1954).

4. Haas, H., Schoch, W., and Strole, U., Papier 9(19/20):469(1955); ABIPC 26:181.

5. Leopold, B., Tappi 44(3):230(1961).

6. Thompson, N., and Kaustinen, O., Tappi 47(3):157(1964).

7. Shimada, I., and Kondo, T., J. Japan. Tappi 22(5):258(1968); ABIPC 39:A3924.

8. Yiannos, P. N., Can. Pat. 814,309(June 3, 1969).

9. Yiannos, P. N., and Britt, K. W., U.S. pat. 3,458,394(July 29, 1969).

10. Rapson, W. H., Wayman, M., and Anderson, C. B., Tappi 48(2):65(1965).

11. Wayman, M., Anderson, C., and Rapson, W. H., Tappi 48(2):113(1965).

12. Yokoo, H., J. Japan. Tappi 20(12):641(1966).

13. Taniguchi, E., J. Japan. Tappi 21(10):538(1967); ABIPC 38:A7616.

14. Polcin, J., and Rapson, W. H., Pulp Paper Mag. Can. 72(3):T114(1971).

15. Sarkanen, K. V., and Suzuki, J., Tappi 48(8):459(1965).

16. Sarkanen, K. V., and Lai, Y.-Z., Tappi 51(10):449(1968).

17. Albrecht, J. S. An investigation of the physical-chemical mechanism of selective delignification of wood with peracetic acid. Appleton, WI, The Institute of Paper Chemistry, 1971. 200 p.

18. Birch ... an American wood. U.S. Department of Agriculture Forest Service No. FS-221, 1973. 11 p.

19. Panshin, A. J., and DeZeeuw, C. Textbook of wood technology. 3rd ed. Vol. 1. p. 552. New York, McGraw-Hill, 1970.

20. Farrand, J. C. The peracetic acid oxidation of 4-methylphenols and their methyl ethers. Appleton, WI, The Institute of Paper Chemistry, 1969. 206 p.

21. Farrand, J. C., and Johnson, D. C., J. Organic Chem. 36(23):3606(1971).

22. FMC Corporation. The operation of a bench scale peracetic acid generator. New York, 1963.

23. Giguere, P. A., and Olmos, A. W., Can. J. Chem. 30:821(1952).

24. Brooks, W. V. F., and Haas, C. M., J. Phys. Chem. 71:650(1967).

25. Brauns, F. E., and Brauns, D. A. The chemistry of lignin — supplement volume. New York, Academic Press, 1965.

26. Behrman, E. J., and Edwards, J. O. Progress in physical organic chemistry. p. 73. Streitwieser, A., and Taft, R. W., eds. New York, Interscience, 1967.

27. Hatakeyama, H., Suzuki, K., Nakano, J., and Migita, N., J. Chem. Soc. Japan, Ind. Chem. Sect. 71(2):247(1968).

28. Wayman, M., Anderson, C. B., and Rapson, W. H., Pulp Paper Mag. Can. 69 (9):51(T225-34)(1968).

29. Endo, A., Saito, M., Yoshida, M., and Fusezaki, Y., J. Chem. Soc. Japan, Pure Chem. Sect. 88(1):83(1967); ABIPC 38:A6908.

30. Sakai, K., and Kondo, T., J. Jap. Wood Res. Soc. 21(1):39(1975).

31. Hatakeyama, H., Nakano, J., and Migita, N., J. Chem. Soc. Japan, Ind. Chem. Sect. 68(5):52A, 972(1965); ABIPC 36:A3213.

32. Ishikawa, H., Oki, T., and Okubo, K., J. Japan. Tappi 20(8):435(1966); ABIPC 37:A8913.

33. Kinoshita, Y., Oki, T., and Ishikawa, H., J. Jap. Wood Res. Soc. 13(7):319 (1967); ABIPC 38:A8316.

34. Oki, T., Okubo, K., and Ishikawa, H., J. Jap. Wood Res. Soc. 18(12):601(1972).

35. Oki, T., Okubo, K., and Ishikawa, H., J. Jap. Wood Res. Soc. 20(2):89(1974).

36. Oki, T., Okubo, K., and Ishikawa, H., J. Jap. Wood Res. Soc. 20(11):549(1974).

37. Strumila, G., and Rapson, W. H., CPPA Ann. Mtg. (Montreal) 60, Preprints Book B:9-18(1974).

38. Ishikawa, H., Okubo, K., Oki, T., and Watanabe, S., J. Japan. Tappi 19(8): 393(1965); ABIPC 36:A5497.

39. Davidage, H., Davis, A. G., Kenyon, J., and Mason, R. F., J. Chem. Soc., 1958:4569.

40. Ishikawa, H., Kinoshita, Y., Oki, T., Okubo, K., J. Japan. Tappi 21(9): 494(1967); ABIPC 38:A7503.

41. Ishikawa, H., Oki, T., and Okubo, K., J. Japan. Tappi 20(9):485(1966); ABIPC 37:A8914.

42. Hatakeyama, H., Nakano, J., and Migita, N., J. Chem. Soc. Japan, Ind. Chem. Sect. 70(6):957(1967); ABIPC 38:A7496.

43. Hatakeyama, H., Suzuki, K., Mishizuka, G., Nakano, J., and Migita, N., J. Chem. Soc. Japan, Ind. Chem. Sect. 70(8):1399(1967); ABIPC 39:A208.

44. Sakai, K., and Kondo, T., J. Jap. Wood Res. Soc. 12(6):310(1966); ABIPC 38: A7518.

45. Sakai, K., and Kishimoto, S., J. Jap. Wood Res. Soc. 14(8):411(1968).

46. Kono, M., Sakai, K., and Kondo, T., J. Japan. Tappi 19(1):27(1965); ABIPC 35:A8076.

47. Anon., Chem. Week 95(18):46, 48(1964).

48. Havel, S., Chem. Prumsyl 15(2):68(1965).

49. Rydholm, S. A. Pulping processes. p. 1093. New York, Interscience, 1965.

50. Swern, D. Organic peroxides. New York, Wiley-Interscience, 1970.

51. Sakai, K., Kuroda, K., and Kishimoto, S., Tappi 55(12):1702(1972).

52. Wiesner, J. V., and Lippman, E. O. V., after Grafe, V., Monatsh. 25:990(1904).

53. Hagglund, E. Chemistry of wood. Chapter 3. New York, Academic Press, 1951.

54. Adler, E., Bjorkqvist, K. J., and Haggroth, S., Acta Chem. Scand. 2(1):93 (1948).

55. Adler, E., and Ellmer, L. R., Acta Chem. Scand. 2(9):839(1948).

56. Brauns, F. E., J. Am. Chem. Soc. 61:2120(1939).

57. Fleck, J. A. The investigation of peracetic acid oxidized loblolly pine by pyrolysis-gas chromatography-mass spectrometry. Appleton, WI, The Institute of Paper Chemistry, 1975. 214 p.

58. Jensen, W., Fremer, K.-E., and Forss, K., Tappi 45(2):122(1962).

59. Forss, K., and Fremer, K.-E., Tappi 47(8):485(1964).

60. Forss, K., and Fremer, K.-E., Paperi Puu 47(8):443(1965).

61. Forss, K., Fremer, K.-E., and Stenlund, B., Paperi Puu 48(9):565; (11):669 (1966).

62. Felicetta, V. F., Glennie, D., and McCarthy, J. L., Tappi 50(4):170(1967).

63. Gupta, P. R., and McCarthy, J. L., Macromolecules 1(3):236(1968).

64. Gupta, P. R., and McCarthy, J. L., Macromolecules 1(6):495(1968).

65. Forss, K., and Stenlund, B., Paperi Puu 51(1):93(1969).

66. Stenlund, B., Paperi Puu 52(2):55(1970).

67. Stenlund, B., Paperi Puu 52(3):121(1970).

68. Krause, T., and Bottger, J., Papier 27(10A):457(1973).

69. Flodin, P. Uppsala, Sweden, Thesis, University of Uppsala, 1962.

70. Ackers, G. K., Biochemistry 3(5):723(1964).

71. DeVries, A. J., LePage, M., Beau, R., and Guillemin, C. L., Anal. Chem. 39(8):935(1967).

72. Cazes, J., J. Chem. Ed. 43(7):A567, A625(1966).

73. Cazes, J., J. Chem. Ed. 47(7):A461, A505(1970).

74. Bly, D. D., Science 168(3931):527(1970).

75. Porath, J., Biochim. Biophys. Acta 39:193(1960).

76. Gelotte, B., J. Chromat. 3:330(1960).

77. Beau, R., LePage, M., and DeVries, A. J., Applied Polymer Symposia 8:137 (1969).

78. Sjostrom, E., and Enstrom, B., Svensk Papperstid. 69(15):469(1966).

79. Simonson, R., Svensk Papperstid. 74(21):604(1971).

80. Ahlgren, P. A., Yean, W. Q., and Goring, D. A. I., Tappi 54(5):737(1971).

81. Rezanowich, A., Yean, W. Q., and Goring, D. A. I., Svensk Papperstid. 66(5): 141(March, 1963).

82. Yean, W. Q., and Goring, D. A. I., Pulp Paper Mag. Can. 65:T127(1964).

83. Yean, W. Q., and Goring, D. A. I., Svensk Papperstid. 71(20):739(Oct., 1968).

84. Albrecht, J. S., and Nicholls, G. A., Paperi Puu 58(2):49(1976).

85. Goring, D. A. I. Polymer properties of lignin and lignin derivatives. In Sarkanen and Ludwig's Lignins. Chapter 17. New York, Wiley, 1971.

86. Ahlgren, P. A., and Goring, D. A. I., Can. J. Chem. 49:1272(1971).

87. Kerr, A. J. Physicochemical mechanisms of delignification. Doctoral Dissertation. McGill University, 1974.

88. Okubo, K., Oki, T., Kinoshita, Y., and Ishikawa, H., J. Japan. Tappi 23(12): 509(1969).

89. Albrecht, J. S., and Nicholls, G. A., Paperi Puu 56(11):927(1974).

90. Sarkanen, K. V., and Hergert, H. L. Classification and distribution. In Sarkanen and Ludwig's Lignins. Chapter 3. New York, Wiley, 1971.

91. Hergert, H. L. Infrared spectra. In Sarkanen and Ludwig's Lignins. Chapter 7. New York, Wiley, 1971.

92. Jones, E. J., J. Am. Chem. Soc. 70(5):1984(1948).

93. Jones, E. J., Tappi 32(4):167(1949).

94. Marchessault, R. H., Pure Appl. Chem. 5(1/2):107(1962).

95. Michell, A. J., Aust. J. Chem. 19(12):2285(1966).

96. Lindberg, J. J., and Kenttamaa, J., Suomen Kemistilehti 32B:193(1959).

97. Lindberg, J. J., Paperi Puu 43(11):672(1961).

98. Lindberg, J. J., Finska Kem. Medd. 69(1):11(1960).

99. Bolker, H. I., and Somerville, N. G., Pulp Paper Mag. Can. 64(4):T187(1963).

100. Michell, A. J., Watson, A. J., and Higgins, H. G., Tappi 48(9):520(1965).

101. Bellamy, L. J. The infrared spectra of complex molecules. 2nd ed. London, Methuen, 1958.

102. Harrington, K. J., Higgins, H. G., and Michell, A. J., Holzforschung 18(4): 108(1964).

103. Durie, I. A., Lynch, B. M., and Sternhell, S., Aust. J. Chem. 13(8):156(1960).

104. Hergert, H. L., J. Org. Chem. 25(3):405(1960).

105. Marchessault, R. H. In Proc. IUPAC Wood Chemistry Symposium, Montreal, 1961. London, Butterworths, 1962.

106. Marchessault, R. H., and Liang, C.-Y., J. Polymer Sci. 59(168):357(1962).

107. Silverstein, R. M., and Bassler, G. C. Spectrometric identification of organic compounds. New York, Wiley, 1968.

108. Higgins, H. G., Stewart, C. M., and Harrington, K. J., J. Polymer Sci. 51(155):59(1961).

109. Liang, C.-Y., Basset, K. H., McGinnes, E. A., and Marchessault, R. H., Tappi 43(12):1017(1960).

110. Marton, J., Alder, E., and Persson, K., Acta Chem. Scand. 15(1):284(1961).

111. Bolker, H. I., Nature 197(2):489(1963).

112. Wexler, A. S., Anal. Chem. 36(1):213(1964).

113. Kolboe, S., and Ellefsen, O., Tappi 45(2):163(1962).

114. Sarkanen, K. V., Chang, H.-M., and Allan, G. G., Tappi 50(12):583(1967).

115. Dandarova-Vasatkava, M., Polcin, J., Kosikova, B., and Joniak, D., Holzforschung 23(4):127(1969).

116. Rydholm, S. A. Pulping processes. p. 182. New York, Interscience, 1965.

117. Sarkanen, K. V., Chang, H.-M., and Ericsson, B., Tappi 50(11):572(1967).

118. Sundholm, F., Acta Chem. Scand. 22(3):854(1968).

119. Pearl, I. A., J. Org. Chem. 24(6):736(1959).

120. Marton, J., and Sparks, H. E., Tappi 50(7):363(1967).

121. Bland, D. E., and Logan, A. F., Biochem. J. 95(2):515(1965).

122. Liang, C.-Y., and Marchessault, R. H., J. Polymer Sci. 39(135):269(1959).

123. Barker, S. A., Bourne, E. J., Stacey, M., and Whiffen, D. H., J. Chem. Soc. 1954:171.

124. Whiffen, D. H., Spectrochim. Acta 7:253(1955).

125. Vodnansky, J., Slabina, M., and Schneider, B., Coll. Czech. Chem. Comm. 28(12):3245(1963).

126. Sjoholm, R., and Bruun, H. H., Suomen Kemistilehti 39A:121(1966).

127. Jayme, G., and Rogmann, E. M., Papier 19(10A):719(1965).

128. Faix, O., and Schweers, W., Holzforschung 28(2):50(1974).

129. Merewether, J. W. T., and Samsuzzaman, L. A. M., Holzforschung 26(1):11(1972).

130. Salama, C., Can. Spectroscopy 9(8):145(1964).

131. Browning, B. L. The methods of wood chemistry. p. 750. New York, Interscience, 1967.

132. Kosikova, V. B., Polcin, J., Dandarova-Vasatkova, M., and Joniak, D., Holzforschung 23(2):43(1969).

133. Smith, D. C. C., J. Chem. Soc. 1955:2347.

134. Nakanishi, K. Infrared absorption spectroscopy. p. 42-8. Tokyo, Holden-Day, 1962.

135. Kawamura, I., and Higuchi, T., J. Jap. Wood Res. Soc. 10(5):200(1964).

136. Sarkanen, K. V., Chang, H. M., and Chang, G. G., Tappi 50(12):587(1967).

137. Ludwig, C. H. Magnetic resonance spectra. In Sarkanen and Ludwig's Lignins. Chapter 8. New York, Wiley, 1971.

138. Ludwig, C. H., Nist, B. J., and McCarthy, J. L., J. Am. Chem. Soc. 86(6): 1186(1964).

139. Ludwig, C. H., Nist, B. J., and McCarthy, J. L., J. Am. Chem. Soc. 86(6): 1196(1964).

140. Katuscak, S., Rybarik, I., Paulinyova, E., and Mahdalik, M., Papper Tra 53 (11):665(1971).

141. Consden, R., Gorden, A. H., and Martin, A. J. P., Biochem. J. 38(3):224 (1944).

142. Chang, H.-M., and Allan, G. G. Oxidation. In Sarkanen and Ludwig's Lignins. Chapter 11. New York, Wiley, 1971.

143. Okubo, K., Oki, T., Kinoshita, Y., and Ishikawa, H., J. Japan. Tappi 23(12):509(1969); ABIPC 40:A9001.

144. Neimo, L., Baczynska, K., and Sihtola, H., Paperi Puu 47(2):43, 54(1965).

145. Taniguchi, E., J. Japan. Tappi 19(6):283(1965); ABIPC 36:A4858.

146. Lindgren, B. O., Acta Chem. Scand. 12(3):447(1958).

147. Dudkin, M. S., and Shkanlova, N. G., Zh. Prikl. Khim. 43(1):206(1970); ABIPC 42:A2444.

148. Cheng, C.-W. Existance and nature of covalent bonds between lignin and polysaccharides in spruce sapwood. North Carolina State University, 1972. 105 p.

149. Simonson, R., Svensk Papperstid. 74(19):604(1971).

150. Bolker, H. I., and Wang, P. Y., Tappi 52(5):920(1969).

151. Harris, E. E., Ind. Eng. Chem. 32(8):1049(1940).

152. Schubert, W. J., and Nord, F. F., J. Am. Chem. Soc. 72(2):977(1950).

153. Schubert, W. J., and Nord, F. F., J. Am. Chem. Soc. 72(9):3835(1950).

154. Pew, J. C., Tappi 40(7):553(1957).

155. Kringstad, K. P., Norsk Skogin. 21(6):210(1967).

156. Biot, B. J., Ann. Chem. Phys. 2:41(1817).

157. Simon, S. J., and Pearson, K. H., Ann. Chem. 45(3):620(1973).

158. Listowski, I., Avigad, G., and Englard, S., J. Am. Chem. Soc. 87(8):1766(1965).

159. Rao, V. S. R., and Foster, J. F., Nature 200(11):570(1963).

160. Haidinger, W., Ann. Phys. 70:531(1847).

161. Djerassi, C., Wolf, H., Lightner, D. A., Bennenberg, E., Takeda, K., Komeno, T., and Kuriyama, K., Tetrahedron 19:1547(1963).

162. Crabbe, P. ORD and CD in chemistry and biochemistry. New York, Academic Press, 1972.

163. Kauzmann, W. Quantum chemistry. New York, Academic Press, 1966.

164. Baumann, R. P. Absorption spectroscopy. New York, John Wiley and Sons, 1962.

165. Crabbe, P., and Klyne, W., Tetrahedron 23:3449(1967).

166. Verbit, L., J. Am. Chem. Soc. 87(4):1617(1965).

167. Hooker, T. M., and Tanford, C., J. Am. Chem. Soc. 86(11):4989(1964).

168. Rosenberg, A., J. Bio. Chem. 241(10):5119(1966).

169. Klyne, W., Tetrahedron 13:29(1961).

170. Djerassi, C., and Geller, L. E., J. Am. Chem. Soc. 81(6):2789(1959).

171. Lyle, G. G., J. Org. Chem. 25(10):1779(1960).

172. Marchessault, R. H., Mukherjee, S., and Sarko, A., Biopolymers 11(1):291, 303(1972).

173. Klyne, W., and Scopes, P. M. Carboxylic acids, lactones, and related compounds. In Snatzke's Optical rotatory dispersion and circular dichroism in organic chemistry. Chapter 12. London, Heyden, 1967.

174. Jennings, J. P., Klyne, W., and Scopes, P. M., J. Chem. Soc. (12):7211(1965).

175. Sticzay, T., Peciar, C., and Bauer, S., Tetrahedron 25:3521(1969).

176. Kirk, D. N., Klyne, W., and Wallis, S. R., J. Chem. Soc. C(2):350(1970).

177. Mulliken, R. S., and Person, W. B. Molecular complexes. p. 121. New York, Wiley-Interscience, 1969.

178. Tsuzuki, Y., Katasoka, S., Funayama, M., and Satsumaboyashi, K., Bull. Chem. Soc. Japan 44(2):526(1971).

179. Tsuzuki, Y., Koyama, M., Aoki, K., Kato, T., and Tanabe, K., Bull. Chem. Soc. Japan 42(4):1052(1969).

180. Geczy, I., Cell. Chem. Tech. 4:245(1970).

181. Whistler, R. L., and Tu, C.-C., J. Am. Chem. Soc. 74:3609(1952).

182. Wolfrom, M. L., and Dacons, J. C., J. Am. Chem. Soc. 74:5331(1952).

183. Bouveng, H. D., and Meier, H., Acta Chem. Scand. 13:1884(1959).

184. Crabbe, P. ORD and CD in chemistry and biochemistry. p. 129-37. New York, Academic Press, 1972.

185. Sully, B. D., and Williams, P. L., The Analyst 87:653(1962).

186. Institute Method No. 3, 1951.

187. Swenson, H. A. Personal communication.

188. Cadotte, J. E., Smith, F., and Spriestersbach, D., J. Am. Chem. Soc. 74(3):1505(1952).

189. Borchardt, L. G., and Piper, C. V., Tappi 53(2):257(1970).

190. Bourne, E. J., Foster, A. B., and Grant, P. M., J. Chem. Soc. (11):4311 (1956).

191. The Gelman Instrument Company. Instructions for rapid electrophoresis. Chelsea, Michigan, 1965.

APPENDIX I

GENERATION OF PEROXYACETIC ACID

PASSIVATION OF GENERATOR

Peroxyacetic acid in the presence of contaminants, especially trace metal ions, readily decomposes to hydrogen peroxide and acetic acid. To prevent this, all materials which were to come into contact with the peroxyacetic acid were passivated by following the procedure outlined by the FMC Corporation (22) which includes the following:

(1) degreasing and washing with Alconox,

(2) rinsing with distilled water,

(3) filling all containers and piping with 0.5% NaOH and allowing it to stand for 15 minutes at room temperature,

(4) draining and rinsing with distilled water,

(5) filling with 35% HNO_3 and allowing it to stand at room temperature for 45 minutes,

(6) repeating Step 4,

(7) filling with 35% H_2O_2 and allowing it to stand overnight at room temperature with venting for O_2 liberation, and

(8) repeating Step 4.

GENERATING PEROXYACETIC ACID

Peroxyacetic acid was generated from a mixture of hydrogen peroxide and acetic acid following the procedure outlined by the FMC Corporation (22).

$$CH_3COOH + H_2O_2 \xrightarrow{H_2SO_4} CH_3CO_3H + H_2O$$

The initial charge to the reactor contained the following:

(1) H_2O, 114 g

(2) H_2SO_4, 115 g

(3) CH_3CO_2H, 51.2 g

(4) 50% H_2O_2, 270 g

(5) dipicolinic acid, 0.275 g

This solution was about 32% H_2O_2.

The feed solution contained the following:

(1) H_2O, 590 g

(2) CH_3CO_2H, 440 g

(3) 50% H_2O_2, 470 g

This solution was approximately 18% H_2O_2.

The generator operating conditions were the following:

(1) bath temperature, 80-84°C

(2) reactor temperature, 57-60°C

(3) vapor temperature, 45-50°C

(4) pressure, 40-60 mm Hg

When these conditions were employed, about 1500 g of 36% peroxyacetic acid were produced at about 2 ml/min.

ANALYSES OF PEROXYACETIC ACID (180)

One-hundred milliliters of 0.1N acetic acid were placed in a 500-ml Erlenmeyer flask immersed in an ice water bath. After the temperature had fallen below 5°C, an accurately weighed sample of the peroxyacetic acid solution was added to the

flask. Ten milliliters of KI (15% w/v) were added, and, at that time, a stopwatch was started. An initial buret reading (x_i) was recorded and the liberated iodine was titrated with 0.1N thiosulfate. As the first end point was reached with thyodene as indicator, the buret reading (x_1) and the stopwatch reading (t_1) were noted when the blue color returned. The titration was continued to a second buret reading (x_2) and corresponding time (t_2) of reappearance of the blue color. The titration was continued to an end point (x_t) after the addition of ammonium molybdate (10% w/v) which remained stable for one minute.

The concentrations of peroxyacetic acid and hydrogen peroxide were calculated using the following equations:

$$\text{PAA titer at time zero, } x_o = x_1 - \frac{t_1(x_2-x_1)}{t_2-t_1}$$

$$\text{PAA, \%} = 0.3803\ (x_o-x_i)/w$$

$$H_2O_2\text{, \%} = 0.1701\ (x_t-x_o)/w$$

where w = solution weight (g). No hydrogen peroxide could be found immediately after peroxyacetic acid production; therefore, the peroxyacetic acid was used immediately after production.

APPENDIX II

COMPUTER PROGRAM FOR NORMALIZING ABSORPTION CURVES

```
DIMENSION FRACNC(200), ABSORB(200), ABNORM(200), IIX(10), IIY(10)
CALL ITLZ
CALL DPT(1,4)
CALL PLOT (0., -11., -3)
CALL PLOT (0., 2., -3)
READ(5,9001) IIX,IIY
FORMAT(10A4/10A4)
CALL AXIS (0.,0.,IIX                    ,-18,13.,0.,0.,12.0)
CALL AXIS (0.,0.,IIY                          , 22,8.,90.,0.,0.005)
IX = 0
WRITE (6,101)
READ (5,201) RXSEG
IF (RXSEG) 2,30,2
WRITE (6,301) RXSEG
READ (5,202) K
WRITE (6,302) K
READ (5,203)(FRACNO(I),ABSORB(I), I=1,K)
SUM = 0.0
DO 10 I = 1,K
SUM = SUM + ABSORB(I)
CONTINUE
WRITE (6,303) SUM
WRITE (6,102)
DO 20 I = 1,K
ABNORM(I) = ABSORB(I)/SUM
CONTINUE
WRITE (6,304)(FRACNO(I),ABNORM(I), I=1,K)
FRACNO(K+1) = 0.0
FRACNO(K+2) = 12.0
ABNORM(K+1) = 0.0
ABNORM(K+2) = 0.005
IX = IX + 1
CALL LINE (FRACNO, ABNORM, K, 1, -1, IX)
GO TO 1
CALL FINAL
CALL EXIT
FORMAT ( '1NORMALIZED ELUTION CURVES FOR REACTION ALIQUOTS FROM DEC.
1973'/)
FORMAT (10X,' FRACTION NUMBER', 10X,' NORMALIZED ABSORBANCE AT 280
NM.'/)
FORMAT (I1)
FORMAT (I3)
FORMAT (2F10.5)
FORMAT (' REACTION SEGMENT NUMBER = ' I1/)
FORMAT (' NUMBER OF FRACTIONS = ' I3/)
FORMAT (' SUM = ' F12.8/)
FORMAT (13X, F10.5, 15X, F12.8)
END
```

APPENDIX III

NORMALIZED ABSORPTION VERSUS FRACTION CURVES

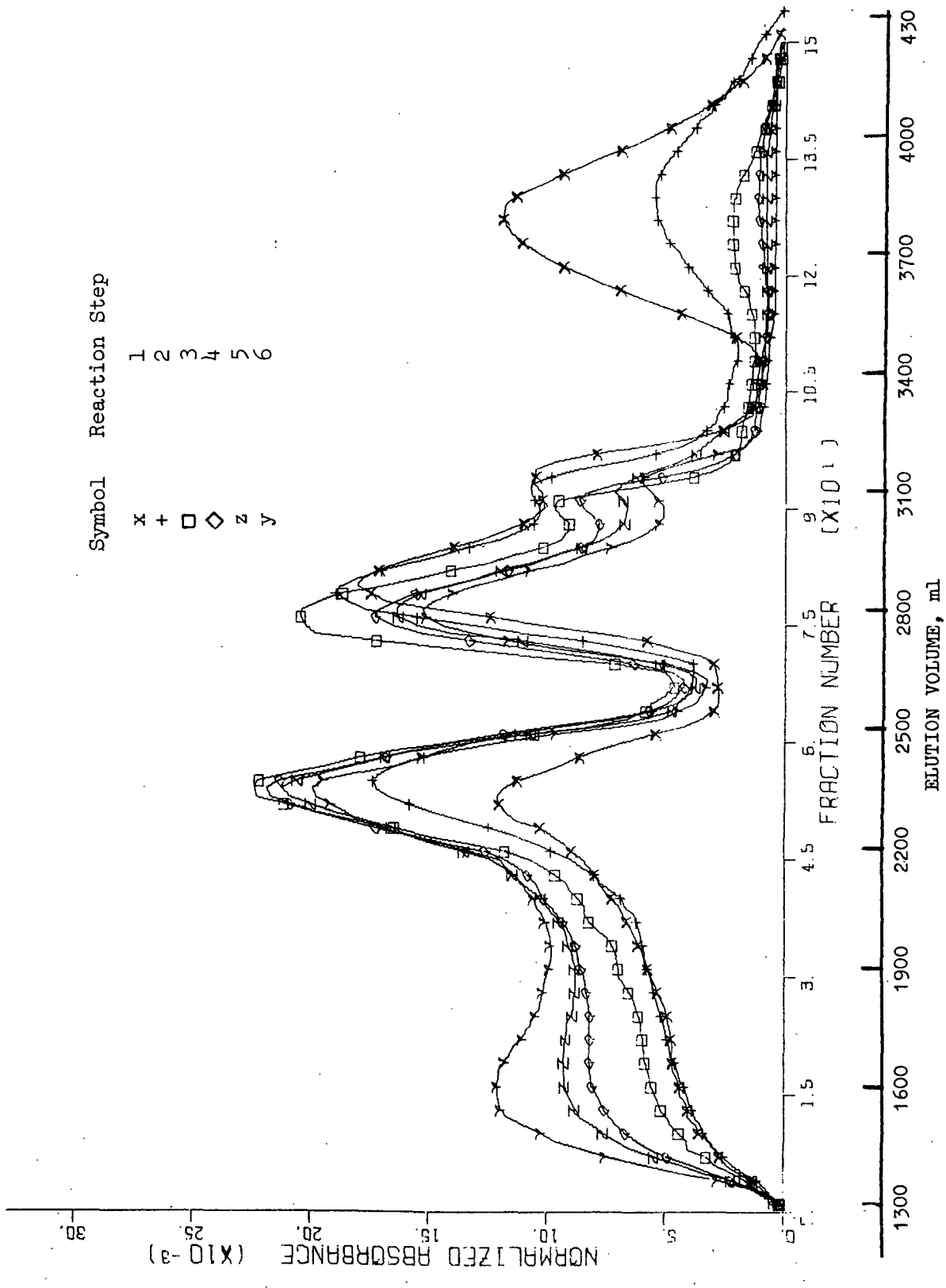

APPENDIX IV

ABSORPTIVITY (1/G CM) OF FREEZE-DRIED FRACTIONS EX-PORASIL B

TABLE XI

Fractions	% Delignification					
	6.3	23.9	45.9	63.1	77.5	84.7
1-7	0.8	2.8	3.5	3.1	2.2	3.1
8-11	4.8	4.7	--	5.2	4.1	4.6
12-15	--	6.6	8.1	5.9	5.5	5.2
16-19	6.0	7.9	8.3	6.4	5.4	5.9
20-23	6.1	7.0	8.8	6.8	--	6.4
24-27	6.4	8.3	8.4	6.2	5.6	6.3
28-30	6.5	7.8	8.4	5.9	5.3	6.1
31-33	6.7	7.3	7.7	6.1	4.8	6.0
34-36	6.7	7.4	7.9	5.9	5.0	6.3
37-39	7.0	6.9	7.7	6.4	5.1	5.9
40-41	6.2	7.1	7.8	7.3	4.8	5.6
42-43	7.4	8.6	7.4	6.5	5.1	5.4
44-45	7.1	5.7	8.0	5.9	5.1	5.3
46-47	10.3	5.3	8.5	7.3	4.8	4.9
48-49	8.9	5.9	9.0	7.2	5.2	5.2
50-51	8.6	7.0	9.3	--	5.3	5.4
52-54	8.3	6.4	9.9	7.4	6.2	6.0
55-57	8.3	8.4	9.0	--	6.6	6.6
58-61	11.3	11.0	9.6	7.9	9.0	7.1
62-65	5.7	6.7	6.7	7.6	5.8	6.6

TABLE XII

Fractions	Sugars	Reaction Step — % Sugar					
		1[b] %[c]	2 %	3 %	4 %	5 %	6 %
12-15	X[a]	2.8(31.1)	2.9(43.3)	4.2(44.7)	7.2(68.6)	12.4(72.9)	19.1(76.7)
	D	2.3(25.6)	1.8(26.9)	3.2(34.0)	0.9 (8.6)	1.3 (7.6)	1.7 (6.8)
	G	2.1(23.3)	1.0(14.9)	1.0(10.6)	1.1(10.5)	1.8(10.6)	2.2 (8.8)
	A	1.2(13.3)	0.5 (7.5)	0.5 (5.3)	0.8 (7.6)	1.1 (6.5)	1.3 (5.2)
	M	011 (1.1)	0.2 (3.0)	0.2 (2.1)	0.2 (1.9)	0.1 (0.6)	0.1 (0.4)
	R	0.5 (5.6)	0.3 (4.5)	0.3 (3.2)	0.3 (2.9)	0.3 (1.8)	0.5 (2.0)
	Total	9.0	6.7	9.4	10.5	17.0	24.9
28-30	X	1.5(42.5)	1.3(48.7)	2.2(56.0)	3.8(64.0)	6.4(69.1)	11.1(79.3)
	D	1.2(34.0)	0.9(33.7)	0.8(20.4)	1.2(20.2)	1.6(17.3)	0.8 (5.7)
	G	0.5(14.2)	0.3(11.2)	0.5(12.7)	0.4 (6.7)	0.5 (5.4)	1.0 (7.3)
	A	0.2 (5.7)	0.1 (3.7)	0.2 (5.1)	0.4 (6.7)	0.6 (6.5)	0.8 (5.7)
	M	0.07(2.0)	0.05(1.9)	0.2 (5.1)	0.1 (1.7)	0.1 (1.1)	0.2 (1.4)
	R	0.06(1.7)	0.02(0.7)	0.03(0.8)	0.04(0.7)	0.06(0.6)	0.09(0.6)
	Total	3.53	2.67	3.93	5.94	9.26	13.99
44-45	X	1.7(42.2)	1.2(53.6)	1.5(55.8)	3.7(69.7)	6.7(77.5)	10.8(83.7)
	D	1.3(32.3)	0.4(17.9)	0.4(14.8)	0.4 (7.5)	0.5 (5.8)	0.4 (3.1)
	G	0.6(14.9)	0.4(17.9)	0.4(14.8)	0.5 (9.4)	0.5 (5.8)	0.6 (4.6)
	A	0.3 (7.4)	0.2 (8.9)	0.3(11.2)	0.5 (9.4)	0.6 (6.9)	0.8 (6.2)
	M	0.1 (2.5)	0.03(1.3)	0.08(3.0)	0.2 (3.8)	0.3 (3.5)	0.2 (1.6)
	R	0.03(0.7)	0.01(0.4)	0.01(0.4)	0.01(0.2)	0.04(0.5)	0.1 (0.8)
	Total	4.03	2.24	2.69	5.31	8.64	12.9
52-54	X	2.0(45.2)	1.4(59.1)	1.9(55.1)	4.4(76.8)	7.9(79.0)	12.9(80.1)
	D	1.2(27.1)	0.4(16.9)	0.5(14.6)	0.2 (3.5)	0.3 (3.0)	0.6 (3.7)
	G	0.6(13.6)	0.2 (8.4)	0.5(14.6)	0.3 (5.2)	0.6 (6.0)	0.9 (5.6)
	A	0.4 (9.0)	0.3(12.7)	0.4(11.7)	0.6(10.5)	0.8 (8.0)	1.0 (6.2)
	M	0.2 (4.5)	0.06(2.5)	0.1 (2.9)	0.2 (3.5)	0.3 (3.0)	0.6 (3.7)
	R	0.02(0.5)	0.01(0.4)	0.03(0.9)	0.03(0.5)	0.1 (1.0)	0.1 (0.6)
	Total	4.42	2.37	3.43	5.73	10.0	16.1
58-61	X	2.0(40.7)	2.2(51.9)	3.0(64.7)	5.0(61.0)	10.3(70.5)	15.1(79.9)
	D	1.3(26.4)	0.7(16.5)	0.3 (6.5)	0.8 (9.8)	1.3 (8.9)	0.7 (3.7)
	G	0.7(14.2)	0.2 (4.7)	0.4 (8.6)	0.7 (8.5)	0.8 (5.5)	0.9 (4.8)
	A	0.5(10.2)	0.6(14.2)	0.5(10.8)	0.9(11.0)	1.2 (8.2)	1.4 (7.4)
	M	0.4 (8.1)	0.5(11.8)	0.4 (8.6)	0.7 (8.5)	0.8 (5.5)	0.6 (3.2)
	R	0.02(0.4)	0.04(0.9)	0.04(0.9)	0.1 (1.2)	0.2 (1.4)	0.2 (1.1)
	Total	4.92	4.24	4.64	8.2	14.6	18.9

[a] Sugars, expressed as a percentage of the total material in the freeze-dried fractions; X = xylan, D = glucan, G = galactan, A = araban, M = mannan, and R = rhamnan.

[b] Reaction Steps: 1 = 6.3%, 2 = 23.9%, 3 = 45.9%, 4 = 63.1%, 5 = 77.5%, and 6 = 84.7% delignification.

[c] Sugars, expressed as a percentage of the total saccharides present in the freeze-dried fractions.

APPENDIX VI

COMPUTER PROGRAM FOR POTENTIOMETRIC TITRATIONS

```
/ID 94000180,AG
/JOB GO,TIME=99
/FTC LIST
BPS FORTRAN D COMPILER
 S.0001            DIMENSION PH(100), BASEML(100), DELTAI(100)
 S.0002            CALL ITLZ
 S.0003            CALL OPT(1,4)
 S.0004            CALL PLOT (0., -11., -3)
 S.0005            CALL PLOT (0., 2.0, -3)
 S.0006       100  WRITE (6,1)
 S.0007            READ (5,200)ALIQBL
 S.0008            WRITE (6,2)ALIQBL
 S.0009            READ (5,300) K
 S.0010            WRITE (6,3) K
 S.0011            WRITE (6,4)
 S.0012            READ (5,301) (BASEML(I), PH(I), I = 1,K)
 S.0013            WRITE (6,302) (BASEML(I), PH(I), I = 1,K)
 S.0014            BASEML(K+1) = 0.
 S.0015            BASEML(K+2) = .0010
 S.0016            PH(K+1) = 0.
 S.0017            PH(K+2) = 2.
 S.0018            CALL AXIS  (0., 0., IIX, -18, 10., 0., 0., 0.0010)
 S.0019            CALL AXIS (0., 0., IIY, 13, 8., 90., 0., 2.0)
 S.0020            CALL LINE (BASEML, PH, K, 1, -1, 2)
 S.0021            CALL PLOT (16.0, 0.0, -3)
 S.0022            L = 0
 S.0023            M = K-1
 S.0024            DO 10 I = 1,M
 S.0025            L = L+1
 S.0026            DELTAI(L) = (PH(I+1) - PH(I))/(BASEML(I+1) - BASEML(I))
 S.0027            BASEML(L) = (BASEML(I+1) + BASEML(I))/2.0
 S   28        10  CONTINUE
 S.0029            BASEML(L+1) = 0.
 S.0030            BASEML(L+2) = .0010
 S.0031            DELTAI(L+1) = 0.
 S.0032            DELTAI(L+2) = 2000.
 S.0033            CALL AXIS (0., 0., IIW, -18, 10., 0., 0., 0.0010)
 S.0034            CALL AXIS (0., 0., IIZ, 13, 8., 90., 0., 2000.)
 S.0035            CALL LINE (BASEML, DELTAI, K-1,1,-1, 2)
 S.0036            CALL PLOT (16.0, 0.0, -3)
 S.0037            GO TO 100
 S.0038          1 FORMAT ('1POTENTIOMETRIC TITRATION OF FRACTIONATED LIGNIN'/)
 S.0039          2 FORMAT (' ALIQUOT AND BLOCK NUMBERS ARE ' 2F5.2/)
 S.0040          3 FORMAT (' NO. OF OBSERVATIONS = ' I2/)
 S.0041          4 FORMAT (10X, ' MILLIEQUIVS. 0.1N NAOH/MG. OF SAMPLE', 10X, ' PH'/)
 S.0042        200 FORMAT (2F5.2)
 S.0043        300 FORMAT (I2)
 S.0044        301 FORMAT (2F10.6)
 S.0045        302 FORMAT (27X, F10.6, 24X, F10.6)
 S.0046            END
                SIZE OF COMMON  00000     PROGRAM  02746
END OF COMPILATION  MAIN
/DATA

POTENTIOMETRIC TITRATION OF FRACTIONATED LIGNIN

1F0031215


END OF JOB.
```

APPENDIX VII

BAND ASSIGNMENTS OF LIGNIN AND CARBOHYDRATE MATERIALS*

Frequency, cm^{-1}	Band Assignment
3600-3200	Hydroxyl group stretch O-H
3450-3400	H-bonded OH stretch
3000-2600	Methyl and methylene CH stretch
1800-1600	Carbonyl stretching
1775-1650	Lactone carbonyl
1600	COO^- after salt formation
1650	Water (OH bending)
1610-1595 and 1515-1500	Aromatic skeletal vibrations
1465-1400 and 1380-1365	C-H bending vibration
1400-1335	OH bending vibration alcoholic
1270-1000	C-O-C ether asymmetric stretching vibration
1225-1215	OH phenolic
1145-1040	OH bands miscellaneous
1100-1000	C-O stretch carbohydrates
900-800	C-H out-of-plane bending vibration
895-890	Anomeric carbon group frequency
560-470	Softwood
535	Hardwood

*For more detailed individual band assignments, see References 94-135.

APPENDIX VIII

INFRARED SPECTRA OF FRACTIONS EX-PORASIL B

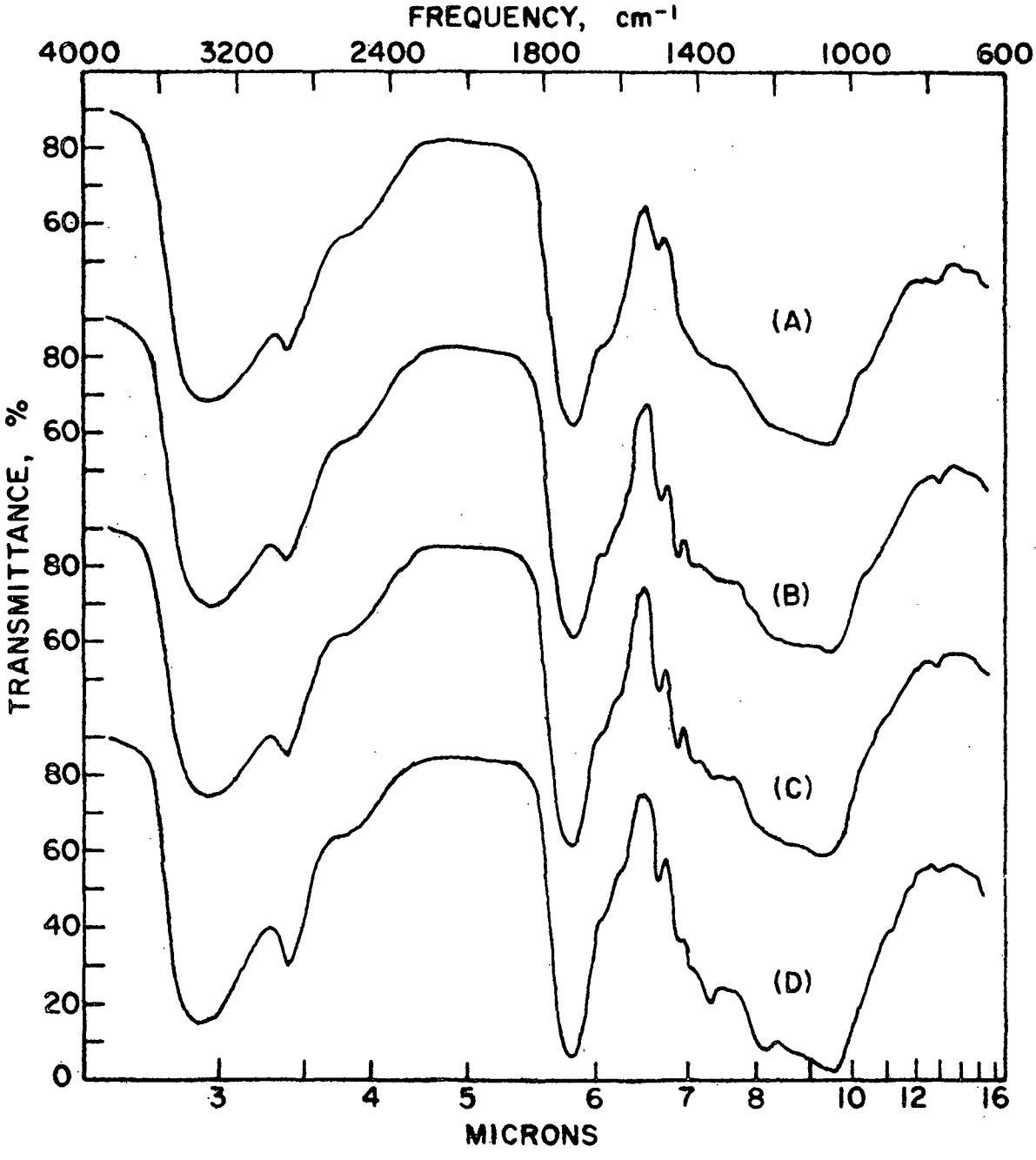

Figure 43. Infrared Spectra of Fractions 12-15 from Reaction Stages 1 (A), 3 (B), 4 (C), and 6 (D)

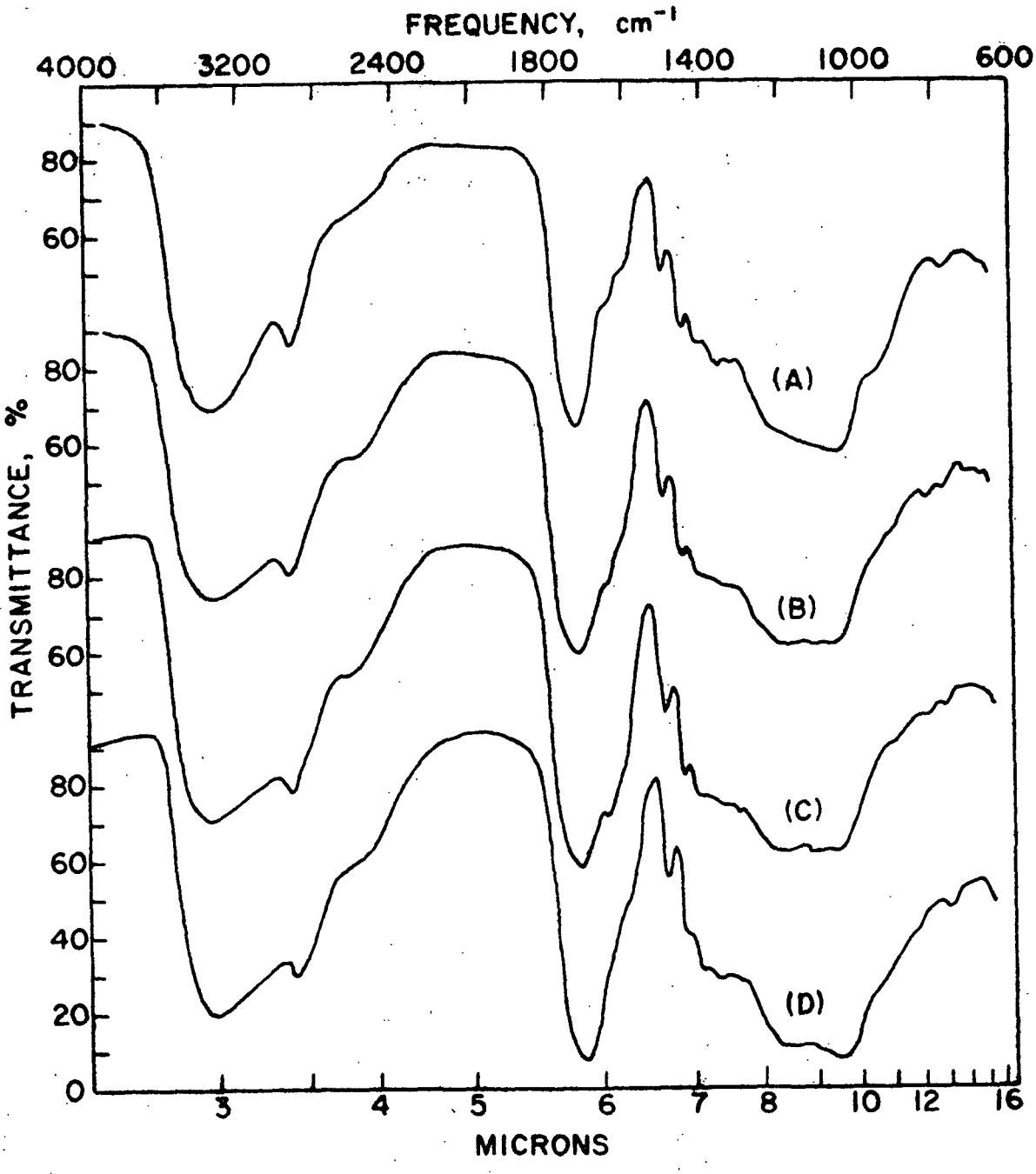

Figure 44. Infrared Spectra of Fractions 1-7 (A), 28-30 (B), 52-54 (C), and 62-65 (D) from Reaction Stage 4

APPENDIX IX

RANGES OF CHEMICAL SHIFTS IN ACETYLATED LIGNIN MODELS (137)

TABLE XIII

Selected Ranges No.	Selected Ranges δ-Values, ppm	Contributing Proton Types	δ, ppm	γ, ppm
1	9.75 to 12.00 (Strongly deshielded protons)	a. Carboxylic	11.00-12.00	-2.00 to -1.00
		b. Aldehydic	9.75-10.00	0-0.25
2	6.35 to 7.90 (Aromatic and α-vinylic protons)	a. Aromatic, ortho to carbonyl:	7.20-7.90	2.10-2.80
		-Hydroxyphenyl type	7.38	2.17
		-Guaiacyl type	7.23-7.78	2.22-2.77
		-Syringyl type	7.24-7.27	2.73-2.76
		b. Other arom. protons	6.35-7.24	2.75-3.65
		-Hydroxyphenyl type	7.02	2.98
		-Guaiacyl type	6.35-7.24	2.76-3.65
		-Syringyl type	6.35-6.61	3.39-3.65
		c. α-Vinylic	6.36-6.72	3.28-3.64
3	5.75 to 6.35	a. Benzylic protons in β-O-4 and β-1 dilignol and arylglycerol acetates	5.75-6.35	3.65-4.25
		b. β-Vinylic	6.12-6.34	3.66-4.25
4	5.30 to 5.70	Benzylic protons in β-5 dilignol acetates	5.30-5.70	4.30-4.70
5	2.35 to 5.30	a. $H-C_\alpha$ in β-β dilignol and $H-C_\beta$ in β-O-4 dilignol acetates. $H-O_\gamma$ in cinnamyl alcohol acetates	4.40-5.30	4.70-5.60
		b. $H-C_\gamma$ in β-5-, β-1-, β-O-4, and β-β dilignol acetates	3.95-4.40	5.60-6.05
		c. Arom. methoxyl protons	3.55-3.95	6.05-6.45
		d. $H-C_\beta$ in β-1-, and β-β dilignol acetates and aliph. methoxyl protons	2.35-3.55	6.45-7.65
6	2.15 to 2.35 (Most arom. acetoxyl protons)	Arom. acetoxyl protons	2.15-2.35	7.65-7.85
7	1.75 to 2.15 (Aliph. acetoxyl protons)	Aliph. acetoxyl and arom. acetoxyl in 5-5 dilignol acetates	1.75-2.15	7.85-8.25
8	0.75 to 1.75 (Highly shielded protons)	Miscellaneous protons	0.75-1.75	8.25-9.25

APPENDIX X

COMMUNICATIONS INVOLVED IN OBTAINING OPTICAL MEASUREMENTS FROM JASCO INC.

A search into the literature and personal communications with Joe Branier (a salesman with Cary Inc.) indicated that a JASCO ORD/CD/UV-5 would probably be the best instrument available and most suited to the samples in question. A call was then made to JASCO Inc. to determine whether an instrument was in the area. During this call, Jacques Bambling (President of JASCO) agreed to have six samples run, rather than bother one of his customers. Thus, six samples were selected and sent to JASCO for ORD and CD determinations.

Results for the ORD analyses were received in the form of raw data as seen in Appendix XI. The raw data were converted to specific rotations for the various wavelengths in question as seen in Appendix XI. The data for these samples were then plotted.

At a later date, CD results for two the samples were received. The CD data were converted and plotted as described for the ORD results.

The validity of the conversion technique was checked by sending JASCO a copy of the raw data, the converted data, and the plots of these data. In addition, a sample (unknown to JASCO) of phenyl-β-D-glucopyranoside was sent out for ORD analysis. Converting the raw data for this known and comparing to the literature would be used to validate the conversion technique.

JASCO looked at the results and conversion technique and said the results and technique looked "quite good." In addition, a comparison of the converted data for the known sample with that of the literature compared favorably.

APPENDIX XI

OPTICAL MEASUREMENTS FROM JASCO INC.

RAW DATA

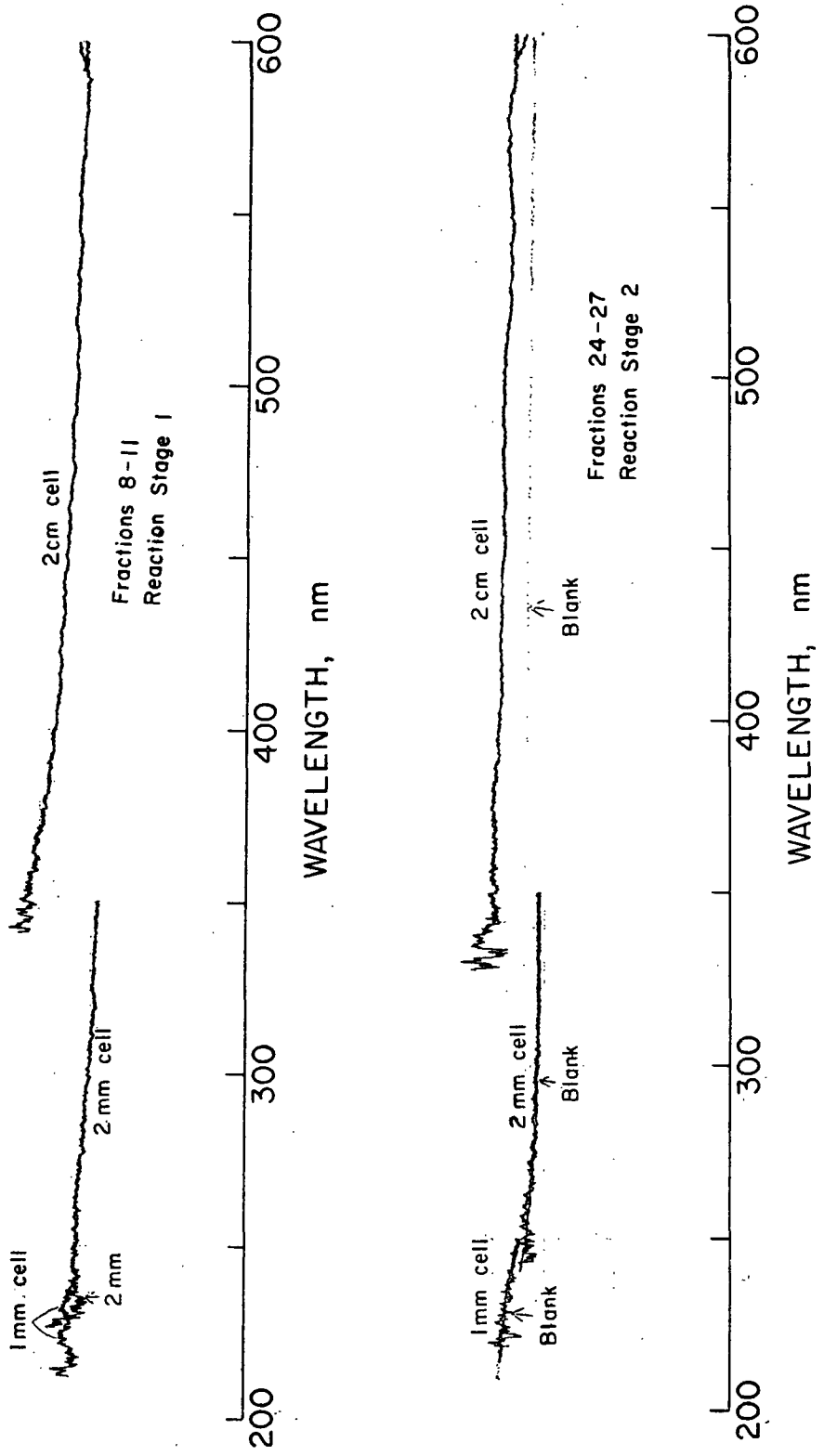

Appendix XI (Continued)

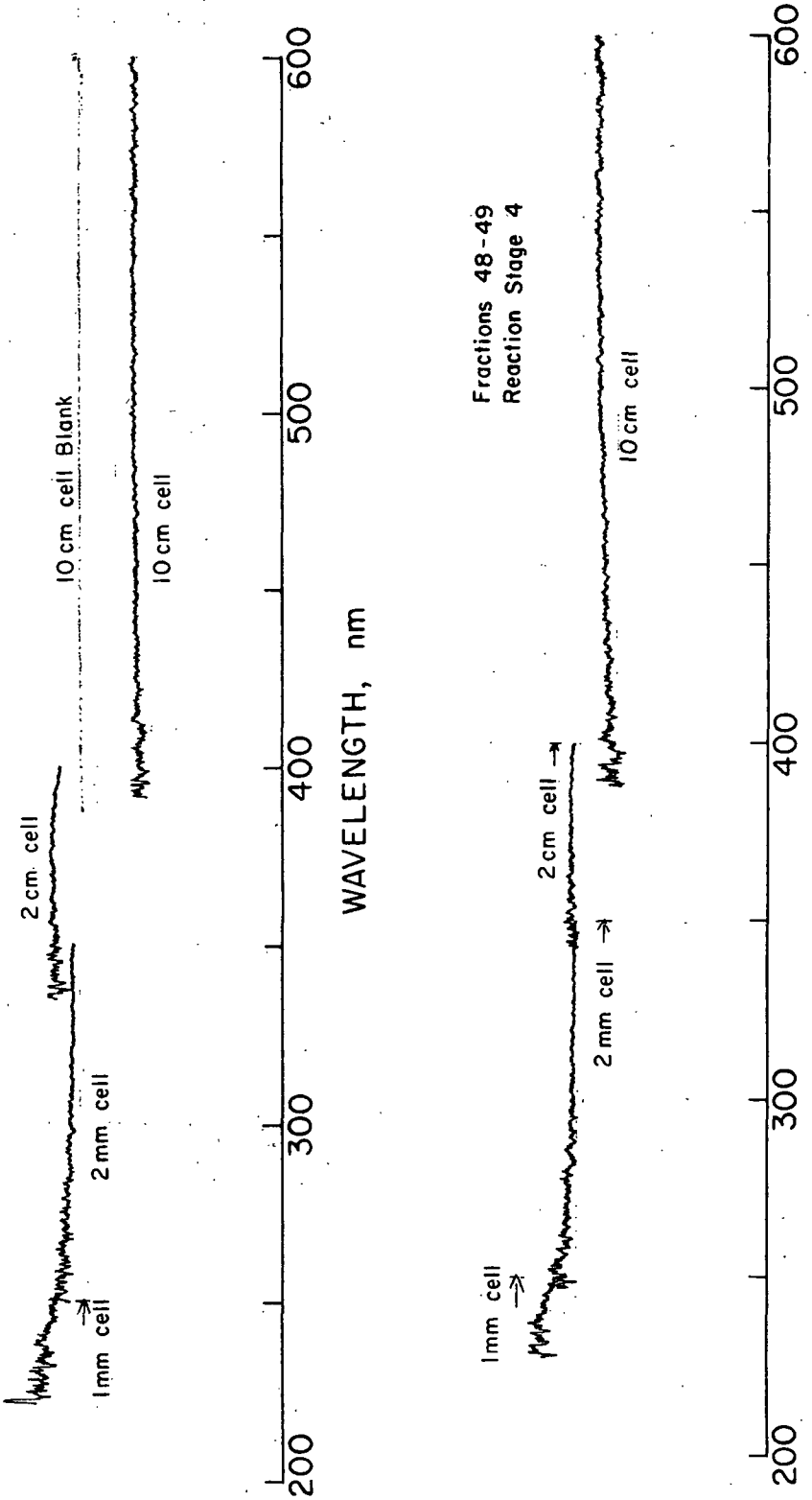

Appendix XI (Continued)

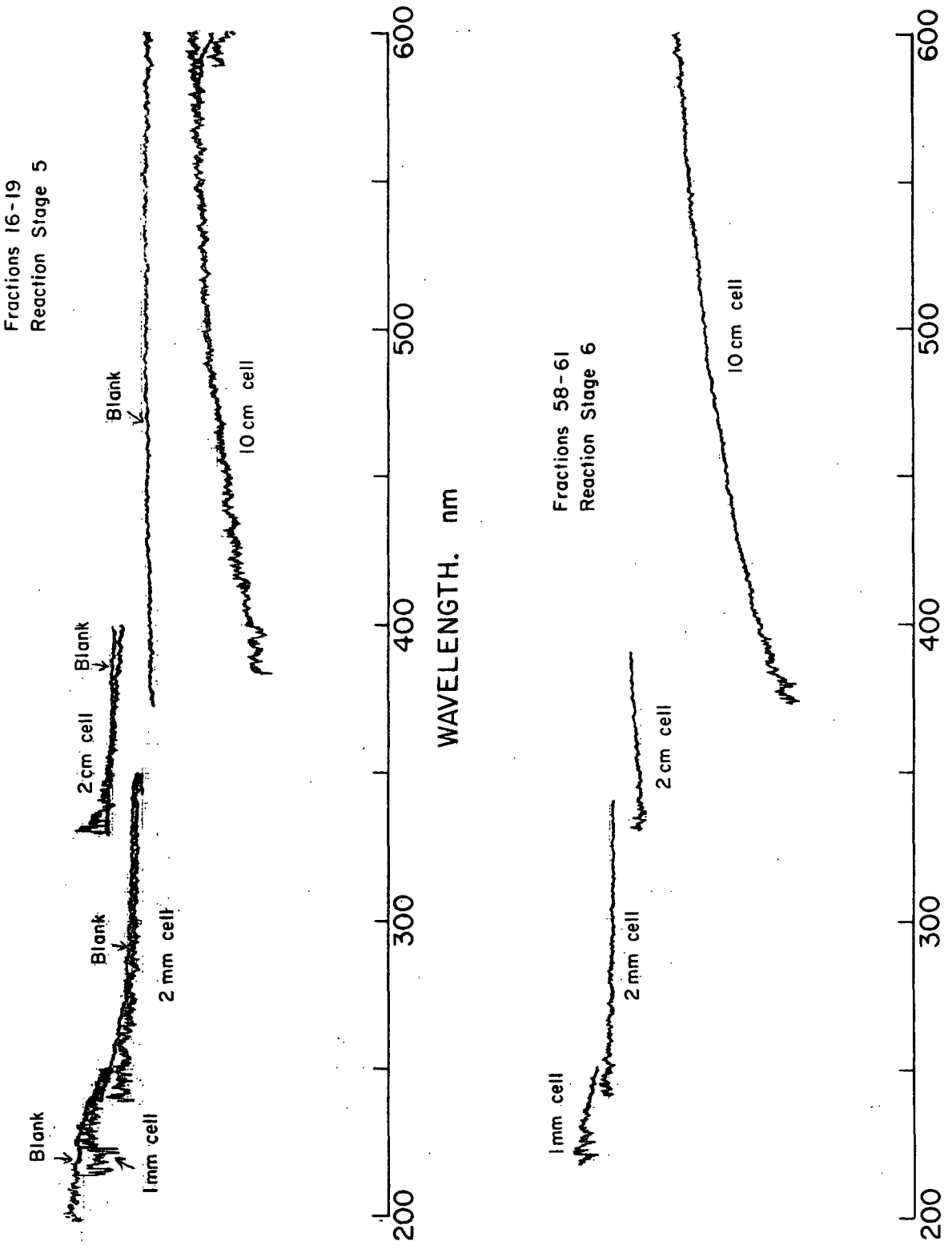

DATA CONVERSION TECHNIQUE

TABLE XIV

λ, nm	α_o	$[\alpha]_\lambda^{23}$
	Reaction Step 1, Fractions 8-11	
600	+0.004(2 cm)	1.98
550	+0.004 "	2.48
500	+0.006 "	2.97
450	+0.008 "	3.96
400	+0.011 "	5.45
350	+0.018 "	8.91
300	+0.003(2 mm)	14.85
290	+0.003 "	14.85
280	+0.004 "	19.80
270	+0.004 "	19.80
260	+0.005 "	24.75
250	+0.004 "	19.80
240	+0.001 (1 mm)	9.90
230	+0.001 "	9.90
220	-0.003 "	-29.70
		$\underline{c}$ = 10.10 mg/10 ml
	Reaction Step 2, Fractions 24-27	
600	+0.005(2 cm)	2.50
550	+0.006 "	3.00
500	+0.008 "	4.00
450	+0.008 "	4.00
400	+0.008 "	4.00
350	+0.009 "	4.50
300	+0.000(2 mm)	0.00
290	+0.000 "	0.00
280	+0.000 "	0.00
270	+0.000 "	0.00
260	+0.000 "	0.00
250	+0.000 "	0.00
240	+0.000 "	0.00
230	+0.000 "	0.00
220	+0.000 "	0.00
		$\underline{c}$ = 10.0 mg/10 ml

TABLE XIV (Continued)

λ, nm	α_o	$[\alpha]_\lambda^{23}$
	Reaction Step 3, Fractions 31-33	
600	-0.015(10 cm)	-1.38
550	-0.015 "	-1.38
500	-0.015 "	-1.38
450	-0.016 "	-1.47
400	+0.000(2 cm)	0.00
350	+0.000 "	0.00
300	+0.000(2 mm)	0.00
290	+0.000 "	0.00
280	+0.000 "	0.00
270	+0.000 "	0.00
260	+0.000 "	0.00
250	+0.002 "	9.17
240	+0.001(1 mm)	9.17
230	+0.002 "	18.35
220	-0.003 "	27.52
		c = 10.9 mg/10 ml
	Reaction Step 4, Fractions 48-49	
600	-0.003(10 cm)	-0.25
550	-0.004 "	-0.33
500	-0.005 "	-0.42
450	-0.007 "	-0.58
400	-0.003(2 cm)	-1.25
350	-0.003 "	-1.25
300	-0.002(2 mm)	-8.33
290	-0.002 "	-8.33
280	-0.001 "	-4.17
270	-0.001 "	-4.17
260	-0.001 "	-4.17
250	-0.001 "	-4.17
240	+0.000(1 mm)	0.00
230	+0.000 "	0.00
220	+0.000 "	0.00
		c = 12.00 mg/10 ml

TABLE XIV (Continued)

λ, nm	α_o	$[\alpha]_\lambda^{23}$
	Reaction Step 5, Fractions 16-19	
600	-0.008(10 cm)	-0.75
550	-0.009 "	-0.84
500	-0.010 "	-0.93
450	-0.028 "	-2.62
400	-0.002(2 cm)	-0.93
350	+0.000 "	0.00
300	+0.000(2 mm)	0.00
290	+0.000 "	0.00
280	-0.001 "	-4.67
270	-0.002 "	-9.35
260	-0.002 "	-9.35
250	-0.002 "	-9.35
240	-0.001(1 mm)	-9.35
230	-0.001 "	-9.35
220	-0.004 "	-37.38
		c = 10.7 mg/10 ml
	Reaction Step 6, Fractions 58-61	
600	-0.020(10 cm)	-1.59
550	-0.026 "	-2.07
500	-0.031 "	-2.47
450	-0.039 "	-3.11
400	-0.012(2 cm)	-4.78
350	-0.016 "	-6.37
300	-0.005(2 mm)	-19.92
290	-0.004 "	-15.94
280	-0.004 "	-15.94
270	-0.004 "	-15.94
260	-0.004 "	-15.94
250	-0.005 "	-19.92
240	-0.003(1 mm)	-23.90
230	-0.003 "	-23.90
220	-0.005 "	-39.84
		c = 12.55 mg/10 ml

Results for the ORD determinations were received in the form of raw data as seen in this appendix. The raw data were converted to specific rotations for the various wavelengths in question as seen in Appendix XI. Rotations were determined by the following equation:

$$[\alpha]_{\lambda}^{23°C} = \frac{100\ (\alpha_o - \alpha_s)}{\ell c}$$

where c = concentration, g/100 ml

ℓ = length of cell, dm

α_o = rotation from chart

α_s = rotation of blank

$[\alpha]_{\lambda}^{23°C}$ = specific rotation

The validity of the conversion technique for the raw data needed to be established. This was checked by sending to JASCO a copy of the raw data, the converted data, and plots of the converted data. An expert opinion about the conversion technique was requested. In addition, a sample of phenyl-β-D-glucopyranoside (sent as an unknown for analysis) described earlier was analyzed for its CD spectrum. The same conversion technique was used on this data and a comparison with a literature ORD spectrum was made as shown in Fig. 34.

The results of the conversion technique were examined and said to be "quite good." In some cases, however, small changes in the raw data gave large shifts or shoulders in some of the plots. It was suggested that these be averaged because the signal to noise ratio was too large in some of these regions.

The raw data from the CD curve for phenyl-β-D-glucopyranoside was converted to specific ellipticity. The CD curve (Fig. 34) had four negative minima corresponding to the inflection points in the ORD curve given by Sticzay in the

literature. Thus, the conversion technique used on the known compound was verified as being valid by comparison with the literature. In addition, the instrument was verified as giving valid results by comparison to the literature.